

5-19-2020

The Apicomplexan-Specific FIKK Kinase is Crucial for Cyst Formation in *Toxoplasma gondii*

Corey Gaylets

Follow this and additional works at: https://touro scholar.touro.edu/nymc_students_theses



Part of the [Medical Microbiology Commons](#)

The Apicomplexan-Specific FIKK
Kinase is Crucial for Cyst Formation in
Toxoplasma gondii

Corey Ethan Gaylets

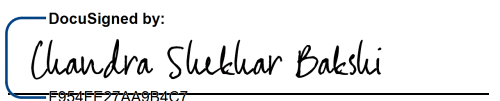
A Doctoral Dissertation in the Program in Microbiology and
Immunology Submitted to the Faculty of the Graduate School of
Basic Medical Sciences in Partial Fulfillment of the Requirements
for the Degree of Doctor of Philosophy

2020

The Apicomplexan-Specific FIKK
Kinase is Crucial for Cyst Formation in
Toxoplasma gondii



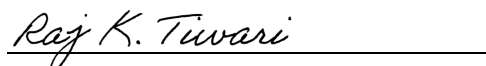
Dana Mordue, PhD
Mentor

DocuSigned by:


F954FE27AA9B4C7...
Chandra Bakshi, PhD, DVM
Chair of Committee



Mary Petzke, PhD
Committee member



Raj Tiwari, PhD
Committee Member



Zhongtao Zhang, PhD
Committee Member

April 24, 2020

Date of approval

© Copyright Corey Ethan Gaylets 2020
All Rights Reserved.

Aknowledgements

My mother, father, and brother who always supported me, my friends in the PhD program, and to my mentor Dr. Dana Mordue who taught me so much.

Table of Contents

The Apicomplexan-Specific FIKK Kinase is Crucial for Cyst Formation in <i>Toxoplasma gondii</i> ..	ii
Aknowledgements	iv
Table of Contents.....	v
List of Figures.....	vii
List of Tables.....	viii
List of Abbreviations	ix
Abstract of Dissertation.....	x
I Introduction.....	1
1 History	1
2 Classification and Natural Cycle.....	2
3 Infection in Humans	5
4 Structure and Lifecycle.....	9
5 The Residual Body and Intravacuolar Network	15
6 Tachyzoite to Bradyzoite Differentiation and Cyst Formation	16
7 Cyst Formation and Structure	18
8 Genetic Regulation of Tachyzoite to Bradyzoite Differentiation.....	24
9 Immune Response to Infection.....	31
10 FIKK.....	32
II Specific Aims	37
III Materials and Methods.....	38
1 HFF Cell Culture.....	38
2 Parasite Culture/Clones	38
3 Parasite Genetic Manipulation	42
4 Electroporation Protocol.....	42
5 Creation of the FIKK-YFP Clone	42
6 Creation of FIKK Gene Deleted Parasite Clones.....	45
7 Creation of Additional FIKK Gene Deletions From a Newly Cloned Pru Parental Line.	49
8 Creation of Pru Δ Ku80 FIKK Complemented Clones	52
9 Live Cell Imaging.....	56
10 Bradyzoite-Inducing Conditions and Cyst Formation <i>In vitro</i>	56
11 Immunofluorescence Staining Procedure	57
12 Cyst Formation <i>in vivo</i>	60
13 Acute Infection <i>in vivo</i>	63
14 Plaque Assay <i>in vitro</i> for Stressed Versus Unstressed Parasites.	63
15 Invasion Assay	66

16	Replication Assay.....	68
17	qRT-PCRs.....	68
18	RNA Sequencing.....	70
19	Proteomics and Phosphoproteomics.....	71
20	Motif Search	74
21	Statistics and Relevant Programs	74
IV	Results.....	75
1	Aim 1: Initial Characterization of the <i>T. gondii</i> FIKK Kinase Gene Deletion	75
2	The FIKK Kinase is Localized to the Basal Complex Throughout the Parasite’s Lytic Cycle But it is Also Localized to the Host Cell Cytosol.....	75
3	Impact of FIKK Gene Deletion on the Global Parasite Transcriptome and Proteome.....	78
4	Aim 2: Functional Characterization of the FIKK Kinase for Acute Infection	84
5	The FIKK Kinase is Not Required for the Parasites’ Lytic Cycle <i>in vitro</i>	84
6	There is No Gross Impact of the FIKK Gene Deletion on Parasite <i>in vitro</i> Growth in HFF Cells.....	86
7	Deletion of the FIKK Kinase Does Not Impact the Efficiency of Parasite Invasion of HFF Cells.....	88
8	The FIKK Kinase Does Not Alter Parasite Replication Within a PV	90
9	The FIKK Kinase is Important for Parasite Virulence During Acute Infection <i>in vivo</i> ...	92
10	Aim 3: Functional Characterization of the FIKK Kinase in Chronic Infection	94
11	The FIKK Kinase is Important for Cyst Formation <i>in vitro</i>	94
12	The FIKK Kinase is Important for Establishment of Chronic Infection in Mice.....	99
13	The FIKK Kinase is Important for Tachyzoite Differentiation to Bradyzoites.....	101
14	FIKK Target Search	105
V	Discussion	111
1	<i>Tg</i> FIKK is Not Important for the Parasite’s Lytic Cycle.....	113
2	Δ FIKK Parasites Retain Growth Characteristics of Tachyzoites When Exposed to Bradyzoite-differentiation Conditions.	113
3	The <i>Tg</i> FIKK Kinase Has a Moderate Impact on Acute Infection in Mice	113
4	<i>Tg</i> FIKK is Important for Early Events that Regulate Tachyzoite to Bradyzoite Differentiation.	116
5	The FIKK Kinase is Important for Chronic Infection.	120
VI	References	123

List of Figures

Figure 1: <i>Toxoplasma gondii</i> Life Cycle in Definitive and Secondary Hosts.	4
Figure 2: Toxoplasmosis in Humans	8
Figure 3: Invasion and PV Formation.....	11
Figure 4: Basal Complex and Parasite Replication.....	14
Figure 5: Transitioning between Stages and TgIF2 α Phosphorylation	21
Figure 6: Cell Cycle and Bradyzoite Transition	22
Figure 7: Cyst Matrix and Wall.....	23
Figure 8: Histone Modifications in <i>T. gondii</i> that Regulate Stage Differentiation	26
Figure 9: Localization of Tagged FIKK Proteins	36
Figure 10: Creation of the Clonal Pru Δ HPT Wild Type (WT) 2 Clone.....	41
Figure 11: VC YFP Plasmid Including the Cloned FIKK Sequence	44
Figure 12: Δ FIKK Plasmid.....	47
Figure 13: Junctional PCR of Δ FIKK Clones.....	50
Figure 14: QPCR of Δ FIKK Clones and Complements.....	51
Figure 15: FIKK Complement Plasmid with BirA Tag	55
Figure 16: Cyst Induction Conditions.....	59
Figure 17: Procedure for Investigating Chronic Infection <i>in vivo</i>	62
Figure 18: Plaque Assay.....	65
Figure 19: Invasion Assay.....	67
Figure 20: Live Cell Imaging of the FIKK-YFP	77
Figure 21: Differentially Expressed Genes Between Pru Δ HPT and Δ FIKK Clones With No Exogenous Stress	80
Figure 22: Differentially Expressed Genes Between Pru Δ HPT and Δ FIKK Clones at 24 Hours Under SNP Stress	81
Figure 23: Differentially Expressed Genes Between Pru Δ HPT and Δ FIKK Clones at 48 Hours Under SNP Stress	82
Figure 24: Differentially Expressed Genes Between Pru Δ HPT and Δ FIKK Clones at 72 Hours Under SNP Stress	83
Figure 25: Parasite Lytic Cycle	85
Figure 26: Plaque Sizes of Pru Δ Ku80, Δ FIKK, and FIKK Kinase Complemented Clones.....	87
Figure 27: Parasite Invasion Assay.....	89
Figure 28: Parasite Replication of WT and FIKK Deficient Parasites in the Presence and Absence of Exogenous Stress.....	91
Figure 29: Survival Curves of Acute Infection.....	93
Figure 30: Cyst Formation <i>in vitro</i> by Pru Δ HPT and Pru Δ HPT Δ FIKK Clones.....	96
Figure 31: Cyst Formation <i>in vitro</i> Pru Δ Ku80.	97
Figure 32: Cysts <i>in vitro</i>	98
Figure 33: Infection with Δ FIKK Parasites Results in Decreased Numbers of Brain Cysts	100
Figure 34: Expression of Canonical Bradyzoite Marker in WT versus Δ FIKK Parasites Cultured in Bradyzoite/cyst-inducing Conditions.....	103
Figure 35: Expression of Ap2 Transcription Factors in WT Parasites, Δ FIKK Clones and FIKK Complemented Parasites	104
Figure 36: Expression of Ap2 Transcription Factors in WT Parasites, Δ FIKK Clones and FIKK Complemented Parasites	105
Figure 37: Alignment of TgFIKK, PfFIKK8, PFIKK8 Active site, and CpFIKK.....	107
Figure 38: Schematic Model of the Current Model of Where and How the FIKK Kinase Functions in Parasite Cyst Formation.	110

List of Tables

Table 1: Ap2 Transcription Factors Known to Regulate Bradyzoite Genes	28
Table 2: Parasite Strains and Genetically Modified Parasite Clones Used in the Thesis.....	40
Table 3: Primers Used to Confirm FIKK Knockout	48
Table 4: Clones Used for <i>in vitro</i> and <i>in vivo</i> Studies of Acute and Chronic Infection	58
Table 5: Primers Used for qRT-PCRs.....	69
Table 6: Experimental Setup for RNA Sequencing and Proteomics	73
Table 7: Genes in the <i>T. gondii</i> Genome that Contain the Putative FIKK Target Sequence.....	108

List of Abbreviations

ANOVA	Analysis of variance
Ap2	Apetala transcription factor
BAG1	Bradyzoite antigen 1
BirA	Biotin ligase
BPK1	Bradyzoite pseudokinase 1
CNS	Central nervous system
CST1	Cyst protein 1
DAPI	4',6-diamidino-2-phenylindole
DBA	<i>Dolichos bifluros</i> lectin
EIF2- α	Eukaryotic initiation factor 2 alpha
ENO	Enolase 1, 2
5-FUDR	5-floxuridine
GRA	Dense granule protein
HA	Hemagglutinin
HDAC	Histone deacetylase
HEPES	4-(2-hydroxyethyl)-1-piperazineethanesulfonic acid
HFF	Human foreskin fibroblast
HPT	HXGPRT Hypoxanthine phosphoribosyl transferase
ICN	Intracyst network
IVN	Intravacuolar network
IF	Immunofluorescence
IFN- γ	Interferon-gamma
LDH,	Lactate dehydrogenase 1,2
MAG2	Matrix antigen 2
MCP4	Microneme adhesive repeat domain-containing protein 4
MORN-1	Membrane occupation and recognition nexus protein 1
MPA	Mycophenolic acid
NHEJ	Non-homologous end-joining
NO	Nitric Oxide
PTM	Post-translational modification
PV	Parasitophorous vacuole
PVM	Parasitophorous vacuole membrane
QPCR	Quantitative polymerase chain reaction
SNP	Sodium nitroprusside
<i>T. gondii</i>	<i>Toxoplasma gondii</i>
<i>TgFIKK</i>	<i>Toxoplasma gondii</i> FIKK
UPRT, UPT	Uracil phosphoribosyltransferase
YFP	Yellow fluorescent protein

Abstract of Dissertation

Toxoplasma gondii is an obligate intracellular pathogen. It is considered the second deadliest foodborne pathogen in the world with up to 1/3 of the human population estimated to be currently infected. The majority of immune competent people may exhibit mild symptoms following *T. gondii* infection. The acute stage of infection is often well controlled by cellular immunity in healthy individuals. However sterilizing immunity does not occur as the tachyzoite stage of the parasite responsible for acute infection differentiates to a slow growing bradyzoite stage contained in tissues cysts that can persist for the life of the host. However, if the host becomes immunocompromised, these parasites can differentiate back to tachyzoites that can cause pneumonia, severe central nervous system pathology and death. Current therapies are effective against the tachyzoite stage but not the chronic cyst stage and so infected patients are susceptible to recurrent disease should they become immunocompromised.

Apicomplexa parasites, including *T. gondii* have a unique family of serine/threonine kinases referred to as FIKK kinases based on the conserved amino acids in its active site: region of amino acid in the protein's active site consisting of a phenylalanine(F), and isoleucine(I), and two lysines(K). *Plasmodium falciparum* has 17 potential FIKK kinases while most Apicomplexa including *T. gondii* have a single FIKK kinase. The goal of the current study was to evaluate the importance of *T. gondii*'s sole FIKK kinase to parasite pathogenesis.

Endogenous tagging of the *Tg*FIKK kinase with YFP followed by live cell florescent microscopy during the parasite's lytic cycle indicated the FIKK kinase localizes to the parasite posterior end, within the parasite basal complex, in both

extracellular and intracellular parasites. It was also transiently found in the host cell cytosol. The FIKK kinase was deleted and complemented in order to study the function of the FIKK kinase in parasite pathogenesis. Studies comparing wild type, Δ FIKK parasites and FIKK complemented parasites indicate that the *Tg*FIKK kinase is not critical for the parasites lytic cycle in human fibroblast (HFF) cells, including parasite replication. Instead, we show that the *Tg*FIKK kinase is critical for the ability of the parasite to form cysts *in vitro* in cell culture and for the establishment of chronic infection in mice. The deletion of the FIKK gene prevents tachyzoite to bradyzoite differentiation. Thus, our current hypothesis is that the *Tg*FIKK kinase may link changes in the parasite's cell cycle at a proposed G1 checkpoint that serves as a gateway for parasite entry into the bradyzoite differentiation pathway.

Introduction

History

Toxoplasma gondii (*T. gondii*) was first discovered in 1908 by researchers studying *Leishmania* by using a rodent native to North Africa called the gundi (*Ctenodactylus gundii*). Infection in the gundi only occurred in captivity while being used to study leishmaniosis at the Pasteur Institute in Tunis (10). After discovery, the transmission was not elucidated until 1938, when doctors in New York treated a newborn baby girl for convulsive seizures, after one month she died, and the autopsy showed lesions in the brain with free and intracellular parasites found upon microscopic study. Tissue from the brain was homogenized in saline and inoculated into rabbits and mice, which subsequently developed encephalitis (91). The parasites were isolated from the brains of these animals and were successfully passed into other mice. Subsequent studies showed congenital transmission in many animal species (40). In the 1960s work demonstrated transmission by consumption of undercooked meat by feeding meat from infected animals to children at a Paris sanatorium. A sampling of the Paris population also showed that 80% of people were seropositive for *T. gondii* (17). Initial characterization showed congenital, and foodborne transmission, however the prevalence of *T. gondii* amongst strict vegetarians in India was the same as non-vegetarians (67). A parasitologist in Scotland, Bill Hutchison, first suspected fecal-oral infection by experimenting with the nematode parasite *Toxocara cati*. He fed cats already infected with *T. cati* with isolated *T. gondii* tissue cysts. Nematode eggs isolated from the cats' feces also caused toxoplasmosis in mice. *Toxoplasma* infectivity was maintained even after eggs were stored for up to twelve months in tap water, which indicated an

undiscovered form of *T. gondii* since the already isolated tachyzoites, and bradyzoites from infected brain tissue could not survive in tap water for that long (44). The final piece of the parasite life-cycle was elucidated in 1970 when several groups independently discovered the oocyst form of the parasite in the feces of cats (22, 31).

Classification and Natural Cycle

T. gondii is a member of the phylum Apicomplexa. This is a diverse phylum with over 5,000 species comprised almost exclusively by intracellular parasites. *T. gondii* belongs to a subset of Apicomplexa called the coccidians, a class of organisms defined by their ability to form oocysts. *T. gondii* is a parasite with a wide host range and it can infect every bird and mammal species tested (54). These species comprise the range of animals that can play secondary host to the parasite. Secondary hosts are infected with the asexual stages of the parasite, the tachyzoite and bradyzoite. However, the oocyst form often transmits infection to secondary hosts through contaminated food and water. The definitive host of *T. gondii* is the cat, where parasite sexual reproduction occurs. In the cat, the parasite infects the intestine and develops into the merozoite stage that undergoes sexual reproduction to form sporozoite-containing oocysts. The oocysts are shed in the feces of cats. The oocysts sporulate in the environment and can remain viable for months. Upon consumption of sporulated oocysts by a secondary host, the sporozoites emerge and invade the small intestine, forming parasitophorous vacuoles in the epithelial cells, and transitioning into tachyzoites (Figure 1). After replicating the tachyzoites will egress from the infected cells, lysing them in the process. After egress the parasites invade new cells repeating the parasite lytic cycle. The tachyzoite parasites disseminate systemically from the intestine and can invade any nucleated cell. During infection, some

of the tachyzoites differentiate into bradyzoites contained in intracellular tissue cysts. While a cell-dependent immune response typically resolves acute infection, sterilizing immunity does not occur due to the persistence of these bradyzoites in tissue cysts. The tissue cysts generally appear invisible to the immune response and do not generate a noticeable inflammatory response. Thus the encysted parasite establishes a chronic infection (54). The cysts also act as a reservoir for parasites. If a host becomes immunocompromised, the encysted bradyzoites can differentiate back into rapidly replicating tachyzoites and cause renewed disease. Tissue cysts may form in any nucleated cell; however, *in vivo*, they are more common in the central nervous system, in the eye, and in both skeletal and cardiac muscles (Figure 2). *In vivo*, bradyzoite transition and cyst formation occur as early as one-day post-infection. Cyst size is variable depending on the number of parasites within, and the type of host cell infected (45).

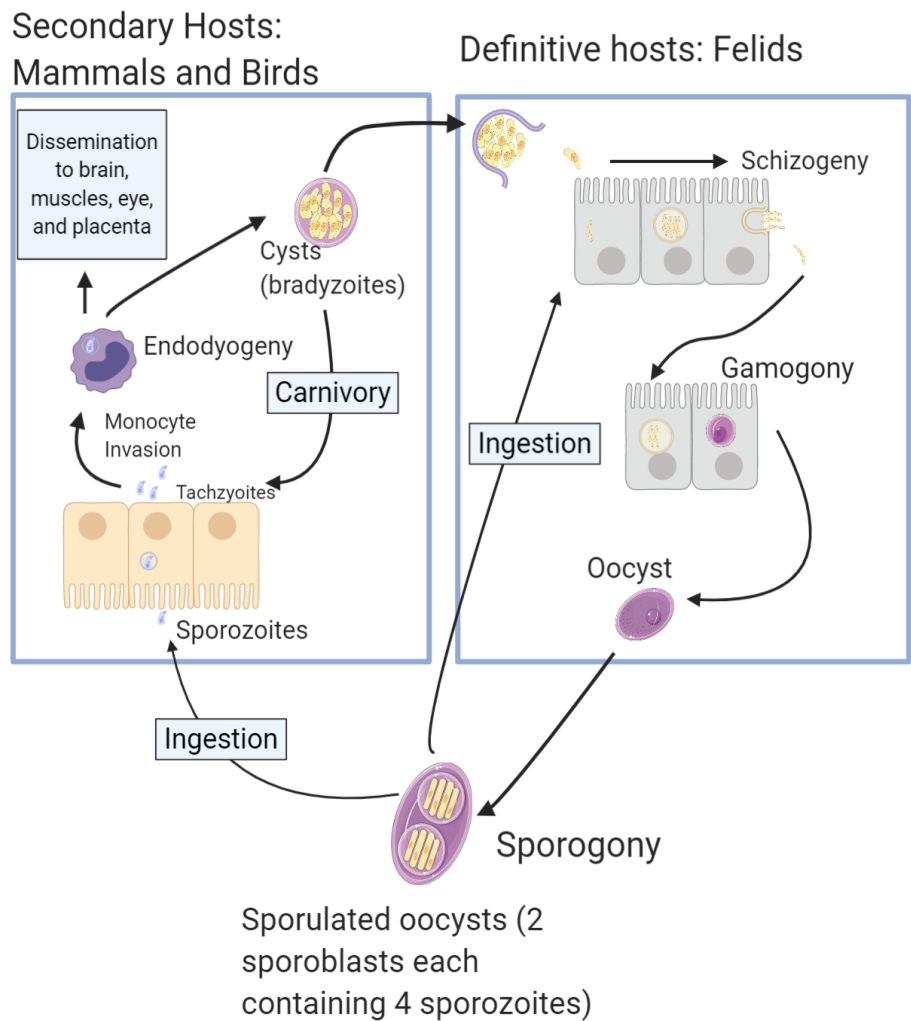


Figure 1: *Toxoplasma gondii* Life Cycle in Definitive and Secondary Hosts. Tissue cysts are also infectious to both the definitive as well as secondary hosts through predation/carnivorism. After ingestion of contaminated meat, the bradyzoites emerge from the cysts, invade the intestinal epithelium, differentiate into tachyzoites and disseminate systematically. Thus both sporozoites in oocysts and bradyzoites in tissue cysts are infectious via oral transmission and follow a similar progression to cause disease

Infection in Humans

Humans act as a secondary host to the parasite. People are infected by the parasite through eating undercooked meat from another infected secondary host, or by consuming oocysts in contaminated food or water. Additionally, if a pregnant woman becomes infected, the parasite can cross the placental barrier and infect the fetus (23). This can result in miscarriage or congenital infection. Less likely sources of infections are blood transfusion, organ transplantation, and contact with contaminated sharps through skin penetration (Figure 2). Infection rates vary based on geography, and the risk of infection generally rises with age. In the United States, overall seroprevalence is 22.5% (47).

There are three primary clonal lineages of *T. gondii* that are predominant in North America and many parts of Europe: Type I, II, and III. These lineages differ in virulence and occurrence (43). Most strains isolated from AIDS patients have been Type II, while both Type I and II have been recorded in congenital disease cases and Type III parasites are primarily found in animal infections (1). Replication times differ between lineages with Type I strains replicating faster than Type II and III (66). Specific immune evasion mechanisms also correlate with differences often conserved between parasite genotypes. Other atypical genotypes of *T. gondii* exist that infect humans. These atypical genotypes are dominant in certain areas of the world, including South America, and some have been associated with increased disease severity.(54)

Severe clinical disease is uncommon in *T. gondii* infection in immune-competent individuals. Clinical disease is more likely in immunocompromised patients and in primary infection during pregnancy (4, 54). When symptoms do manifest in healthy hosts, they occur within the first two weeks after infection. In these cases, the disease is

generally mild, non-specific, and self-limiting. Very rarely infection in healthy patients can result in myocarditis, polymyositis, pneumonitis, hepatitis, or encephalitis (54).

In immunocompromised patients, the infection can be debilitating, and life-threatening with most cases due to reactivation of a latent infection (62). The central nervous system is most commonly affected by reactivated disease resulting in *T. gondii* encephalitis, which can vary in presentation. Symptoms include mental status changes, seizures, motor deficits, sensory abnormalities, movement disorders, and neuropsychiatric findings. Often reactivated toxoplasmosis is confused with other infections and diseases delaying diagnosis and treatment. Outside of central nervous system (CNS) manifestations, reactivated toxoplasmosis can cause chorioretinitis, pneumonitis, or multiorgan involvement leading to shock (62). *T. gondii* encephalitis is life-threatening and requires rapid intervention to avoid fatal outcomes.

In congenital infection, the infected fetuses may appear normal on ultrasound, and if there are findings on ultrasound, they usually are intracranial calcifications, ventricular dilation, hepatic enlargement, ascites, and increased placental thickness (33). However, spontaneous abortion of infected fetuses is common early in pregnancy. The presentation of disease in newborns is variable and can include hydrocephalus, microcephaly, intracranial calcifications, chorioretinitis, strabismus, blindness, epilepsy, physical or mental retardation, petechia, and anemia (81). These clinical signs are non-specific and may be caused by other infections. (54)

Treatment for toxoplasmosis is rarely given in immunocompetent individuals unless symptoms are persistent or severe. If treatment is required a combination of pyrimethamine, sulfadiazine, and folinic acid are administered for 2-4 weeks. Treatment

is not required for women with prior exposure to *T. gondii*, as confirmed by IgG serology as a memory response is normally capable of suppressing parasite replication and prevent cross-placental transmission. If the infection is newly acquired, then spiramycin is given for the first and early second trimesters, and pyrimethamine and sulfadiazine for the late second and third trimesters (23, 33). The triple combination of pyrimethamine, sulfadiazine, and folinic acid is recommended in immunocompromised patients. Treatment is given pre-emptively in immunocompromised patients with suspected reactivated infection. After resolution of symptoms, a maintenance regimen is given using half of the dosage of the combination used in treatment. Maintenance is continued indefinitely or until the immunosuppression has resolved (54).

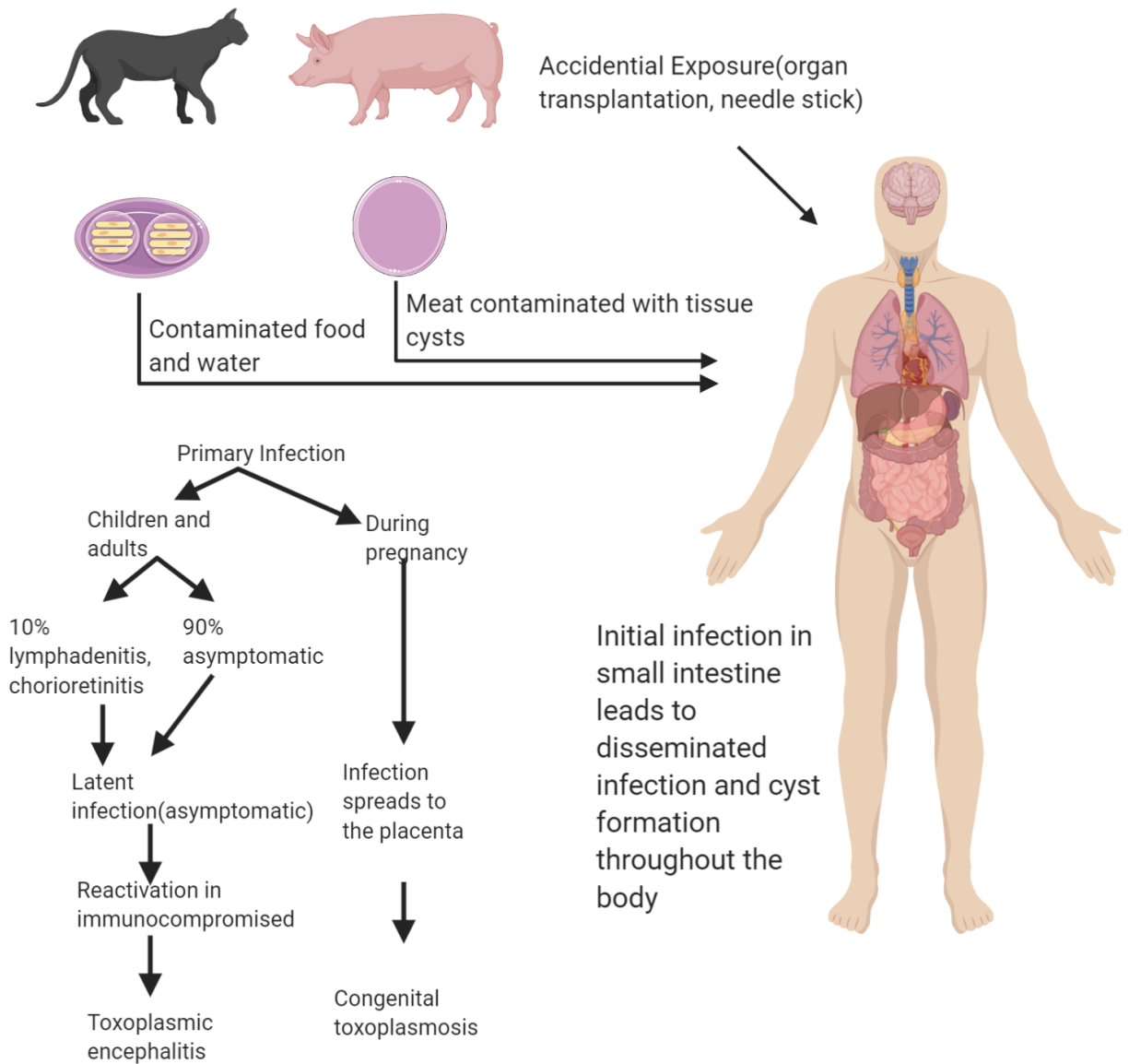


Figure 2: Toxoplasmosis in Humans

Toxoplasmosis in humans can be acquired by various sources in the environment and the food supply. Initial infection is often asymptomatic or mild, followed by a latency that can last for up to a lifetime of the host. *T. gondii* can infect any nucleated cell in the body, but tissue cyst forms preferentially in the muscles and nervous system.

Structure and Lifecycle

There are three infectious stages of *Toxoplasma gondii*, the sporozoite, tachyzoite, and bradyzoite. The bradyzoite and sporozoite stages are relevant to the transmission of infection; the tachyzoite and bradyzoite stages are relevant to human disease.

The term tachyzoite comes from the Greek word for speed (tachos) and was coined in 1973 (30). The tachyzoite is crescent-shaped, 2 by 6 micrometers with a pointed anterior end, and a rounded posterior end. The tachyzoite cell contains a pellicle that surrounds the cell membrane, apical and polar rings, a conoid at the apical end, rhoptries, micronemes, dense granules, a micropore, mitochondrion, microtubules, rough and smooth endoplasmic reticula, Golgi body, nucleus, and an apicoplast (21). *T. gondii* is an obligate intracellular parasite. The tachyzoite stage is the stage that invades host cells. Parasites only spend a short amount of time outside of a host cell, after egress, where they move by gliding motility to find a new host. Upon contact with a host cell, parasites adhere using glycosylphosphatidylinositol (GPI) anchored surface antigens which recognize proteoglycans on the host cell surface (41). After binding to the host cell, the parasite interacts more tightly with the host cell membrane; proteins are secreted from the micronemes that lead to the formation of the moving junction (MJ), which forms the interface between the invading parasite and the plasma membrane. The moving junction acts as an anchor point in the membrane, using this anchor point the parasite invaginates the host cell membrane which leads to the formation of the nascent parasitophorous vacuole membrane (PVM) (Figure 3). During the parasite invasion, the nascent parasitophorous vacuole (PV) forms from the host cell lipid bilayer but excludes host cell transmembrane proteins as well as proteins in lipid rafts (75). The PVM is

created in a process independent of phagocytosis. The parasite invasion process and formation of the PV creates an intracellular niche for the parasite that does not fuse with lysosomes, preventing the host cell from degrading the parasite. This results in the creation of a favorable PV for parasite survival and growth that is largely separated from the host cell cytosol and the vesicular network (4). Proteins secreted from the parasite's rhoptries and dense granules modify the PVM and the host cell structures surrounding it giving parasites within the PV access to the nutrients in the cytosol. Nutrients are also acquired through recruitment of host cell organelles brought into close proximity with the PVM that allow nutrient and lipid exchange. *T. gondii* is auxotrophic for key nutrients such as tryptophan, arginine, cholesterol, and iron, and so the PVM functions as a barrier permeable to these and other small molecules (11).

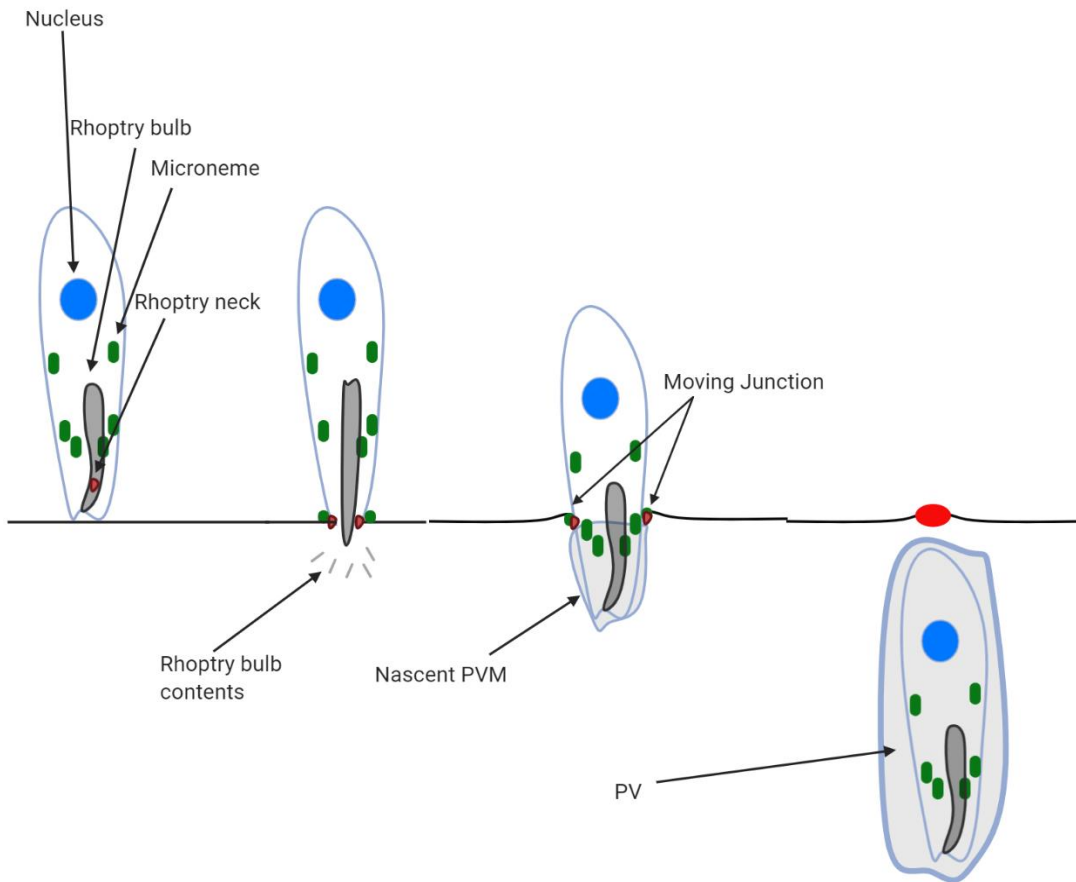


Figure 3: Invasion and PV Formation

Invasion of the host cell by tachyzoites involves binding to the host cell membrane and the secretion of various effector proteins that form the moving junction. The parasite invades and secretes effectors which create the nascent PV and PV.

Parasite replication only occurs in a parasitophorous vacuole through a unique process called endodyogeny (49). During endodyogeny, daughter cells form within the mother cell and upon maturation, the mother cell breaks apart releasing the new daughters (Figure 4) (29, 73). The *T. gondii* cell cycle is different from most eukaryotes in only having a G1 and S phase which is followed by mitosis with only a small G2 phase, while cytokinesis occurs late during the S phase. Genes expressed in G1 are primarily biosynthetic and metabolic genes common to all eukaryotes, however the transcriptome of S/M contains genes unique to the Apicomplexa. The expression of genes during G1 also occurs in two distinct phases. The genes expressed during the early part of G1 encode for ribosomal proteins, RNA polymerases and processing factors, and proteins needed for translation. In the second half of G1 the transcriptome becomes enriched for genes for DNA replication and proteasomal degradation (14). Additionally quiescent stages of the parasite, the sporozoite and bradyzoite, are considered to be in G0 (49).

The second stage found in humans is the bradyzoite stage. The name, coming from the Greek word for slow (brady), was used to describe parasites slowly replicating within tissue cysts (30). Structurally bradyzoites are similar to tachyzoites; the only differences are the location of the nucleus, central in tachyzoites, closer to the posterior end in bradyzoites, longer rhoptries, and the presence of amylopectin granules (21). Bradyzoites have also been reported as losing the apicoplast. In contrast to tachyzoites, bradyzoites are growth-arrested, and while considered quiescent some motility and replication have been observed and bradyzoite egress and reinvasion is possible (25, 39). Bradyzoites are found in intracellular cysts. In vivo cysts are most prevalent in the brain, eye, and in skeletal and cardiac muscles (20). The smallest cysts contain two parasites

and are about 5 μm in size, with the largest being 10-70 μm in size containing potentially thousands of bradyzoites. In vivo formation of bradyzoites occurs as early as one day post-infection (13).

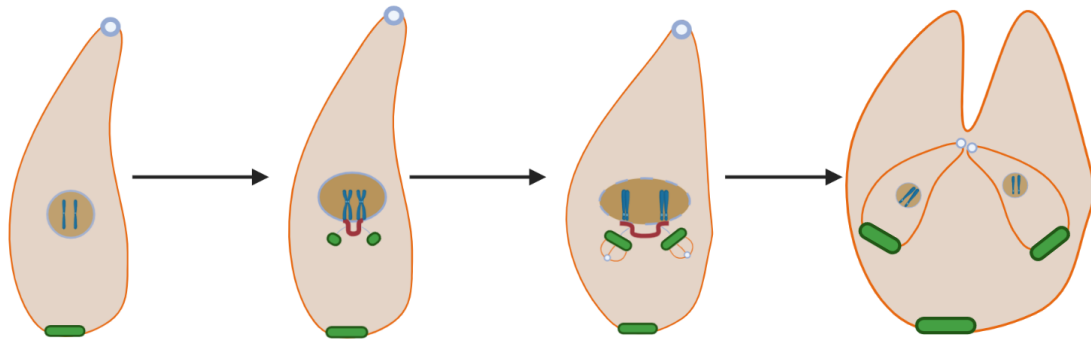


Figure 4: Basal Complex and Parasite Replication

The *T. gondii* basal complex is important for endodyogeny, the process by which the parasite reproduces. During endodyogeny the basal complex is one of the first organelles formed in the nascent daughter cells, its constriction is important for the separation of the daughter cells and their subsequent maturation. The basal complex is shown in green in both the mother cell and the nascent daughter cells.

The Residual Body and Intravacuolar Network

After host cell invasion and formation of the PV, the parasites replicate through endodyogeny. During replication nascent daughter cells form within the mother cell and release upon maturation; this leads to the breakdown of the mother cells (29). Remnants of the mother cell remain at the posterior ends of the mature daughter cells forming a structure called the residual body. The residual body is important for organizing the parasites in the characteristic rosette structure within the PV (55). Membrane connectivity exists between the residual body and the parasites within a parasitophorous vacuole until the parasite egresses from the host cell. Additionally, the residual body is not found within mature cysts. Consistent with the lack of a residual body, bradyzoites are not linked together in the same rosette like pattern as tachyzoites within a PV. The connections formed within the residual body are believed to facilitate communication between parasites to insure synchronization within a PV. Parasite actin is important for the formation of the residual body as conditional actin knockouts lack the structure. These actin conditional knockouts also replicate in an asynchronous manner. Actin polymers within the parasites were also discovered to extend into the residual body. This actin network is important for transport of material between the parasites within a PV (61, 82).

An intravacuolar network forms within the PV and appears to originate from the posterior end of the parasites. However, once formed the intravacuolar network extends throughout the PV and connects parasites within the PV to the PVM. The network proteins are made of tubules that are 5nm thick but are more than 100nm long. The intravacuolar network is shaped by dense granule proteins (GRAs) GRA2, GRA4, GRA6,

GRA9, and GRA12. Deletion of any of these proteins results in a major deficiency in cyst formation *in vivo* (38, 53, 83).

Within the cyst is the intracyst network (ICN). The ICN may be a modification of the IVN as there are similarities in its composition to the intravacuolar network that connect tachyzoites to the PVM (71). Electron microscopy studies suggest that elements of the ICN and cyst wall components may originate from a cytoskeletal pore in the posterior end of parasites. These secretions lead to the formation of the network, matrix, and wall of the cyst (Figure 7). However, dense granule proteins and rhoptry proteins are secreted from the apical end of the parasites during invasion and are important for the formation of both the ICN and IVN. Thus the origins and formation of the IVN, the ICN and cyst matrix and cyst wall components remain very poorly defined (38, 71).

Tachyzoite to Bradyzoite Differentiation and Cyst Formation

Stage differentiation from the tachyzoite stage to the bradyzoite stage requires the tachyzoite to fall out of the cell cycle and enter G0. Experiments have shown that the transition can begin before parasite invasion of the host cell as stressing extracellular parasites is sufficient to induce the formation of cysts after invasion (92). Bradyzoite induction occurs at a G1 checkpoint during which time the cell commits to either continued replication as a tachyzoite or to transition into a bradyzoite (66). Evidence points to translational control through modification of the homolog of eukaryote initiation factor 2 alpha, TgIF2 α (90). When tachyzoites are exposed to different stressors that induce bradyzoite transition TgIF2 α becomes phosphorylated (66). Treatment of encysted parasites using inhibitors of eIF2 α dephosphorylation such as guanabenz inhibits bradyzoite to tachyzoite differentiation. Additionally, TgIF2 α is phosphorylated in

bradyzoites (50, 56). After phosphorylation of parasite TgIF2 α , translation becomes dramatically reduced (Figure 5). This stall in protein translation allows the parasite to reprogram its genome to respond to stress and to transition to bradyzoites. mRNAs preferentially translated while TgIF2 α is phosphorylated have been identified.

Translation of a group of transcription factors unique to the Apicomplexa transcription factors are completely unaffected by TgIF2 α phosphorylation. These Apicomplexan apetalas (ApiAp2 or just Ap2) transcription factors have an important role in regulating the cell cycle and tachyzoite to bradyzoite transition (60). This transition between stages is closely linked to the parasite's cell cycle. Transition does not occur when the cell cycle is blocked presumably because the parasite does not reach the required G1 checkpoint to enter the bradyzoite differentiation pathway. A gene set enrichment analysis on the parasite shows that genes associated with the S/M phase of the cell cycle are enriched in bradyzoites, while genes enriched in G1 were found primarily in tachyzoites (13, 14).

Gene silencing is crucial to bradyzoite differentiation. In other eukaryotes gene silencing occurs during S phase, in *T. gondii* initiation of bradyzoite gene expression also requires the parasite to enter into S phase. While the timing of transition, in relation to the cell cycle, occurs during G1 (Figure 6); the resulting changes in gene expression requires epigenetic remodeling that occurs during S phase. Thus parasite replication and bradyzoite differentiation are tightly linked together (65). Approximately 1000 genes are differentially expressed in tachyzoites versus bradyzoites although few of these genes are annotated other than as hypothetical proteins (14). Surface proteins and metabolic genes are substantially changed between tachyzoites and bradyzoites. Canonical markers of bradyzoites include surface antigen 4 (SAG4), bradyzoite antigen 1 (BAG1), surface

antigen 2/2d (SAG2/2D), bradyzoite pseudokinase 1 (BPK1) and specific metabolic enzyme isoforms lactate dehydrogenase 2 (LDH2), enolase 2 (ENO2), and enolase 1 (ENO1) (6, 8, 14, 16, 45, 95, 96, 97).

Cyst Formation and Structure

The *T. gondii* tissue cyst consists of the parasites within a cyst matrix that is surrounded by a cyst wall contained within a membrane. The cyst wall is 270 to 850 nm in thickness and is organized in two layers (84). Qualitatively, *in vitro* cysts are similar to ones formed *in vivo* but there are clearly differences between *in vitro* cysts and *in vivo* cysts that may undergo significant additional maturation over time (45).

The defining feature of a cyst that separates it from a PV is the presence of the cyst wall, which forms underneath the PVM (32). Cyst walls can be detected using various fluorescently labeled lectins. The *Dolichos biflorus* lectin recognizes *N*-acetyl galactosamine on the glycoprotein CST1. It is used to label the cyst wall and to identify cysts in culture (31, 95). In addition to CST1 other proteins that comprise the cyst wall are just beginning to be identified. To date proteins in the mature cysts are dense granule proteins: GRA1, GRA2, GRA3, GRA6, GRA7, bradyzoite pseudokinase 1 (BPK1), microneme adhesive repeat domain-containing protein 4 (MCP4); and matrix antigen 1 (MAG1) (9, 52, 86).

The three lineages of *T. gondii* differ in their ability to form cysts. The faster replicating Type I parasites are generally poor cyst formers in mice; in part because they are almost always lethal during the acute stage of infection and the infected mice die prior to establishment of chronic infection. However, even *in vitro* in cell culture they tend to remain as tachyzoites and differentiate poorly *in vitro* in cyst inducing conditions.

Type II and III parasites are better cyst formers and are less virulent in mice (43). A Type I strain labeled RH, after the initials of the patient from which it was isolated, is the most commonly used laboratory strain. It is easy to manipulate genetically and is primarily parasite strain that has been studied to date to model tachyzoite biology and the parasite's lytic cycle in host cells *in vitro*. However, it is no longer able to complete the parasite's life cycle including differentiation to oocysts and differentiation to bradyzoite-containing cysts (8, 43). Thus, the RH strain cannot be effectively used to study stage conversion and cyst formation. However, under certain conditions, RH strains can produce bradyzoite specific proteins (8).

Cyst induction and bradyzoite conversion can be studied using Type II and Type III genotypes of the parasite. Tachyzoite to bradyzoite differentiation and formation of nascent cysts can be induced efficiently *in vitro* in cell culture using a variety of diverse exogenous environmental stresses. Bradyzoite-inducing conditions *in vitro* include alkaline stress by culturing parasites in host cells in pH 8 media for approximately three days. As an alternative a brief treatment of extracellular parasites in alkaline conditions can be used. Other methods include treatment with sodium nitroprusside (SNP) to induce nitric oxide (NO), arginine deprivation, incubation with mycophenolic acid, and CO₂ deprivation (8, 28, 45). While these stress conditions can be used to induce cyst formation, cystogenic strains will spontaneously convert at low levels even in non-stress culture conditions particularly if there is a low multiplicity of infection. Although cysts can form in any nucleated cell, certain cell types are more conducive to cyst formation than others (45). Cyst formation is highest in neurons and muscle cells, and cysts can form in these cells easily even in the absence of external stressors (78). The

permissiveness of host cells to cyst formation may be determined by the cell cycle stage of the host cell as terminally differentiated mouse skeletal muscle cells restrict tachyzoite replication and promote bradyzoite differentiation more than their myoblast progenitors. The terminally differentiated state of both muscle cells and neurons may explain the relatively greater numbers of cysts in these tissues *in vivo* (45, 78, 86).

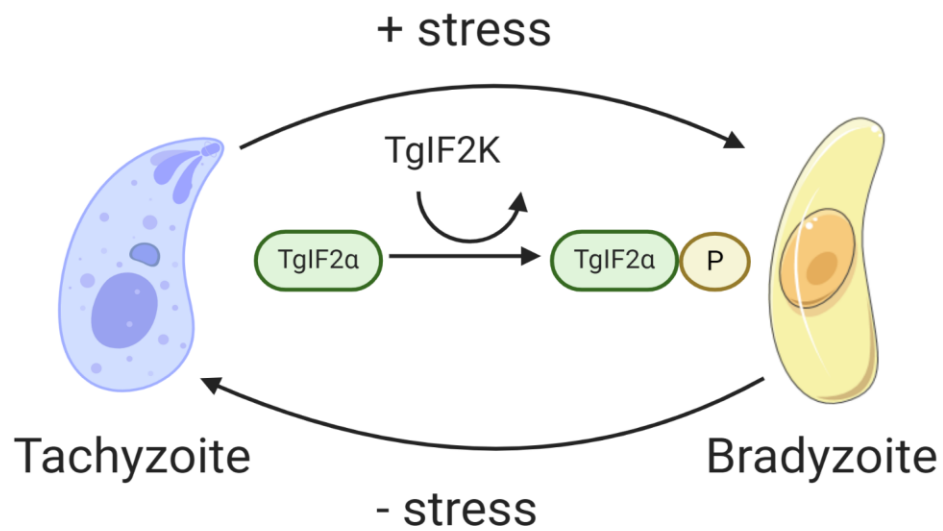


Figure 5: Transitioning between Stages and TgIF2 α Phosphorylation

Transition between stages involves numerous changes to genetic regulation in the parasite. These changes include epigenetic changes leading to differential expression of necessary genes, and phosphorylation and dephosphorylation of TgIF2 which affects translation.

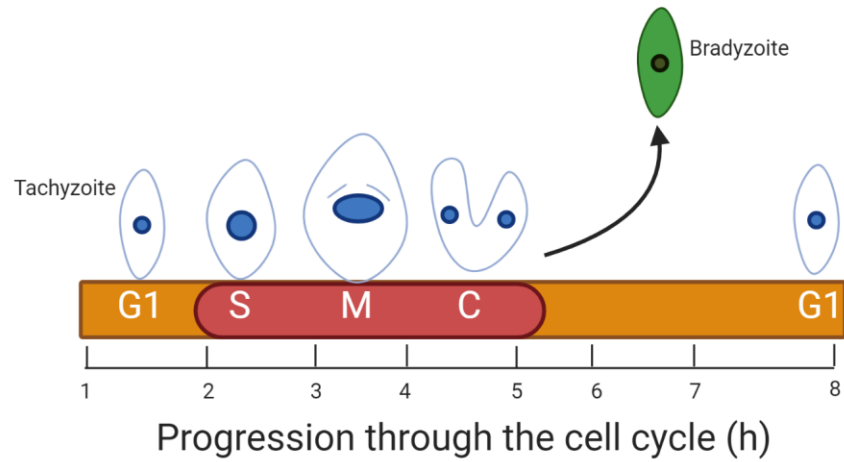


Figure 6: Cell Cycle and Bradyzoite Transition

The parasite progresses through the cell cycle intracellularly inside of the PV. The cell lacks a G2 phase with cytokinesis occurring simultaneously with S/M. At the G1 checkpoint the parasite either commits to further growth and replication, or it commits to transitioning to the bradyzoite stage.

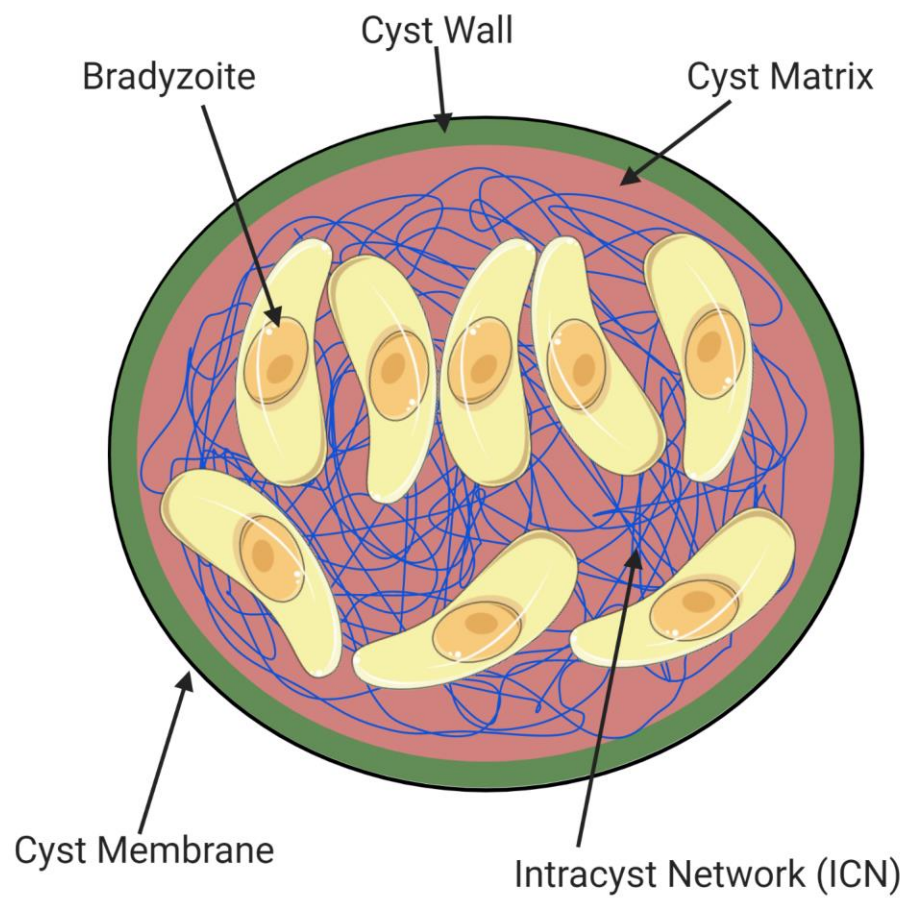


Figure 7: Cyst Matrix and Wall

Graphical representation of a tissue cyst illustrating the presence of the outer cyst wall, the inner cyst membrane, the intracyst network (ICN) and the cyst matrix

Genetic Regulation of Tachyzoite to Bradyzoite Differentiation

The regulation of parasite differentiation between tachyzoites and bradyzoites as well as sporozoites remains poorly understood. However, regulation of the bradyzoite transition occurs at both the transcriptional and epigenetic levels. A series of studies have demonstrated that epigenetics and histone post-translational modifications (PTMs) play a vital role in protozoan parasite biology. More specifically, *Toxoplasma* epigenetics has been linked with the regulation of genes expressed during oxidative stress responses, cell cycle, and DNA repair mechanisms, as well as during tachyzoite to bradyzoite stage conversion (6, 15, 69).

Histones are small basic proteins that assemble in an octamer consisting of two copies of histone proteins H2A, H2B, H3, and H4. These proteins combine with ~147 bp of DNA wound around the octamer core to form the nucleosome. Nucleosomes are linked together by stretches of unbound DNA called linker DNA. Post-translational modifications (PTMs) of histones are important to regulate gene expression (57, 80). PTMs of residues on histones, such as methylation and acetylation, increase or decrease DNA binding, and recruit transcription factors all of which can promote gene expression or gene silencing (68, 80). Acetylation of histone in *T. gondii* is associated with gene activation (35). *T. gondii* also expresses unique variants of histones H3.3 and CenH3 of H3, H2A.Z and H2A.X and H2B.Z variants of H2 (15). Histone PTMs are dynamic and change with the conditions of the cell. The *T. gondii* genome encodes diverse chromatin remodeling proteins including histone deacetylases, acetyltransferases, demethylases, lysine and arginine methyltransferases, kinases, ubiquitin ligases, and small ubiquitin related modifier (SUMO) conjugating enzymes (57, 70). Of all the histone modifying

genes the three that are most studied include the histone acetyltransferases GCN5-A and GCN5B and the histone deacetylase HDAC3 which are implicated in regulating tachyzoite to bradyzoite transition. Attempts to delete GCN5B were lethal suggesting its importance to parasite growth (39, 88). A catalytically inactive GCN5B expressed under an inducible promoter revealed that parasites expressing inactive GCN5B could not replicate. In addition, several transcription factors belonging to the APiAp2 family were found to interact with GCN5B: Ap2IX-7, Ap2X-8, Ap2XI-2, and Ap2XII-4. HDAC3 activity prevents bradyzoite transition as chemical inhibition of it *in vitro* induced stage switching (6, 70). In *T. gondii* histone acetylation is associated with gene activation. Acetylation decreases the charge of histone proteins weakening their association with DNA and opening the chromatin to allow binding by transcription factors and RNA polymerase II. It is theorized that activating transcription factors recruit histone acetyltransferases, while repressive factors recruit histone deacetylases or alternatively compete with activating transcription factors for the same DNA motifs (Figure 8) (49, 88).

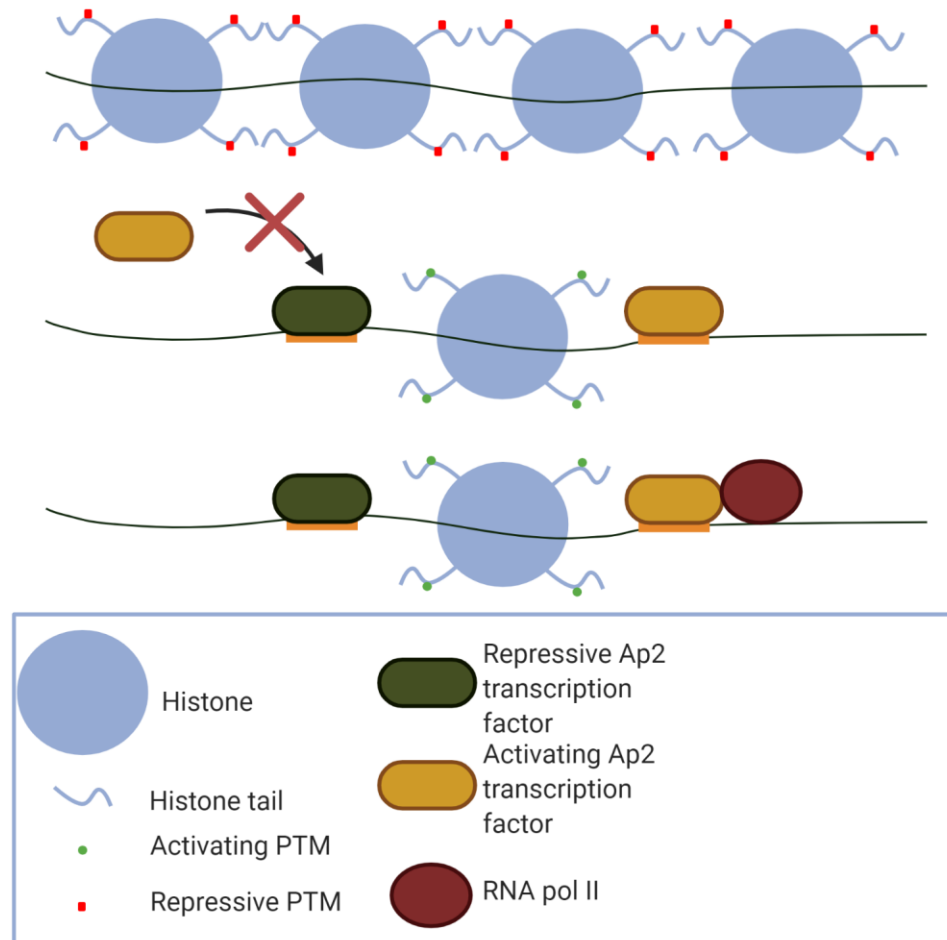


Figure 8: Histone Modifications in *T. gondii* that Regulate Stage Differentiation
 Chromatin remodeling is important for stage differentiation. Post-translational modifications on histone tails either restrict access to DNA, or open chromatin for binding of Ap2 transcription factors, Ap2 factors exist in competition with repressing Ap2s preventing the binding of activating factors, activating Ap2s recruitment of RNA polymerase II to transcribe mRNA.

The ApiAp2 (A2P2) family of transcription factors are major regulators of the cell cycle and bradyzoite transition in *T. gondii*. There are sixty-eight proteins with Ap2 DNA binding domains in the parasite's genome; twenty-four are cell cycle-related, eleven are induced in bradyzoite conditions, twenty-seven are constitutively expressed, and six are not expressed in tachyzoites (2, 3). Several Ap2 genes are induced during stress conditions that lead to bradyzoite transition and are crucial both to activate and repress bradyzoite associated genes (3, 42). Six Ap2s have been identified that contribute to the regulation of tachyzoite to bradyzoite transitions; three are described as repressors of bradyzoite genes, and three as activators of bradyzoite differentiation (Table 1).

Table 1: Ap2 Transcription Factors Known to Regulate Bradyzoite Genes

Repressors of Bradyzoite Genes	Ap2IX-9(42), Ap2IV-4(42), Ap2IX-4(52)
Activators of Bradyzoite Genes	Ap2IV-3(42), Ap21b-1(42), Ap2XI-4(39)

The relationship between Ap2 transcription factors and bradyzoite differentiation is complicated. Factors are annotated as activators or repressors based on experiments in which the gene is either knocked out or conditionally expressed. The resulting impact of their deletion, conditional expression or over-expression results in their definition as either a “repressor” or “activator” of tachyzoite differentiation to bradyzoites. However, in some cases the Ap2 transcription factor only impacts expression of a relatively small subset of genes. Thus, a label as a “repressor” or “activator” does not fully capture the relationship of each Ap2 transcription factor to stage differentiation. For example, Ap2IX-9 increases in expression during transition even though it is a repressor of bradyzoite associated genes.

As mentioned above the relationships between the various Ap2 transcription factors can be complicated as is their individual contribution to tachyzoite to bradyzoite transitions. However, while many factors may turn off bradyzoite genes, paradoxically they themselves are associated with bradyzoite transition. Two Ap2s, a repressor, Ap2IX-9, and an activator Ap2IV-3 exist in a related expression pattern under cyst inducing conditions (43, 50). Both factors bind to the promoter of the bradyzoite associated antigen 1 (BAG1), considered to be the definitive marker of bradyzoites, with opposite results on gene expression. However, Ap2IX-9 expression increases at 48 hours post stress during which time parasites are well into transitioning to bradyzoites. After this initial increase there is a subsequent decline that correlates to an increase in Ap2IV-3. All of this indicates a complicated process of tachyzoite to bradyzoite transition. It is not a binary state, but rather a multi-step process. The interaction of Ap2IX-9 prevents premature commitment to bradyzoite development and expression of bradyzoite associated genes too early in the transition process (42). Early bradyzoite development is associated with four additional Ap2 genes Ap21b-1, Ap2VI-3, Ap2VIII-4 that in addition to APXIX-9, and Ap2IV-3 are not expressed in tachyzoites. As tachyzoites differentiate more completely into bradyzoites, Ap2IV-3 is upregulated. Thus, it could compete for control of bradyzoite genes with Ap2IX-9. Eventually as bradyzoite mature Ap2XI-4 appears to replace Ap2IX-9 (42, 46, 52).

In addition to the current understanding of transition control by Ap2 transcription factors, recent work has detailed a possible master regulator of bradyzoite transition (87). While knocking out or overexpression of certain Ap2 transcription factors impacts bradyzoite transition and cyst formation, these experiments have failed to completely

inhibit these processes (47, 54). A Myb-like domain containing protein annotated as BFD1 was found in a recent study to be critical for stage differentiation. Clones deleted for BFD1 were completely incapable of forming cysts in induction conditions despite normal growth in non-stressed conditions. BFD1 was found to bind to 652 sites in the genome corresponding to 509 genes most of which were differentially regulated under stressed conditions (87). The binding sites were near the transcriptional start sites of these genes and conditional expression was sufficient to induce cyst formation absent of normal induction conditions. Ap2 transcription factors can still be crucial to this process as downstream mediators of bradyzoite transition, although further work must be done to determine their precise relationship to this new regulator.

Twenty-four different Ap2s in *T. gondii* showed expression changes during replication and may have a role in timing of gene expression over the course of the cell cycle (3). A study of parasites arrested at the G1 phase of replication showed that Ap2X-7, Ap2VIIa-6, Ap2XII-4, and Ap2VIII-4 were upregulated showing a potential role for these factors in preventing the cell from entering S phase. Another factor Ap2XI-5 is expressed throughout the cell cycle and was found to regulate virulence genes. Disruption of this transcription factor led to an increase in virulence along with a reduction in invasion (63).

Other than the presence of the Ap2 domain, Ap2 transcription factors have a low degree of similarity. Ap2 domains are about sixty amino acids in size and consist of 3 beta-strands and one C-terminal alpha helix. Between the second and third strand is a hairpin-like structure that is positively charged which enhances affinity to DNA (47, 62).

Ap2 transcription factors bind to DNA motifs found in regulatory regions upstream of gene promoters. DNA motifs have been discovered for several Ap2s in *T. gondii* (47, 54).

Immune Response to Infection

The host immune system can effectively control the acute infection. Since stress is an important determiner of cyst induction, it has been proposed that the immune response in the host is crucial to induce cysts *in vivo* (36). However, it appears that rather than specific host immune factors triggering cyst formation, the effective suppression of the acute infection by the immune system simply keeps the parasite's attempts to reinitiate acute infection in check. The reemergence of the infection in the immunocompromised is due to the lack of suppression of tachyzoites, rather than the withdrawal of an immune factor that causes the parasite to remain encysted (24). Cell mediated immunity is critical for suppression of the parasite and survival of the host both during acute and chronic infection as well as reactivation of infection. Increased susceptibility of hosts to the parasite has been observed in patients with impaired T-cell numbers and/or function and in mice that lack CD8+ and CD4+ T-cells (16, 24, 79). The maintenance of CD8+ function is crucial during the chronic infection to control parasite recrudescence. Highly virulent strains have evolved strategies to inhibit CD8+ T-cells (16, 48). CD8+ function becomes compromised during infection by RH strain parasites. Although RH parasites are capable of forming cysts the infection never progresses to the chronic stage, as the host immune system is easily overwhelmed resulting in death (79, 93). The key cytokine needed to control *T. gondii* infection is IFN- γ , as mice deficient in this cytokine succumb to infection by avirulent strains of *T. gondii*. Mice with chronic infection that are administered IFN- γ antibodies develop reactivation of toxoplasmosis.

IFN- γ stimulates the production of reactive oxygen species and nitric oxide (NO) in macrophages, microglia, and astrocytes (34, 76, 77). Nitric oxide is the effector that induces bradyzoite transition and cyst production, however it is not a necessary factor as cyst formation occurs in inducible nitric oxide synthase deficient mice, as well as in mice treated with aminoguanidine, an inhibitor of NO synthesis (9). Additionally, tumor necrosis factor alpha (TNF- α) has also been shown to play a role in the establishment of chronic infection. It may work synergistically with IFN- γ as treatment of infected macrophages with these cytokines induced cyst formation (77, 96). Interleukin 6 (IL-6) induces cyst formation in cultured human foreskin fibroblast cells, and IL-12 is important to control both acute and chronic infection as it drives production of IFN- γ (31, 54, 72, 73).

FIKK

The Apicomplexa have a unique family of putative serine/threonine kinases designated as FIKK for the conserved region of amino acids found in their kinase domains consisting of a phenylalanine (F), isoleucine (I), and two lysines (K). This family of kinases is unique and divergent from any other eukaryotic kinase family. While almost universal in the Apicomplexa, with the exception of piroplasms, the number of FIKK kinases differ between species with *Plasmodium falciparum* having 21 while both *Cryptosporidium parvum* and *Toxoplasma gondii* having only one each. Most *P. falciparum* FIKK kinases contain a PEXEL motif which designates the proteins for export, these proteins have known targets in the cytoskeleton of erythrocytes. The closest homologues of TgFIKK are the *C. parvum* FIKK (CpFIKK), and FIKK 8 in *Plasmodium falciparum* (PfFIKK8). A potential target of these two FIKK kinases

consists of a short peptide sequence (RAPSFYR). This sequence is essentially a serine residue flanked by two hydrophobic amino acids terminated with arginines in the +3 and -3 positions. The study showed that modifying the terminal arginines substantially reduced enzymatic activity (58).

The architecture of FIKK kinases include a highly variable N-terminal region with a conserved C-terminus where the kinase domain with the eponymous amino acid sequence is found (18, 19, 89). Most of the catalytically important residues of eukaryotic protein kinases are conserved in FIKK proteins, except for the glycine triad.

Bioinformatic analysis of the *T. gondii* genome confirmed the presence of a single FIKK kinase (TGME49_289050) in the parasite genome on chromosome IX (72). cDNA sequencing and subsequent RNA sequencing data indicate that it is comprised of nine exons interrupted by introns. Two isoforms were detected based on cDNA sequencing in both Type I and Type II parasites. *TgFIKK* isoform I predominates in tachyzoites and encodes an approximately 280 kDa protein encoded by 2762 amino acids. *TgFIKK* isoform 2 is created by differential splicing that results in an in frame stop codon that truncates the protein resulting in an incomplete catalytic domain. The FIKK kinase transcript appears to be expressed in all strains of *T. gondii* examined to date. The localization of the predominant *TgFIKK* Isoform 1 full length FIKK kinase in *T. gondii* was investigated in our lab previously by creating a RH parasite with an endogenous tagged FIKK kinase that expressed the fluorescent YFP protein on its 3' end (72). The FIKK-YFP endogenous tag was used to visualize the FIKK-YFP protein by immunofluorescence during the parasite's lytic cycle *in vitro* in tissue culture. HFF cells infected with FIKK-YFP containing parasites were examined by immunofluorescence

using a Zeiss inverted Axiovert 200 System. We were unable to visualize the FIKK-YFP protein using the endogenous fluorescence of the YFP protein as the protein was not sufficiently abundant. Thus we used a mouse monoclonal antibody cocktail to GFP followed by a secondary Alexa 488-conjugated goat anti-mouse antibody to amplify the FIKK-YFP signal (Figure 9).

These studies showed that the protein localized to the basal end of the parasite. In independent studies MJ Gubbles at Boston College created a TY-tagged FIKK protein. His group showed that FIKK-Ty co-localized with membrane occupation and recognition nexus protein (MORN-1) a component of the parasite organelle called the basal complex. He showed that the FIKK-Ty protein colocalizes with MORN1 inside the basal complex. Furthermore, that FIKK-Ty sits apical to inner membrane complex 5 (IMC5) and apical to the posterior cup marker Centrin 2. Thus, the FIKK kinase is toward the apical end of the basal complex rather in the basal end that would be closer to a putative gap in the parasite membrane cytoskeleton that has been hypothesized to function as a posterior pore in the parasite. While FIKK colocalization with MORN1 occurred in the mother cells, the FIKK kinase was restricted to the mature parasites and was not found in developing daughter cells (Figure 9). The FIKK kinase is the only parasite protein published to date that is found in association only with the mother's basal complex and not the daughters'. Proteomic analysis of the parasite basal complex using MORN1 revealed that MORN1 and FIKK are associated with one another and not just proximal to one another in the basal complex (40). The FIKK kinase localization with the basal complex suggested that the protein may be important for parasite replication via endodyogeny (Figure 4). However the work in our lab indicated that deletion of the FIKK

gene from the genome of RH parasites had no effect on parasite replication *in vitro* in HFF cells (72).

These previous studies in our laboratory only indicate that the FIKK kinase is not essential for the parasite lytic cycle *in vitro* in RH strain parasites. While this is an important finding, the function of the *TgFIKK* kinase remains unknown as does its potential contribution to pathogenesis. Furthermore, the Type I strain RH is not representative of the infections typically found in humans nor is it able to complete the parasite life cycle in terms of its sexual cycle in feline hosts or its cyst cycle in secondary hosts including humans. Kinases have clearly been implicated in tachyzoite to bradyzoite differentiation and cyst formation (77). Thus, in the current study we evaluated the contribution of the FIKK kinase in stage differentiation and cyst formation. To more readily address the role of the FIKK kinase in stage differentiation and cyst formation, we deleted the entire FIKK kinase gene in the Type II Prugnaud strain of the parasite. We also complemented the FIKK gene deletion in trans using the FIKK kinase using its endogenous promoter and full-length genomic region of *TgFIKK* Isoform1. We show that the FIKK kinase contributes to acute infection by the Type II Prugnaud strain in mice even though it does not significantly contribute to the parasite lytic cycle *in vitro*. Furthermore, we show that the FIKK kinase is important for the parasite's ability to form cysts *in vitro* or chronic infection *in vivo*. Although its mechanism of action remains unknown, our data suggest that the FIKK kinase plays a critical role in the ability of the parasite to enter the bradyzoite differentiation pathway in order for the parasite to differentiate to bradyzoites and to form tissue cysts to establish chronic infection.

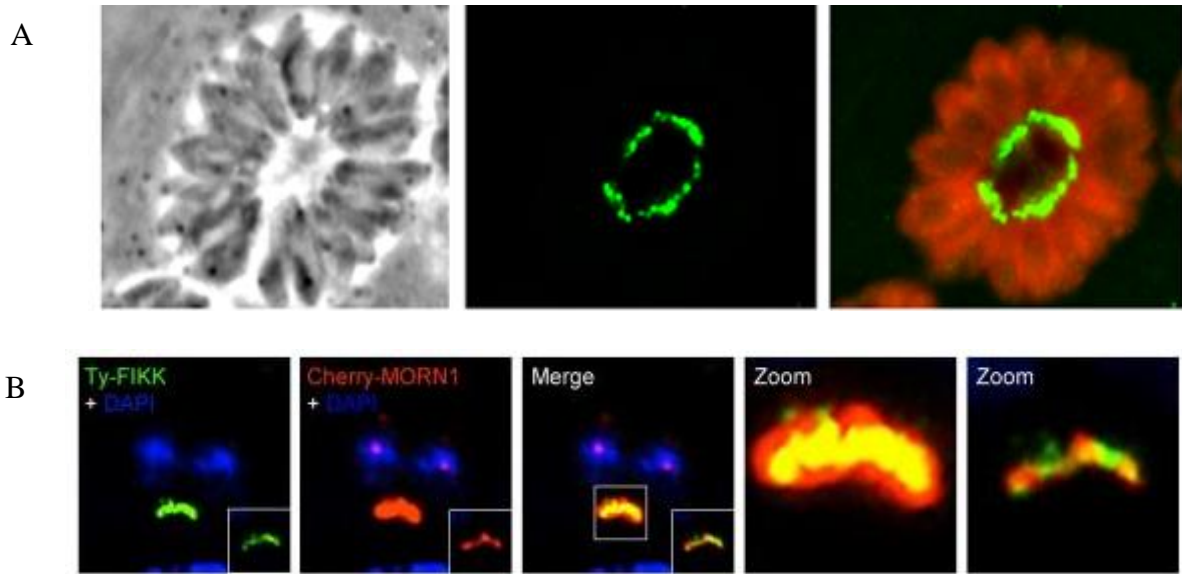


Figure 9: Localization of Tagged FIKK Proteins

Part A: Human foreskin fibroblast cells were infected with parasites over the course of 36 hours. Images were taken at 100x. The localization of FIKK YFP in immunofluorescence with the signal enhanced by an anti-GFP antibody with the parasite labeled with an anti-toxoplasma antibody (red) Images were taken on Zeiss inverted Axiovert 200 System
 Part B. Colocalization of the Ty-FIKK and Cherry-MORN1 (72).

Specific Aims

- I. Initial Characterization of the *T. gondii* FIKK Kinase Gene Deletion
 - I. Localization in Live Cell imaging
 - II. RNA sequencing- Does the deletion affect the expression of other genes
 - III. Proteomics
 - IV. Phosphoproteomics
- II. Functional Characterization of the FIKK Kinase for Acute Infection
 - I. Lytic Cycle- invasion, replication, and plaque assay
 - II. Mouse model of toxoplasmosis
- III. Functional Characterization of the FIKK Kinase in Chronic Infection
 - I. In vitro- HFF cells
 - II. Identify the step in cyst formation where the FIKK is acting
 - III. Chronic infection *in vivo*

Materials and Methods

HFF Cell Culture

Human foreskin fibroblast cells were obtained from the American Type Culture Collection (ATCC, SCRC1041). HFF cells were passaged in tissue culture flasks (T25, T75, and T150s.) Cells were grown in T150s and allowed to come to confluency. Cells were passed into new flasks at least every four weeks. Confluent T150 flasks of HFF cells were split by a two-minute incubation with trypsin (Gibco) at 37°C until cells lifted off of the bottom of the flask. Trypsin was inhibited by adding 5mL of D10 [DMEM (Gibco) high glucose supplemented with 10% FBS (Gibco) and L-glutamine, to inhibit the trypsin enzyme. The cells were centrifuged at 270 x g for 5 minutes to pellet the cells. For seeding T150s, the cell pellet was resuspended in D10 and the cell suspension divided between six new T150 flasks. For seeding T25 flasks the cell pellet was resuspended in 50mL of D10 and the cell suspension divided between ten T25 flasks. All flasks of HFF cells were kept in a 37°C incubator with ambient air plus 5% CO₂.

Parasite Culture/Clones

Parasites were grown in T25 flasks with a confluent monolayer of HFF cells by transfer of 1mL of parasites from a lysed out T25 cell culture into a new T25 flask with confluent HFF cells every two days. Four *T. gondii* parental strains/clones were used for genetic manipulations. The Type I genotype strain RH with both Ku80 and HPT deleted (RHΔKu80ΔHPT) was used to create the YFP-tagged FIKK for the FIKK localization studies. The *T. gondii* Type II genotype Prugnaud (Pru) with either both Ku80 and HPT deleted (ME49 lineage; PruΔKu80ΔHPT) or only HPT deleted (PruΔHPT) were used to create gene deletions for the FIKK gene. Additionally, a second line of PruΔHPT was

clonally purified (Pru Δ HPT WT2) (Figure 10). The Pru Δ Ku80 Δ FIKK clone was used to create the FIKK complement clones (Table 2).

Table 2: Parasite Strains and Genetically Modified Parasite Clones Used in the Thesis

Background Strain	Parental Strain	Created Clones
RHΔKu80ΔHPT	RH (Type 1 genotype). Acute infection and tachyzoites <i>in vitro</i>	RH-FIKK-YFP
PruΔKu80ΔHPT	Pru Δ Ku80 (Type 2 genotype). Acute and chronic infection and <i>in vitro</i> studies including cyst formation	Pru Δ Ku80 Δ FIKK Pru Δ Ku80 Δ FIKK+FIKK1 Pru Δ Ku80 Δ FIKK+FIKK2 Pru Δ Ku80 Δ FIKK+FIKK3
PruΔHPT	Pru Δ HPT WT1 Pru Δ HPT WT2	Pru Δ HPT Δ FIKK 1, 2 Pru Δ HPT Δ FIKK 3, 4

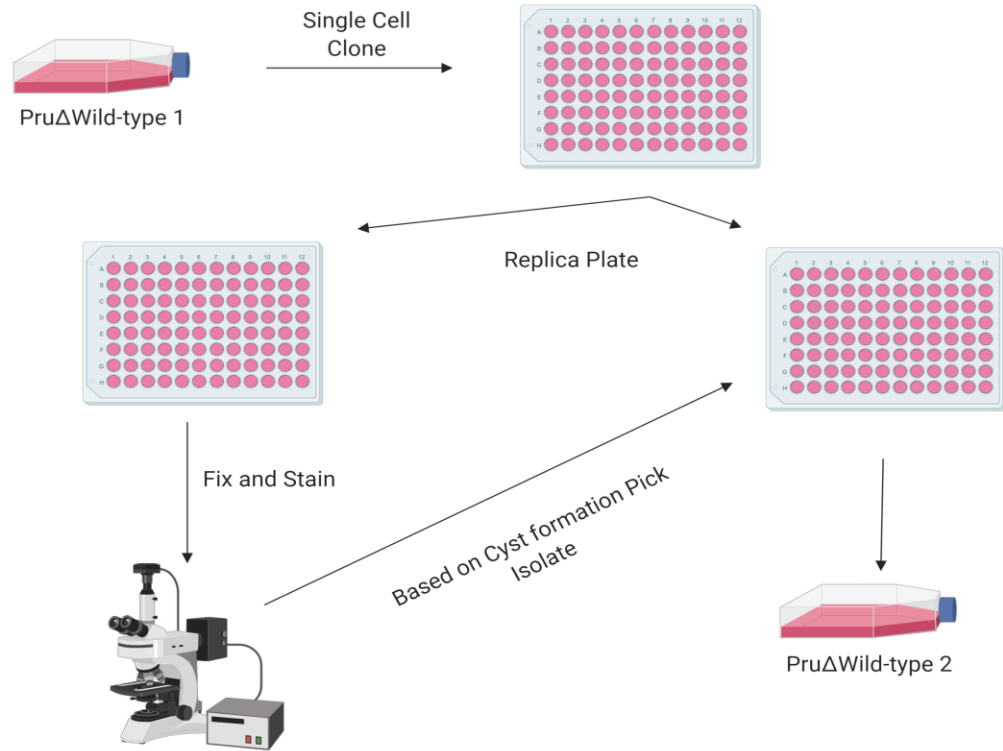


Figure 10: Creation of the Clonal PruΔHPT Wild Type (WT) 2 Clone

PruΔHPT WT2 was created by cloning WT1 by single cell cloning in 96 well plates with confluent HFF cells. The first plate was replica plated and parasites were stressed using sodium nitroprusside to induce cyst formation. Parasites were stained using FITC-conjugated DBA and cystogenic isolates were identified. A number of these clones were selected from the replicate plate in culture. One was randomly chosen and labeled PruΔHPT WT2 and used to create a PruΔHPTΔFIKK clone.

Parasite Genetic Manipulation

Electroporation Protocol

Plasmids were grown in bacterial culture by transfecting Oneshot Top10 chemically competent *Escherichia coli* (*E. coli*) (Thermo Fischer) and grown in Lysogeny broth (LB) supplemented with 100 micrograms per milliliter of carbenicillin to select for the plasmids. The plasmids were purified using the Qiagen Plasmid Midi Kit and prepared for electroporation by mixing with Cytomix (120 mM KCl, 0.15 mM CaCl₂, 10 mM K₂HPO₄/KH₂PO₄ pH 7.6, 25 mM HEPES pH 7.6, 2 mM EGTA, 5 mM MgCl₂). Parasites from two lysed T25s were centrifuged at 1200 RPM for 10 minutes and washed twice with cytomix. Plasmids were suspended in 400 microliters of cytomix and mixed with parasites. The mixture was placed into a 2mm cuvette and pulsed at 1.5Kv, resistance 25Ω, capacitor setting of 25Uf using B7 X ECM 630. After electrotransformation, the parasites were placed under selection in HFF cells.

Creation of the FIKK-YFP Clone

The *T. gondii* FIKK in the RHΔKu80 strain was endogenously tagged at the 3' end with a yellow fluorescent protein tag. A FIKK-YFP fusion transcript was created by amplifying a 1.5KB fragment of FIKK without the stop codon and inserted into a PacI digested VC-YFP plasmid (Figure 11) using ligation independent cloning to fuse the FIKK fragment in frame with YFP. The resulting FIKK-YFP plasmid construct was linearized with BsiWI and electroporated into wild-type RHΔKu80 parasites and selected using 50ug/mL of mycophenolic acid with 25ug/mL of xanthine in D10 medium. After selection parasites were single cell cloned in HFF cells using 96 well plates to isolate

single parasite isolates. Positively tagged isolates were identified by amplifying a region of the genome containing the FIKK-YFP fusion by PCR.

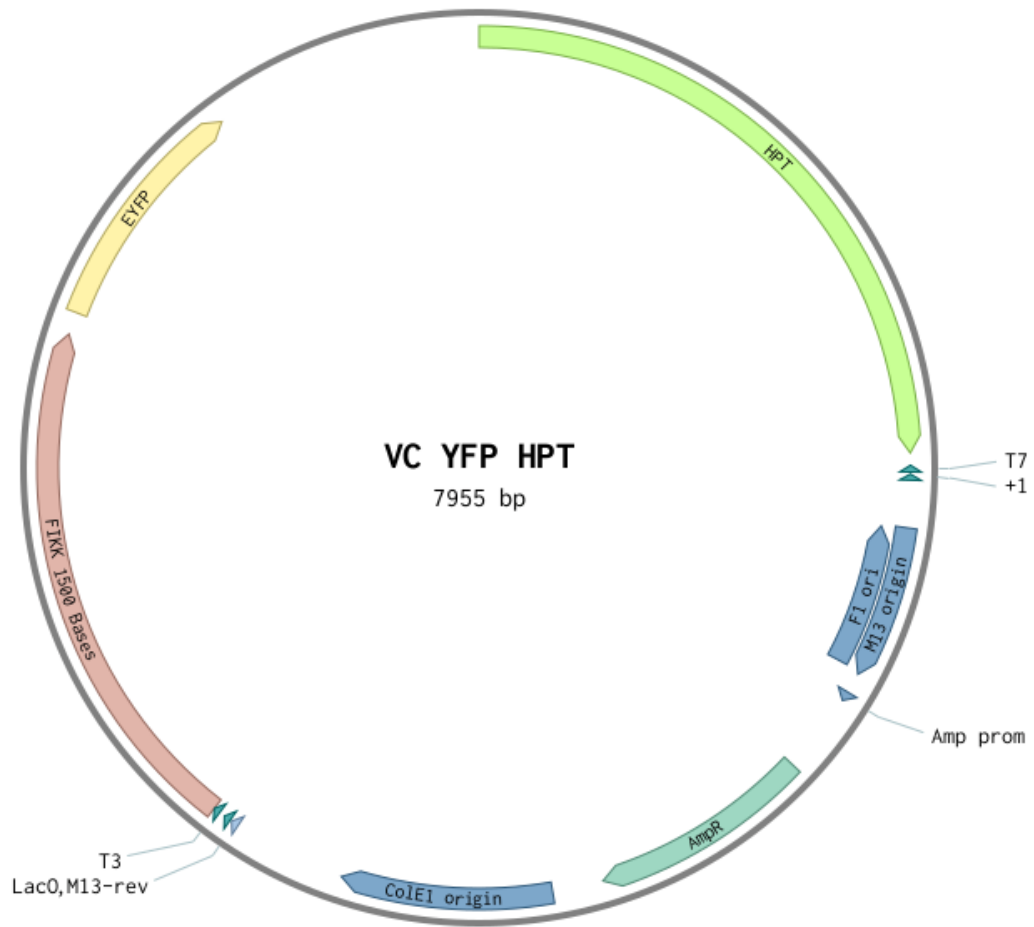


Figure 11: VC YFP Plasmid Including the Cloned FIKK Sequence

The YFP-FIKK plasmid used for endogenous tagging of the 3' end of the FIKK gene with yellow fluorescent protein (YFP). VC YFP plasmid with the final 1500 base pairs homologous to the 3' end of the FIKK gene (and the stop codon removed) cloned immediately upstream of the YFP tag.

Creation of FIKK Gene Deleted Parasite Clones

Wild-type Pru Δ HPT and Pru Δ Ku80 strains were used to create FIKK gene deletion clones. The FIKK gene deletion targeting construct (Figure 12) was created by PCR amplification of 2176 bps of the *T. gondii* genome sequence 313 bps upstream of the FIKK predicted start site using Phusion High-Fidelity PCR Master Mix with HF. The amplified product was validated and cloned upstream of the HPT gene in the *T. gondii* plasmid HPT mini. A 2142 bp *T. gondii* genomic sequence 126 bp downstream of the FIKK gene 3' poly A sequence was PCR amplified, validated, and cloned into the FIKK targeting plasmid downstream of the HPT gene. The completed FIKK targeting plasmid was named "pmini stko2". The targeting plasmid was linearized using the NotI restriction enzyme and 60ug of plasmid was electroporated into wild-type strains. Selection was performed for 5-7 days using 50ug/mL of mycophenolic acid with 25ug/mL of xanthine in D10 in confluent HFF cells in T150 flasks. After selection a population PCR was performed for the presence of the HPT gene, if positive the population was single cell cloned in 96 well plates to isolate single parasites based on plaque formation. After isolation parasites were cloned into 24 well plates and DNA was purified using the Qiagen DNeasy Blood and Tissue Kit as per the kit instructions. Junctional PCR was used to identify parasite clones that had inserted the HPT gene in place of the FIKK genetic locus. Junctional PCR used two sets of primers. One primer set was designed to amplify the junctional region 5' upstream of the FIKK gene targeting plasmid and the 5' end of the HPT gene. The other primer set was designed to amplify the junctional region in the 3' end of the HPT gene and the 3' end of the *T. gondii* genome downstream of the FIKK gene targeting plasmid (Table 3). The amplified ~3KB regions thus included a

section of the HPT gene, the region of the genome used to insure efficient recombination and an area of the genome immediately outside of this area. This ensures that the HPT gene inserted into and replaced the entire FIKK gene (Figure 13). Gene deletion of the FIKK gene was confirmed by isolation of RNA using the RNAeasy plus kit (Qiagen), removal of residual DNA using the Turbo DNase kit (ThermoFisher), and synthesis of cDNA using the SuperScript First-Strand Synthesis System (Invitrogen) (Figure 14, Table 5).

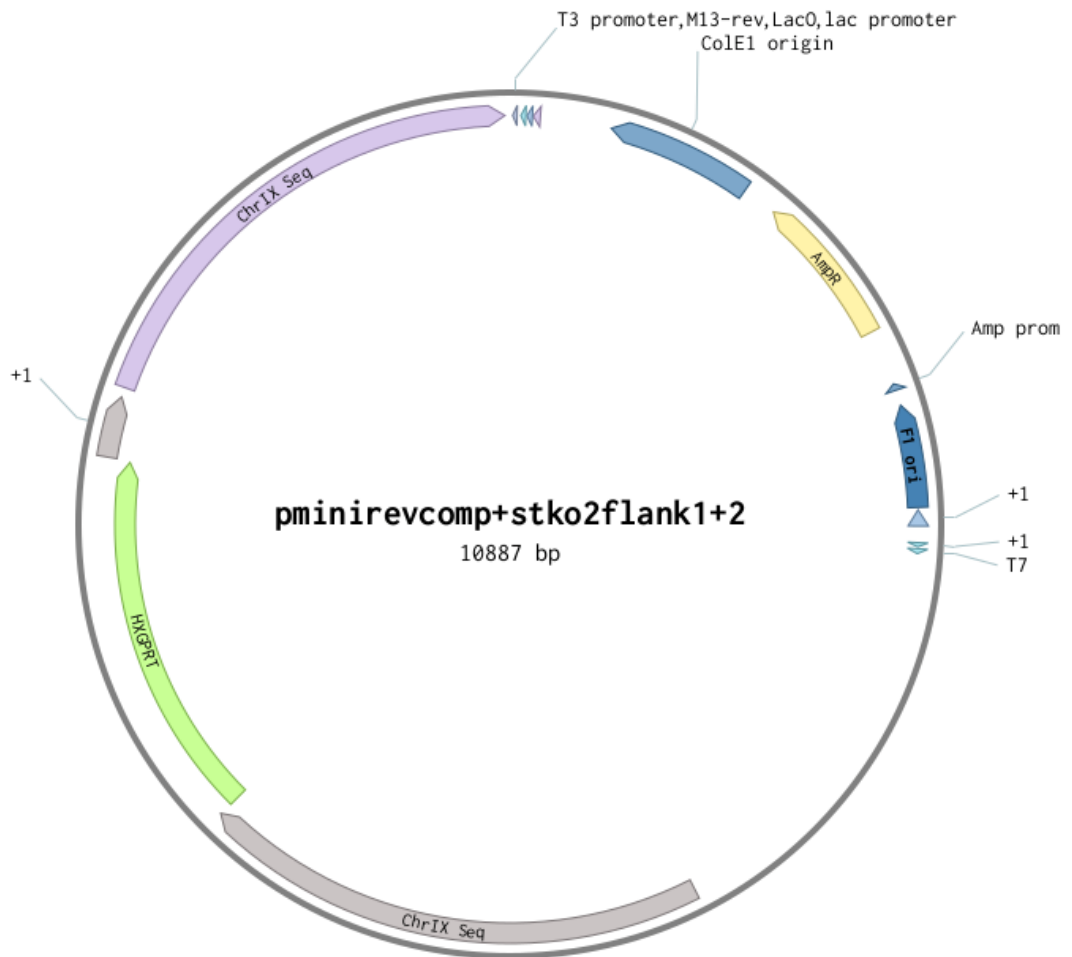


Figure 12: Δ FIKK Plasmid

A schematic of the Pmini stko2 plasmid used to delete the entire FIKK gene. The plasmid includes the HPT gene flanked 5' with approximately 2KB upstream of the 5' FIKK gene locus, and 3' with approximately 2 KB downstream of the FIKK gene locus. The plasmid is designed to promote homologous recombination in the FIKK gene locus and replace entire endogenous FIKK gene with HPT.

Table 3: Primers Used to Confirm FIKK Knockout

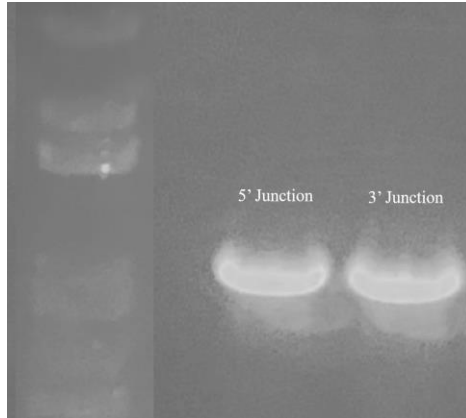
FIKK external forward in sequence	tgatgctaggctcctcttagt
HPT in sequence forward	GGCGTATGACATCCACAGAA
HPT Rev Primer in sequence	GAGCCTTTCAGGATGCAAATG
FIKK external rev in sequence	cggagacacctcaagtataatg

Primers Used in Junctional PCR to confirm FIKK deletion.

Creation of Additional FIKK Gene Deletions From a Newly Cloned Pru Parental Line.

Initial attempts to complement the Pru Δ HPT Δ FIKK were unsuccessful. In lieu of complementation a second set of FIKK deletion clones was created as an alternative method of confirming any potential phenotype associated with deletion of the FIKK gene. There was concern that genetic drift over time may have introduced variation in the population of Pru Δ HPT parasites used in the lab. To eliminate any potential complications due to genetic drift a clonal line of Pru Δ HPT was created. This line was then used to make a second set of Δ FIKK clones. First, the parental parasites were single cell cloned into 96 well plates containing confluent monolayers of HFF cells. After 7 days the plates were checked to identify wells that contained only a single plaque indicating the presence of a single parasite clone within the well. Single clones of the parasite were used to create two replicate 96-well plates containing confluent HFF cells. After three days of culture of one plate in the presence of sodium nitroprusside (SNP) wells were fixed with 4% paraformaldehyde, permeabilized and stained with FITC-conjugated *Dolichos biflorus* (DBA) lectin. Each well of the 96 well plates were screened for cyst formation (DBA positive vacuoles) by fluorescent microscopy with a 20X objective. Most parasite clones appeared similar in terms of their ability to form cysts in the presence of SNP. A robust cyst forming parasite clone was used to create the second set of FIKK gene deletion parasites.

Pru Δ Ku80 Δ FIKK



Pru Δ HPT Δ FIKK

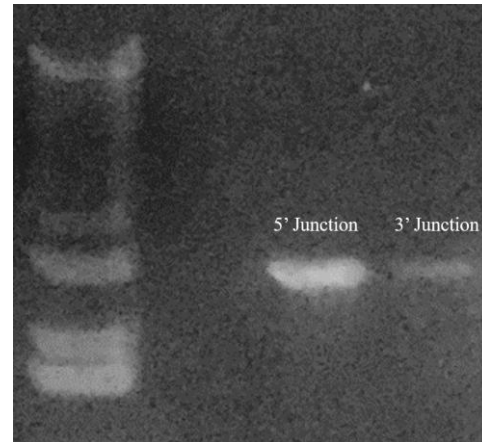


Figure 13: Junctional PCR of Δ FIKK Clones

The deletion of the FIKK kinase was confirmed using junctional PCR with positive junctional PCR bands indicating the replacement of the FIKK gene with HPT.

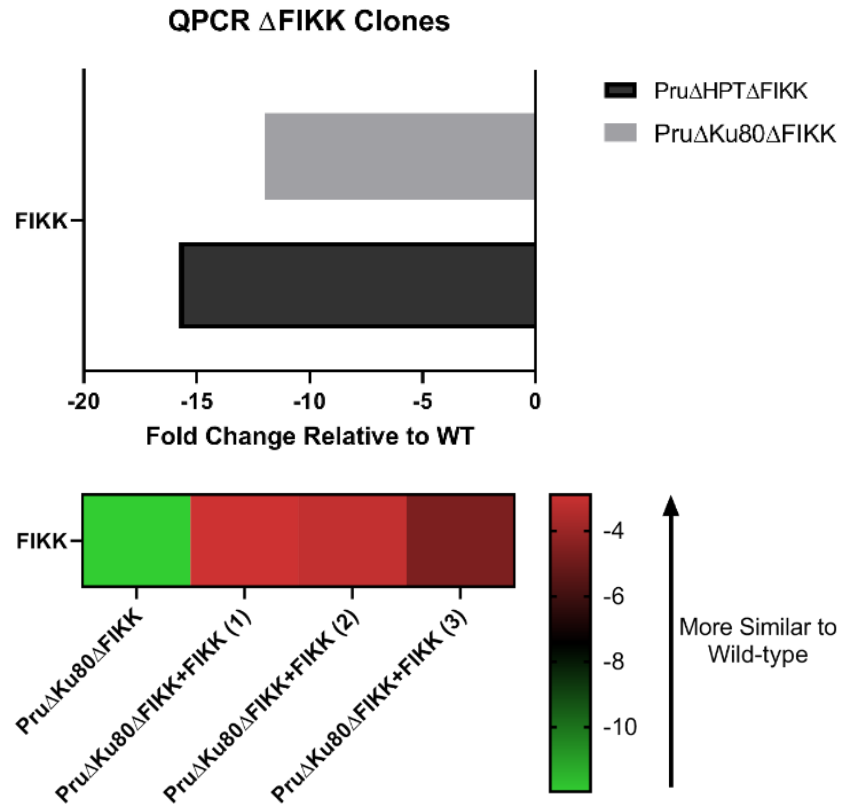


Figure 14: QPCR of Δ FIKK Clones and Complements
 Quantitative real time reverse transcriptase PCR was performed on the wild-type (Pru Δ HPT, Pru Δ Ku80) and Δ FIKK clones to confirm deletion of the FIKK gene. After complementation it was used to confirm the expression of the FIKK gene in the complemented clones.

Creation of Pru Δ Ku80 FIKK Complemented Clones

Deletion of the FIKK kinase was performed in the original Pru Δ HPT line, the single cell clone Pru Δ HPT line, and in a Pru Δ Ku80 line. Attempts at complementation in the Pru Δ HPT Δ FIKK clones were unsuccessful. This was not surprising due to the presence of the robust non-homologous end joining repair system in *T. gondii*. Also, HPT is one of only a few efficient selectable markers for gene deletion in *T. gondii* and its use for complementation was precluded as it had been used for the creation of the FIKK gene deleted clone. Also the plasmid used for complementation included both the entire FIKK gene, plus 2 kb homologous regions on either side of the gene resulting in a large plasmid (24163 bp) that may have further complicated attempts to complementation (Figure 15). To overcome the NHEJ repair system the Pru Δ Ku80 Δ FIKK clone was used as the parental line was missing the ku80 gene which renders the NHEJ repair pathway non-functional. Additionally, to overcome the lower transformation efficiency of large plasmids the complementation construct was not digested as supercoiled plasmids have a higher efficiency in terms of uptake. Complementation was done in trans in the UPRT locus with positive selection using 5-floxuridine. Current trans complementation protocols for *T. gondii* recommend using 5 μ m 5-FUDR for positive selection, the lower dose recommended to counterbalance any toxic effect on the host cells needed to grow the parasites. However, repeated attempts at genetic complementation were unsuccessful using standard protocols even in the Pru Δ Ku80 Δ FIKK clone. 5-FUDR targets actively replicating cells by incorporating into growing DNA strands during the S phase of the cell cycle, hence its application as a chemotherapy drug and immunosuppressant agent. HFF cells are a primary cell line and exhibit contact inhibition and thus when they are

confluent become quiescent. It was theorized that a higher concentration of 5-FUDR could be used to select for transformants to help compensate for a potentially low rate of recombination. To determine the highest concentration of 5-FUDR that can be tolerated by the HFF cells a 24 well plate was seeded with cells and allowed to become confluent. The medium in the wells was aspirated and replaced with D10 containing varying concentrations of 5-FUDR ranging from 5 μ m to 100 μ m by 5 μ m steps and incubated for one week and checked every day for signs of cell death (rounding, lifting off, and the accumulation of dead cell debris in the culture). After one week no well showed any signs of cell pathology. Based on these results 100 μ m 5-FUDR was used for selection.

The uncut complementation plasmid (Figure 15) was used for electroporation. After electroporation the parasites were inoculated into a single T150 containing confluent HFF cells and left to invade for 24 hours at 37°C then DMEM containing 100 μ m of FUDR was added and selection was performed for 5-7 days. After selection parasites were subcloned into five 6-well plates and grown under further selection until lysis of the HFF cell monolayer. Parasite populations were transferred to new wells containing HFF cells, and remaining parasites not used for passage were used to isolate DNA for PCR to detect the presence of the FIKK gene in each parasite population. Parasites from positive wells were single cell cloned into 96 well plates and grown for 5 days. Parasites from wells with single plaques were subcloned into 24 well plates and grown until lysis of the HFF monolayer. After lysis, single parasite clones were evaluated by junctional PCR to identify the presence of the FIKK gene within the UPRT locus. Three parasite clones out three 24 well plates were isolated that were positive by PCR for

the FIKK gene and the junctional 5' and 3' PCRs. These isolates were confirmed by quantitative reverse transcriptase PCR using primers to the FIKK mRNA (Figure 14).

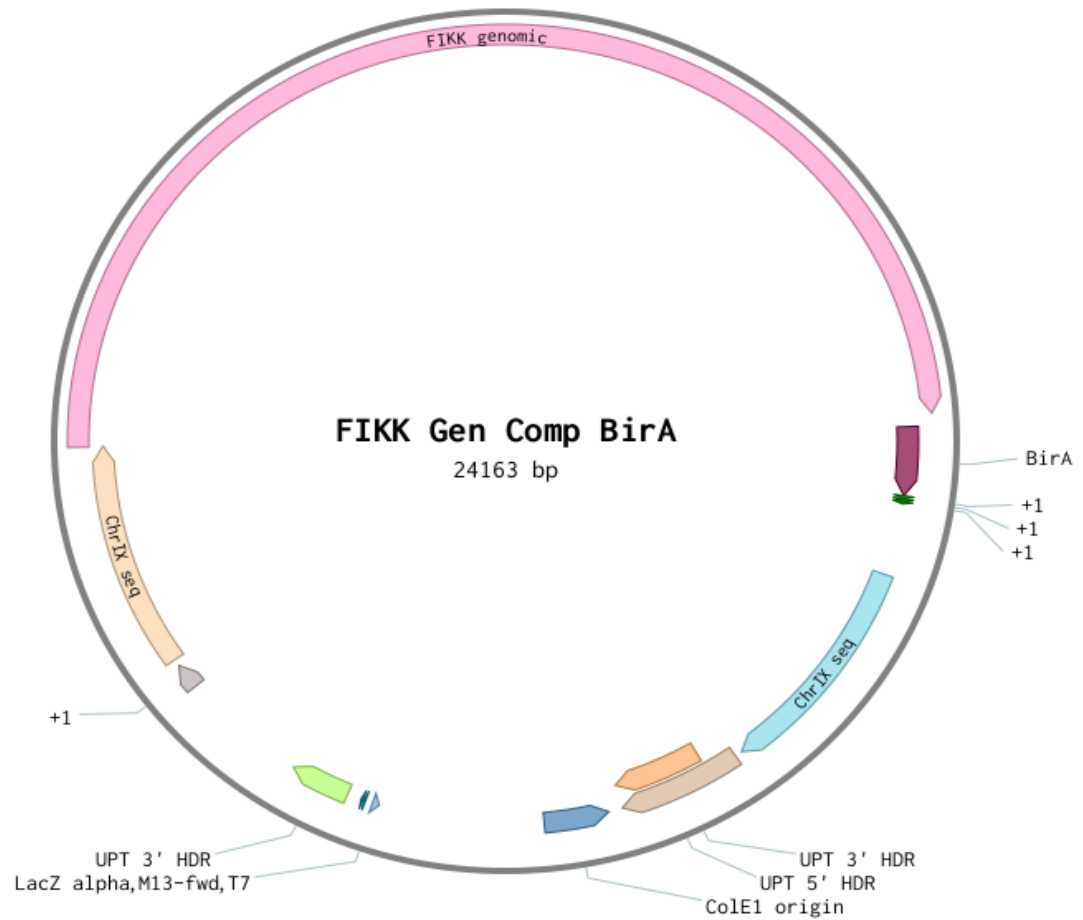


Figure 15: FIKK Complement Plasmid with BirA Tag

The plasmid used for complementation of the Δ FIKK clones with the full length genomic FIKK gene and its endogenous promoter and 3' untranslated region (UTR). The FIKK complement contains a BirA tag for proximal biotinylation labeling and a HA tag. Flanking regions 5' and 3' of the FIKK gene locus contain approximately 2 KB regions homologous to the *T. gondii* UPT locus to target the transgene to the UPT locus to enable selection by 5-floxuridine (FUDR).

Live Cell Imaging

Live cell imaging of the RH Δ Ku80 with FIKK-YFP was performed on a Nikon TiE inverted fluorescent microscope. For live cell imaging of parasites, HFF cells were grown to confluence overnight in D10 phenol red-free media on Eppendorf cell imaging chambers with a glass coverslip bottom. The chambers were placed in a 37°C chamber with 5% CO₂ that was mounted on the stage of the Nikon Eclipse TiE system. The confluent HFF cells were challenged with RH FIKK-YFP parasites. A Nikon CFI Plan Apo100x objective (1.45/0.13mm oil) was used for live-cell imaging. Images of multiple parasites/chambers were taken every twenty minutes over a thirty-six-hour timespan.

Bradyzoite-Inducing Conditions and Cyst Formation *In vitro*

HFF cells were grown to confluency in either 8 well chamber slides, or 24 well plates (Eppendorf). 50,000 parasites were inoculated, and different stress conditions were used to induce cyst formation (Figure 16).

1. Nitric Oxide Stress: Sodium nitroprusside was dissolved to a concentration of 115uM in D10 DMEM. The SNP supplemented medium was replaced every day.
2. Arginine Starvation Stress: Stable isotope labeling with amino acids in cell culture (SILAC) medium without arginine and lysine was supplemented with lysine HCl to 0.146g/l to make Arg⁻ medium supplemented with 1% FBS. The D10 used to grow the HFF cells was replaced with Arg⁻ medium for 24 hours before parasite infection.
3. Drug Treatment Stress: Parasites were incubated in D10 supplemented with 50ug/mL of mycophenolic acid extracellularly without CO₂ for four hours before infection in cells in D10 medium with 10% FBS.

4. Alkaline Stress: D10 supplemented with 10uM of HEPES was adjusted to a pH of 8 with sodium hydroxide. The parasites were incubated for 3 days in alkaline medium.
5. Non-stress: Parasites were used to infect HFF cells and cultured in normal D10.

Immunofluorescence Staining Procedure

Plates with HFF cells infected with parasites were fixed for 20 minutes in 4% paraformaldehyde in PBS then rinsed with PBS to remove residual fixative. Cells were permeabilized using 0.2% Triton X-100 in PBS for 5 minutes at room temperature and rinsed with PBS. Plates were then blocked in 10% FBS in PBS for 30 minutes at room temperature. Primary antibodies were used at a dilution range of 1:1000 to 1:500 in blocking solution and plates were stained for 1 hour at room temperature or at 4°C overnight. Plates were rinsed with 0.05% Tween 20 in PBS three times and then with PBS once. Fluorochrome-conjugated secondary antibodies were used at a dilution of 1:200 to 1:100 in PBS and left on plates for 1 hour at room temperature. Plates were rinsed three times with 0.05% Tween 20 in PBS and once with PBS. Then plates were stained with 4',6-Diamidino-2-Phenylindole, Dihydrochloride (DAPI) (ThermoFischer) diluted to 300nM in PBS for 5 minutes at room temperature to stain the parasite and host cell nuclei. Plates were washed once with PBS and then 500ul of PBS was left on plates to prevent cells from drying. Plates were examined immediately or kept at 4°C for up to a week before examination on the microscope. Determination of cyst formation was done using the Nikon Tie series inverted fluorescent microscope by counting cysts at 40X magnification.

Table 4: Clones Used for *in vitro* and *in vivo* Studies of Acute and Chronic Infection

PruΔKu80ΔHPT	PruΔKu80 (Type 2: acute and chronic infection)	PruΔKu80ΔFIKK PruΔKu80ΔFIKK+FIKK1 PruΔKu80ΔFIKK+FIKK2 PruΔKu80ΔFIKK+FIKK3
PruΔHPT	PruΔHPT WT1 PruΔHPT WT2	PruΔHPTΔFIKK 1, 2 PruΔHPTΔFIKK 3, 4

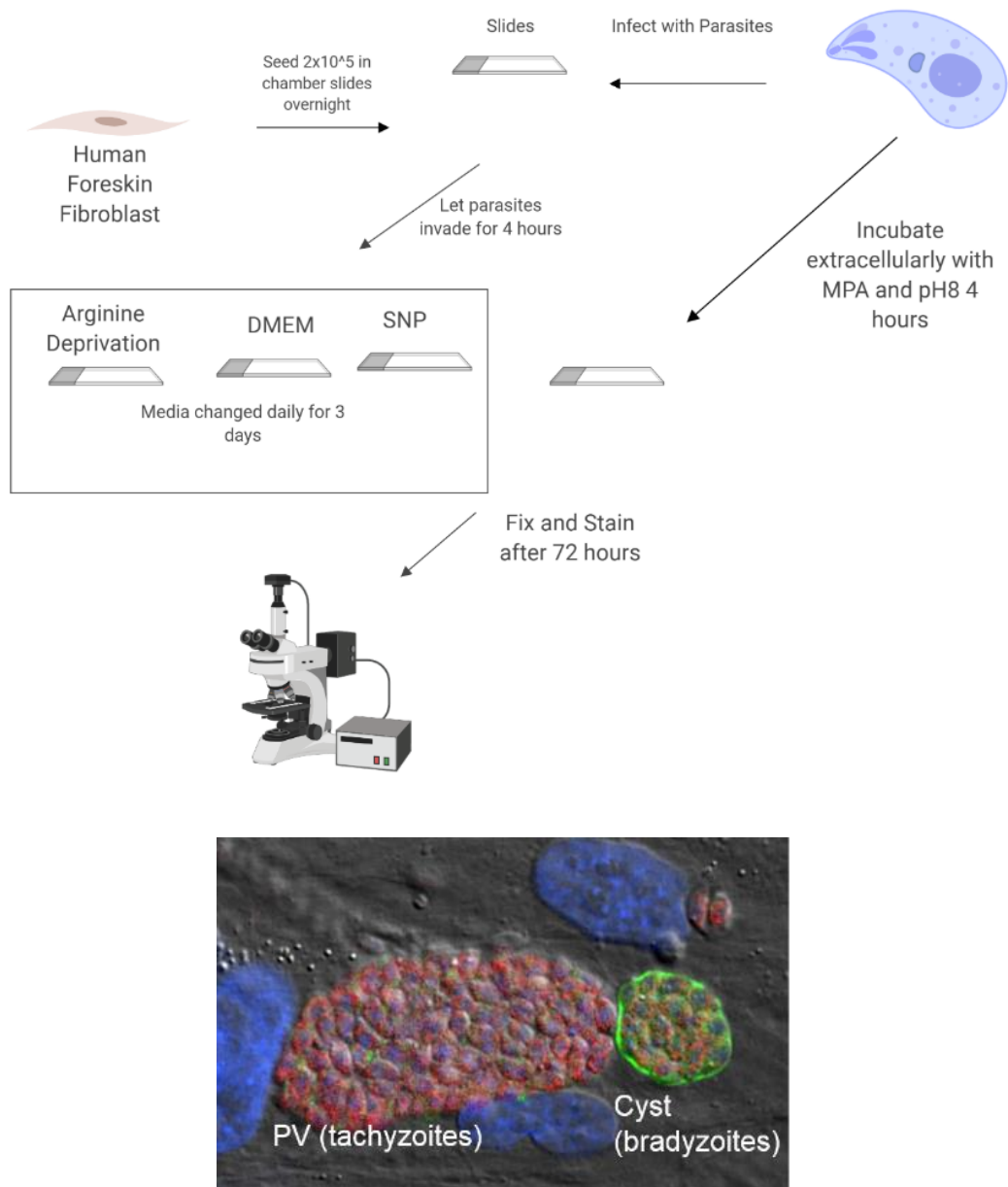


Figure 16: Cyst Induction Conditions

Top panel: A schematic showing the different exogenous inducers of bradyzoite-differentiation that were analyzed to compare cyst production by wild type, Δ FIKK clones, and FIKK complement clones. Bottom panel: The picture shows a fluorescent image superimposed with differential interference contrast (DIC) of parasite vacuoles within an HFF monolayer. Parasites were stained with a polyclonal mouse anti-*T. gondii* antibody followed by an Alexa 594 goat anti-mouse secondary antibody (red) and FITC-conjugated *Dolichos biflorus* Agglutinin (DBA) (green). The number of cysts compared to the number of total PVs was determined to quantify percent cysts/PV. The picture was taken with a Nikon Eclipse Tie Florescent microscope using a 100X oil objective.

After infection parasites were grown for three days at 37°C after which they were fixed in 4% paraformaldehyde for 20 minutes at room temperature. They were then permeabilized for 5 minutes in 0.2% TritonX-100 at room temperature and blocked with 10% FBS for 30 minutes. A polyclonal anti-*Toxoplasma* antibody from mouse serum was used to label the parasites with secondary staining using a goat-anti mouse antibody conjugated to Alexa-594 (Jackson). Cysts were stained using a FITC-conjugated DBA lectin. Four counts of 100 parasitophorous vacuoles were evaluated in the red channel, with cyst counts evaluated in the green channel. The number of cysts as a percentage of total PVs was calculated. A student's T-test was used to compare the numbers between clones.

Cyst Formation *in vivo*

To measure *in vivo* infection, cyst burdens were calculated in the chronic infection in two strains of mice CD-1 and BALB/c. For CD-1 mice infection two experiments were performed using the two sets of PruΔHPT wild-type parasites and their respective FIKK gene deletions. In BALB/C mice the PruΔKu80, ΔFIKK, and FIKK complements were used for infection. Mice were infected intraperitoneally with parasites. After 30 days post-infection the mice were anesthetized using isoflurane and euthanized by cervical dislocation. Brains were then removed and mixed with 1mL of PBS. The brains were homogenized with a mortar and pestle to make a brain suspension (Figure 17). The suspension was fixed for 30 minutes in 2.5% paraformaldehyde in PBS. After fixation 100uL of the brain homogenates were stained using a 1:200 dilution of FITC-conjugated DBA to stain cysts. A wet mount on slides was created for three independent 5uL smears of the brain and cysts were counted in each wet mount. Total cyst burden in a

brain was calculated by multiplying by the dilution factor (10 due to the 100uL volume taken from the 1mL brain homogenate).

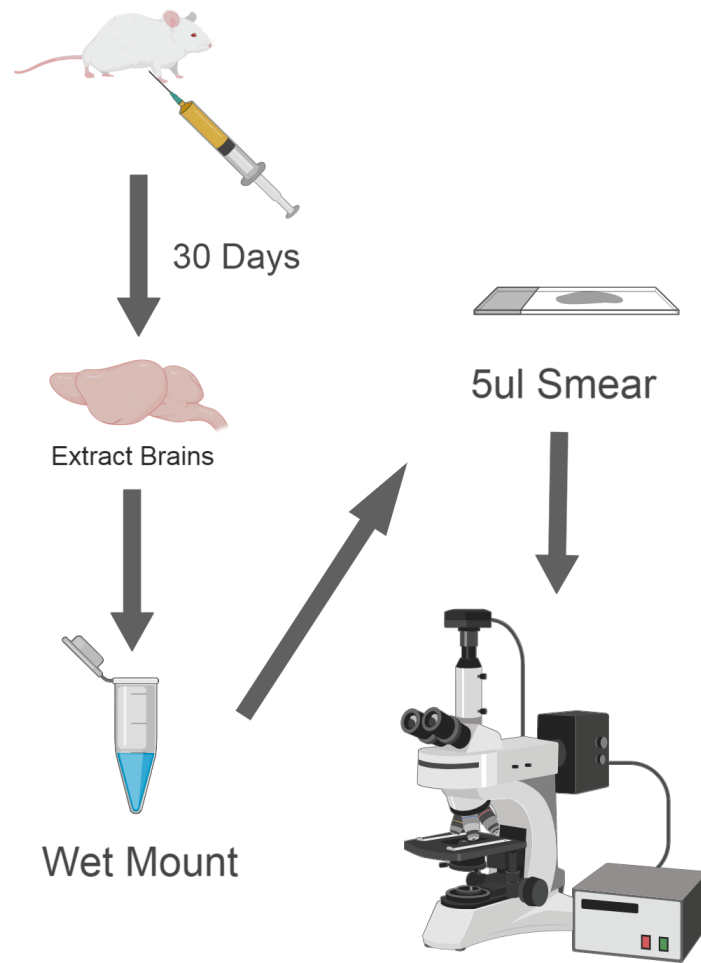


Figure 17: Procedure for Investigating Chronic Infection *in vivo*

Mice were infected intraperitoneally with parasites. Animals were maintained for 30 days post-infection at which point they were euthanized, brains were extracted, and wet mounts made with cyst stained using FITC-DBA. Counts were performed on Nikon Tie inverted fluorescent microscope at 40X magnification.

Acute Infection *in vivo*

Acute infection was evaluated using the Pru Δ Ku80 and the clones derived from it (Table 4). C56BL6 mice were infected with parasites and observed twice daily for seven days post-infection and then once a day for an additional seven days. Mice were observed to evaluate the onset of symptoms that included ruffled fur. Any mice that appeared moribund showing lack of movement, shacking, and cold temperature were anesthetized with isoflurane and euthanized by cervical dislocation.

For all mouse studies parasites were taken from lysed T25 flasks, parasites were counted using hemocytometer and the appropriate number of parasites needed were calculated. To ensure the proper number of parasites were injected, plaque assays were used by inoculating the parasites from the diluted volume onto 24 well plates with confluent HFF cells and counting plaque numbers between the volumes used to infect the mice.

Plaque Assay *in vitro* for Stressed Versus Unstressed Parasites.

Two 24 well plates were seeded with HFF cells and allowed to become confluent. Parasites were taken from a lysed T25 and divided into two groups. One group of parasites was centrifuged for 10 minutes at 1300 RPM and the parasite pellet resuspended in D10 pH 8 supplemented with 50 micrograms of mycophenolic acid. These conditions stress the parasites by starving them of pyrimidines, this was done in order to induce stage differentiation. These parasites were incubated at 37°C for 4 hours extracellular in order to stress the parasites. The other group of parasites were resuspended in D10 pH 7 and immediately allowed to invade HFF cells (non-stressed parasites). Fifty parasites from stressed or non-stressed groups were inoculated per well in a 24 well plate

containing confluent HFF cells and incubated at 37°C for 5-7 days to allow plaques to form. The plates were then fixed with 100% ethanol for 5 minutes and stained with a solution of 0.05% w/v of crystal in violet in a solution of 20% ethanol in PBS for 5 minutes. Images of wells were taken on using an inverted Nikon Eclipse Tie fluorescent microscope at 10X magnification. Plaque sizes were measured using the FIJI image analysis software (Figure 18)

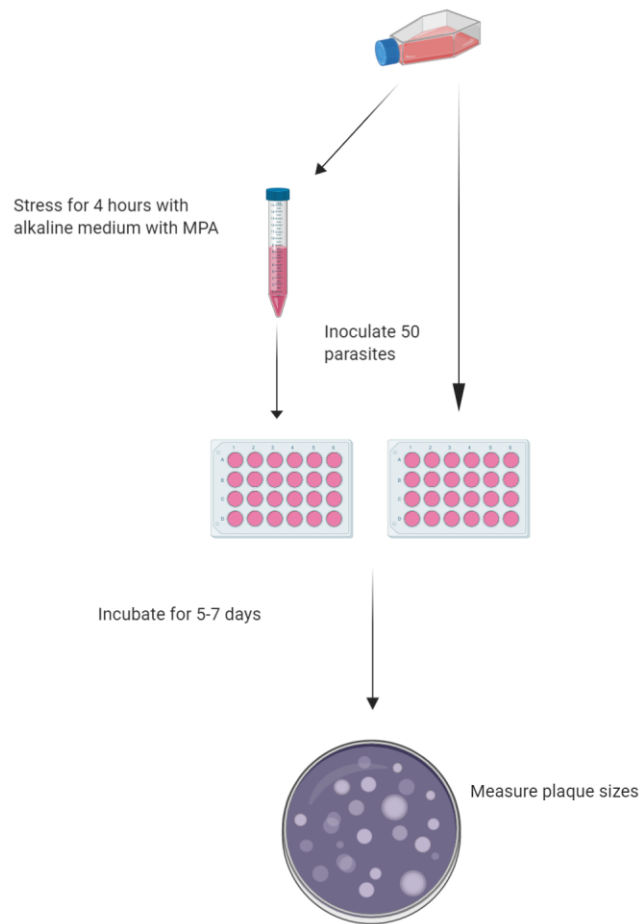


Figure 18: Plaque Assay

Parasites were taken from lysed T25s and divided into two groups. One group was stressed for 4 hours in alkaline medium at pH of 8 supplemented with 50 micrograms of MPA/mL for 4 hours to stress parasites and induce bradyzoite transition. Parasites were inoculated onto 24 well plates with confluent HFF cells at 50 parasites per well and incubated for 5-7 days. After plaques formed plates were fixed and stained with crystal violet and images were taken at 10X on the Nikon Tie Inverted Fluorescent microscope in brightfield. Plaque area was measured by taking the area of plaques.

Invasion Assay

Parasite invasion was measured using differential permeabilization to detect extracellular versus intracellular parasites (in versus out assay). The invasion assay was performed using confluent 24 well plates of HFF cells. Medium from the cells was aspirated, 500uL of medium from lysed T25 flasks containing 10^6 parasites was added and the plates were incubated for 10 minutes at room temperature. After inoculation, PBS warmed to 37°C was placed in the reservoir around the wells, and the plates were placed in a 37°C incubator for 30 minutes to induce parasite invasion of the HFF cells. After the 30 minutes incubation the plates were washed with PBS, fixed with 4% paraformaldehyde for 20 minutes, and blocked with 10% FBS for 30 minutes. The extracellular parasites were stained with a polyclonal anti-*toxoplasma* rabbit antibody. Plates were then washed three times with PBS. plates were incubated with a FITC-conjugated anti-rabbit secondary for one hour at room temperature, and again were washed three times with PBS. The cells were permeabilized for 5 minutes with 0.2% Triton X-100 in PBS for 5 minutes, washed again, and then blocked a second time with 10% FBS for 30 minutes. Intracellular parasites were labeled with a mouse polyclonal anti-*toxoplasma* antibody for one hour at room temperature, washed 3x with PBS and then incubated with Alex-fluor 647 conjugated anti-mouse secondary antibody for one hour at room temperature (Figure 19). The plates were washed three times with PBS and parasites were counted on the Nikon TiE inverted fluorescent microscope. Four counts of 100 parasites were taken, invasion was quantified by calculating the percent of parasites that invaded out of the total parasites.

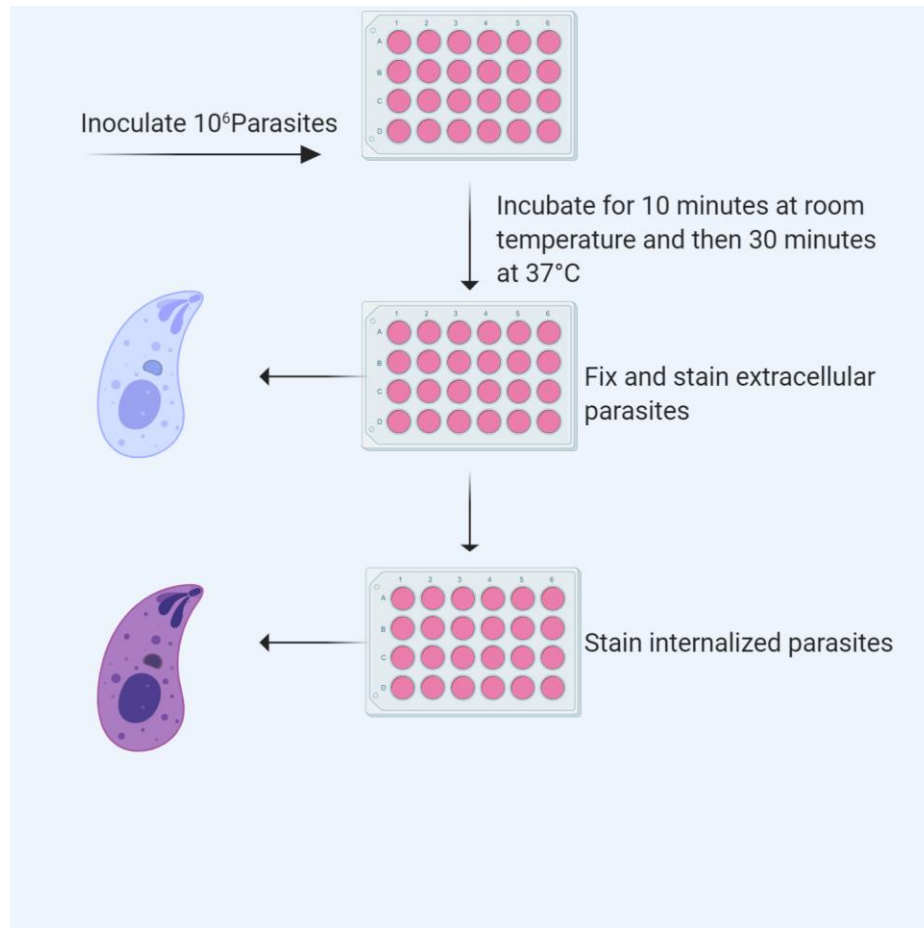


Figure 19: Invasion Assay

Parasites were taken from lysed T25s and inoculated onto 24 well plates with confluent HFF cells for 10 minutes at room temperature. Warm PBS at 37°C was then added to the reservoir around the wells and the plates were placed in a 37°C incubator to induce invasion. After incubation plates were fixed and stained to label extracellular parasites, then permeabilized and stained to label internalized parasites.

Replication Assay

Intracellular parasite replication was quantified by measuring the parasites per vacuole over time. 24 well plates with confluent HFF cells were inoculated with 50,000 parasites. Two sets of plates were used, stressed and non-stressed. Stressed plates were inoculated with parasites stressed for four hours in MPA/pH 8 D10 medium. At 24, 48, and 72 hours plates were fixed with 4% paraformaldehyde for 20 minutes, permeabilized with 0.2% triton X 100 for 5 minutes, and stained for one hour with a mouse-polyclonal anti-*Toxoplasma* antibody and then washed three times with PBS. Plates were then stained with a secondary antibody, Alexa Fluor 595 conjugated goat anti-mouse for 1 hour, rinsed again and counterstained with DAPI. At each time point in each condition, 100 vacuoles were counted and the total parasites per vacuole were counted. Data was binned into four categories based on parasites per vacuole: 1-2, 3-6, 6-10, 10 and more. Replication was quantified by calculating the percent of vacuoles out of the total within each bin for each time point.

qRT-PCRs

Quantitative reverse-transcriptase polymerase chain reaction was used to confirm FIKK deletion, and complementation. Also, to determine gene expression in response to cyst inducing conditions. qRT-PCR was performed using an Applied Biosystems Quantstudio 5 thermocycler using primers against various genes in the *Toxoplasma gondii* genome using the NCBI primer design tool and checked against both the *T. gondii* and human genomes. qRT-PCRs were performed using the Applied Biosystems Fast SYBR Green Master Mix. Expression change was determined by the $\Delta\Delta C_t$ method and normalizing to the parasite's housekeeping gene tubulin (Tub1) (Table 5).

Table 5: Primers Used for qRT-PCRs

		Bradyzoite Markers	
Housekeeping Gene		BAG1QF	GGAGCCATCGTTATCAAAGGAGA
Tub1QF	ATCAGCAGTACCAGGACGCC	BAG1QR	CGGACACTCGCTCAGTCAAA
Tub1QR	GAGAAAAGCCACTACGCGCC	ENO1QF	GCGAGATTTTGGATTCTCGCGG
		ENO1QR	CGCCTTTCCCAAGTACCGT
FIKK		LDH2QF	GTAACAGGCATGCCAGAAGGG
FIKKqf	ACTTCCTGATCGAGGTTCCCA	LDH2QR	GACATCCGATCCGGCGATCT
FIKKqr	GGACTTGGACGACCGTTTGA	CST1QF	ACCTCCGGTCCAAGAAACCG
		CST1QR	GCGGGTCGACTTTGGGAAAC
		BPK1QF	CGCATTCCCCTGCAGATATGA
		BPK1QR	CACTAACTCTCTGGCGGGCA
		MCP4QF	CGGATGATTGGGCGTGCTTT
		MCP4QR	TGAATGAAGTTGCTCTGGCACG

Ap2 Transcription Factors	
Ap2XII-Vlf	CTGGCCCCTAGGCAAGAGTT
Ap2XII-Vlr	GCCTAGCTCAGAAACCAGTTCG
Ap2XI-IVf	GGAGCCACCCCATGATGAA
Ap2XI-IVr	CCGAGCAAAGTCGTCGAGTG
Ap2IX-IXf	TGCGCGCCAAAAGGAAAATATC
Ap2IX-IXr	TGCGTCCTGCAAGAGAGATATTTT
Ap2IX-IVf	TCTACGAGGCCGATTGCAGG
Ap2IX-IVr	AGGAGGCGTCGTCATAACCG
Ap2IV-III f	ACACAGGGCAGTCGTTTCCA
Ap2IV-III r	ATGGCTTGGCGGAGTATCT
Ap2IV-IVf	GATGCGCTTCCGACGTCAAG
Ap2IV-IVr	CGACTGGCGATTGGCTGTTC

RNA Sequencing

The parasite genome is approximately 66 MB and encodes approximately 8920 genes. The expectation was that purified parasite RNA would contain approximately 10 percent HFF cell contamination. These values were used to determine RNA sequencing depth including the number of lanes and barcoding and multiplexing of samples.

Samples from Pru Δ HPT and Pru Δ HPT Δ FIKK 3 were prepared and sent off for RNA sequencing by Cornell University's Genomics Core. The samples were prepared under SNP stress with three-time points 24, 48, and 72 hours. Three biological samples were used for group. Additionally, a non-stressed extracellular time point was taken at 24 hours which was labeled as T0. Parasites were grown in HFF cells and then they were liberated from the host cells by passage through a 25-gauge needle. Subsequent passages through a 27-gauge needle ensure lysis of parasites. Fresh D10 media was added to wash parasites and remove HFF cell debris and parasites were pelleted by centrifugation. Parasites were also passed through a 3 μ m nucleopore filter to further purify parasites. RNA was isolated from parasites using the Qiagen RNAeasy Plus Kit. RNA was further treated with TURBO DNA-free removal kit (Thermo Fisher) to ensure removal of any contaminating DNA. The parasites were pelleted and sent to Cornell on dry ice. RNA quality was validated using the Agilent 2100 Bioanalyzer. RNA sequencing (polyA-selected, paired read, barcoded and multiplexed using 3 lanes) was performed using an Illumina HiSeq 2000 sequencer. Parasite sequences were aligned using STAR to the *Toxoplasma gondii* ME49 reference genome from ToxoDB (<https://toxodb.org/toxo>). Uniquely mapped sequences were intersected with composite gene models from ToxoDB.org (32). Composite gene models for each gene consisted of the union of exons

of all transcript isoforms of that gene. Uniquely mapped reads that unambiguously overlapped with no more than one composite gene model were counted for that gene model.; the remaining reads were discarded. The counts for each gene model correspond to gene expression values and were used for gene expression analysis. Preliminary exploration of the data was achieved via simple error ratio estimates, principle component analysis, and multidimensional scaling. Differential gene expression was performed with default normalization strategies using limma, edgeR and DeqSeq2. Only genes with adjusted p-values less than 0.5 were considered differentially expressed. Log2fold change and p-values were also calculated using the Benjamini-Hochberg method.

Proteomics and Phosphoproteomics

Parasite groups and biological replicates for RNAseq and proteomics are shown in Table 6. For proteomic analysis of both Pru Δ HPT and Pru Δ HPT Δ FIKK3 parasites in HFF cells were grown for 72 hours under SNP stress and for 24 hours without stress (T0). At these time points parasites were intracellular. Parasites could not be purified from HFF cells without losing the proteins in the PV and PVM as well as in nascent cysts. Thus, the predominant proteins were from HFF cells rather than parasites. A high multiplicity of infection was used to maximize the ratio of parasites to HFF cells. However, this also resulted in overall poor differentiation of parasites to cysts. Parasites were pelleted and shipped to the Proteomics and Mass Spectrometry Facility at the Donald Danforth Plant Science Center, St. Louis, MO. Ribosomal proteins in parasites versus HFF cells are different sizes and based on their expression following horizontal gel electrophoresis the estimate was that approximately 10 percent of the proteins in each

sample were of parasite origin. Proteins were extracted from each sample, normalized for protein concentration, digested and labeled with TMT-10plex reagent (omitting two channels) and then pooled together. The set for phosphopeptide analysis were enriched with TiO_2 (or iron iMAC). Both sets were prefractionated using high pH reversed phase HPLC and individual fractions were analyzed by nanoLC-MS/MS. Relative phosphorylation site usage in WT and ΔFIKK parasites was analyzed by quantitative mass spectroscopy. Bioinformatic filtering was used to reduce the site and protein false discovery rate to less than 1% and 3% respectively. HFF proteins and parasite proteins were filtered by bioinformatics based on each of their respective genomes and analyzed separately. Peptides homologous to both HFF and parasite proteins were excluded. Protein alignment was performed using Scaffold 4.

Table 6: Experimental Setup for RNA Sequencing and Proteomics

	T0(24h no stress)	24h Stress (SNP)	48h Stress	72h Stress
PruΔHPT WT2	Triplicate	Triplicate	Triplicate	Triplicate
PruΔHPTΔFIKK 3	Duplicate	Duplicate	Duplicate	Duplicate

Proteomic and Phosphoproteomic

	T0(24h no stress)	72h Stress
PruΔHPT WT2	Triplicate	Triplicate
PruΔHPTΔFIKK 3	Duplicate	Duplicate

Motif Search

Previous analysis of PfFIKK8 and CpFIKK by Osman et al. 2015 determined that both the FIKK kinases in *P. falciparum* and *C. parvum* targeted a protein motif consisting of seven amino acid residues (RAPSFYR). Based on the sequence a search was performed using ToxoDB to identify potential FIKK targets based on the presence of this motif. The search was performed using Perl style regular expression, which allows the search to be based on specific amino acids with other amino acids being represented by a number indicating the chemical profile of the amino acid. The motif translated into the Perl expression was R66S66R indicating the presence of the flanking arginines and central serine which Osman et al. identified as crucial to the enzymatic activity of the PfFIKK8 and CpFIKK enzymes (58).

Statistics and Relevant Programs

Statistical analysis was performed using Graphpad Prism 8 based on the recommendations of the program. After normalization and preliminary analysis by Cornell or Danforth, files containing genes, log₂fold change, and p-values were evaluated by us. Data mining these files was performed using R Studio (<https://rstudio.com/>), and Volcano plots were produced using Glueviz (<http://glueviz.org/>). Primers were designed using the NCBI primer design tool (<https://www.ncbi.nlm.nih.gov/tools/primer-blast/>). Plasmid maps and alignments were made using Benchling (<https://www.benchling.com/>), and images were analyzed using FIJI (<https://imagej.net/Fiji>). All graphical images were made using Biorender (<https://biorender.com>).

Results

Aim 1: Initial Characterization of the *T. gondii* FIKK Kinase Gene Deletion

The FIKK Kinase is Localized to the Basal Complex Throughout the Parasite's Lytic Cycle But it is Also Localized to the Host Cell Cytosol.

In previously published studies, the endogenously tagged FIKK protein tagged with YFP or Ty (FIKK-YFP/FIKK-Ty respectively) localized to the basal end of *T. gondii* and colocalized with MORN1 in the parasite basal complex1 (Figure 9) (72). However, a limitation of these previous studies was that the FIKK-YFP tagged protein required amplification with both a mouse anti-GFP primary antibody followed by an anti-mouse goat secondary antibody conjugated with Alexa Fluor 488 in order to be visualized by fluorescence microscopy (Figure 9). Such amplification can increase non-specific background fluorescent signals. Thus, it was not clear from previous studies whether parasite expression of FIKK-YFP was exclusive to the parasite basal complex throughout the parasites' lytic cycle or whether lower amounts of the protein were localized to other areas of the parasite or infected host cell. In order to overcome these limitations, live cell imaging was performed with the RH FIKK-YFP parasite clone using a Nikon Eclipse TiE fluorescent microscope. New advances in microscopic imaging with the Nikon Eclipse TiE system results in greater fluorescent light capture than the previously utilized Zeiss inverted Axiovert 200 System. Still images are shown in the first panel in Figure 20. In the first panel, two extracellular parasites are shown prior to invasion into the adjacent HFF cell. The FIKK-YFP protein (green) is evident exclusively in the basal end of the extracellular parasites. In the next panel, a parasite is shown in the process of invasion of the HFF cell. The constriction within the parasite marks the tight junction/moving junction that is formed between the parasite and host membrane during parasite invasion.

It is clear that during parasite invasion the FIKK kinase is unchanged in the parasite basal end. In the next panel, two parasites are shown that have replicated by endodyogeny and are linked to one another through their basal ends. The FIKK-YFP protein is associated with each of the parasite's basal ends but surprisingly is also evident in the host cell cytosol surrounding the parasitophorous vacuole (PV). This suggests that the FIKK-YFP protein may be exported or otherwise traffic from the PV to the infected host cell cytosol, perhaps transiently, during the parasite's lytic cycle (Figure 20). The last panel shows 8 parasites/PV in a rosette formation with the FIKK-YFP in the basal end of each parasite. Thus live-cell imaging of parasites and HFF cells during the parasites' lytic cycle was consistent with previous immunofluorescence that showed a continuous localization to the basal end of the parasite throughout the lytic cycle. However, live-cell imaging disclosed a previously unknown potential localization of the FIKK-YFP to the host cell cytosol. The significance and mechanism of FIKK-YFP localization to the host cell cytosol is beyond the scope of this thesis. However, its potential localization in the host cell outside of the parasite and its PV must be considered in terms of the potential role of the FIKK protein during infection.

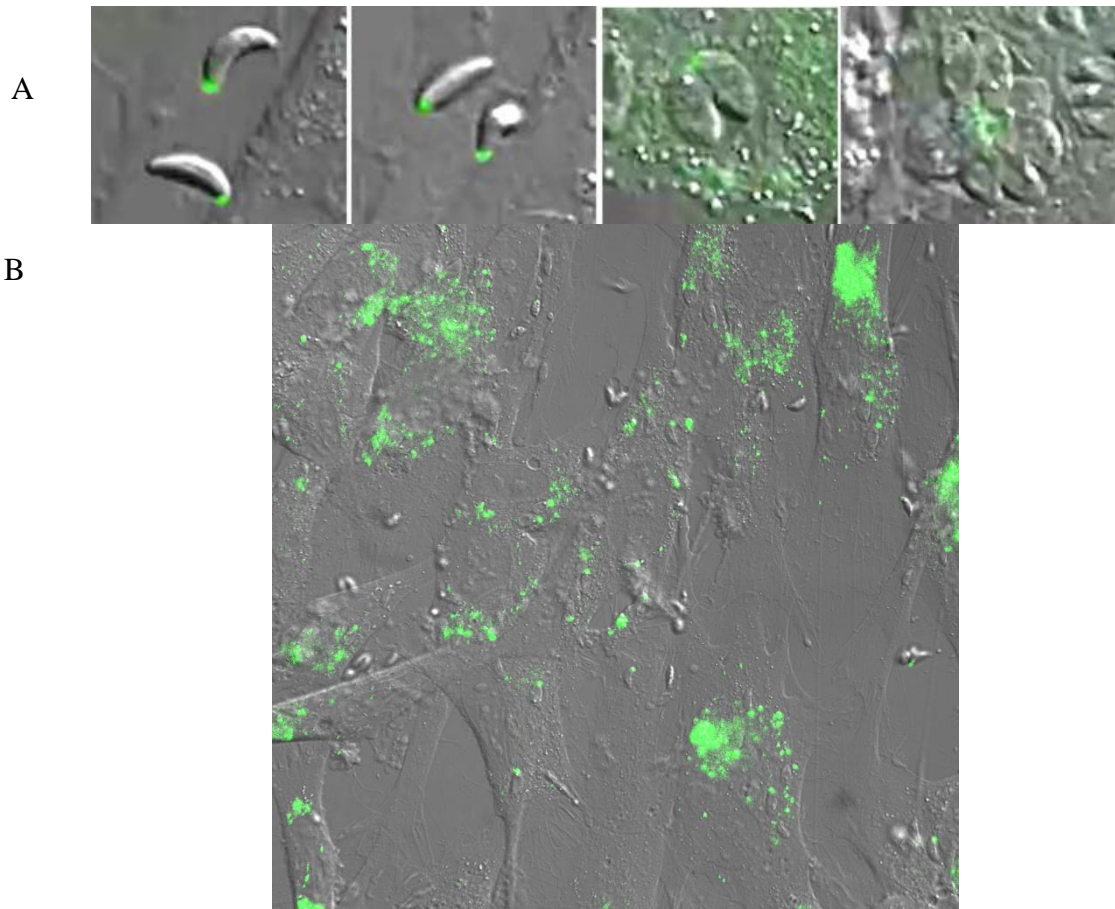


Figure 20: Live Cell Imaging of the FIKK-YFP

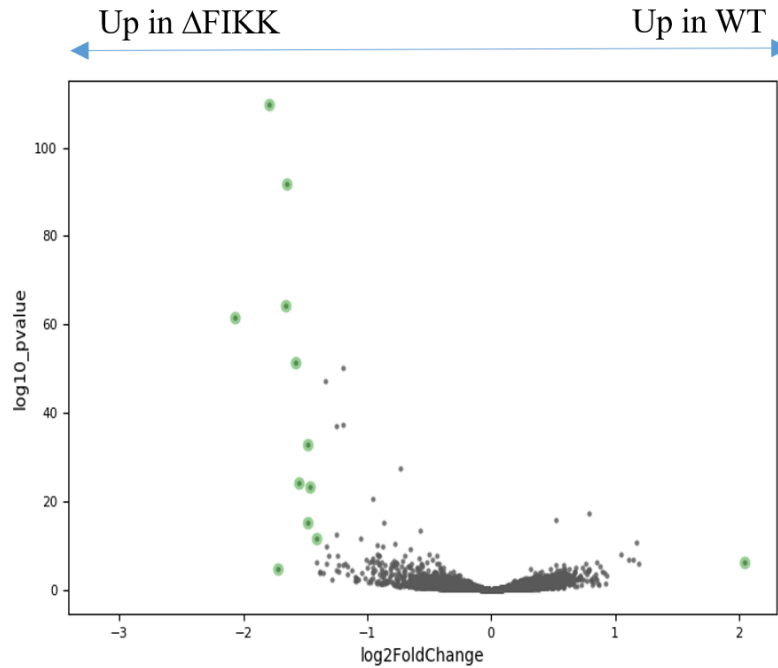
Part A: Live cell imaging of the parasite expressing FIKK YFP over the course of 36 hour in HFF cells showing extracellular parasites, parasites invading HFF cells, two parasites per vacuole and approximately 8 parasites per vacuole. Part B: A single snap shot of an entire microscope field containing parasites that express FIKK YFP in HFF cells. FIKK-YFP can be seen on the basal end of intracellular and extracellular parasites. It is also clear that there are foci of FIKK-YFP expression in areas that appear to contain few or no parasites. This suggests that the FIKK-YFP enters host cells that may not contain parasites.

Impact of FIKK Gene Deletion on the Global Parasite Transcriptome and Proteome.

The FIKK gene was deleted in the Type II Pru strain of *T. gondii* in order to examine the importance of the FIKK gene in cystogenic parasite strains as well as those that are the more common agents of toxoplasmosis in humans. In order to evaluate whether deletion of the FIKK gene impacted the expression of downstream genes we performed global RNA-sequencing of the intracellular wild type parasite versus the FIKK gene depleted parasites. RNA sequencing was performed after the creation of first set of FIKK gene deletions in the clonally purified line of Pru Δ HPT. It was unknown how the FIKK deletion would impact the organism and these molecular techniques allowed us to cast a wide net and catch any potential differences between wild-type and Δ FIKK parasites. RNA sequencing was compared between WT parasites and FIKK gene deleted parasites first in the absence of exogenous stress in intracellular parasites, and then in response to sodium nitroprusside to evaluate the impact on genes induced in bradyzoite-inducing conditions. Since we used a high multiplicity of infection, exogenous SNP did not induce cyst formation or pronounced expression of bradyzoite genes. Differentially expressed genes were compared between WT and Δ FIKK parasites in the presence and absence of exogenous SNP. A list of differentially expressed genes (DEGs) was created based on Log₂fold changes between wild-type and Δ FIKK clone and adjusted p-values to take into account false discovery. A volcano plot is shown in Figure 21 that shows differentially expressed genes in intracellular parasites between WT and Δ FIKK clones in the absence of exogenous stress. A limited set of genes (12) were found to be different between wild-type and Δ FIKK in the RNA sequencing analysis in non-stressed conditions. As expected, the expression of the FIKK gene was decreased in the Δ FIKK

clones and the expression of the HPT gene was increased. However, no definitive pattern could be found in the limited number of differentially expressed genes, particularly since many of the changed genes are hypothetical proteins with no annotated functional domains or function (Figure 21, Figure 22, Figure 23, Figure 24). There was also a minor difference in gene expression between WT and Δ FIKK clones in the presence of SNP for 24, 48 or 72 hrs. Thus deletion of the FIKK kinase has very minimal impact on parasite gene expression in tachyzoites.

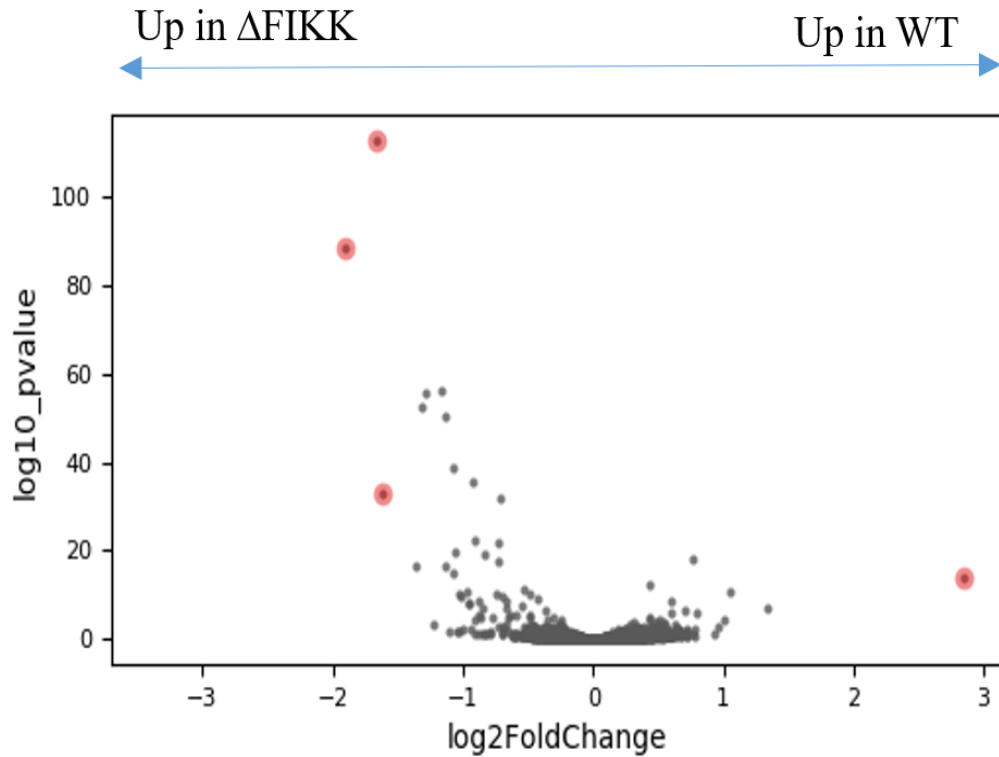
Global proteomic and phosphoproteomic analysis was performed that compared intracellular wild type and Δ FIKK clones in the presence and absence of SNP. We were unable to detect the FIKK protein in these studies which made it clear that the depth of the study in terms of protein detection in parasites was limited. This is consistent with the fact that parasite proteins represented potentially less than 10% of total proteins due to HFF cell numbers compared to parasites. Our analysis showed that when wild-type was compared to Δ FIKK clones in either the presence or absence of exogenous stress no proteins met the criteria for differential expression (\log_2 Fold change of 1.5) and statistical significance (adjusted $p < 0.05$).



Product Description	log2FoldChange	padj
HXGPRT	-1.658058295	4.98E-65
hypothetical protein	-1.579784939	4.23E-52
RNA-dependent RNA polymerase RDP	-1.651995989	1.97E-92
hypothetical protein	-1.484182196	1.77E-33
hypothetical protein	-1.466494673	5.11E-24
dynein heavy chain family protein	-2.065296607	2.20E-62
hypothetical protein	-1.405118414	1.97E-12
hypothetical protein	-1.47969181	7.04E-16
hypothetical protein	-1.551629019	8.91E-25
hypothetical protein	-1.719097313	2.66E-05
RuvB family 2 protein	-1.796142202	2.34E-110
FIKK kinase, putative	2.044706223	4.67E-07

Figure 21: Differentially Expressed Genes Between Pru Δ HPT and Δ FIKK Clones With No Exogenous Stress

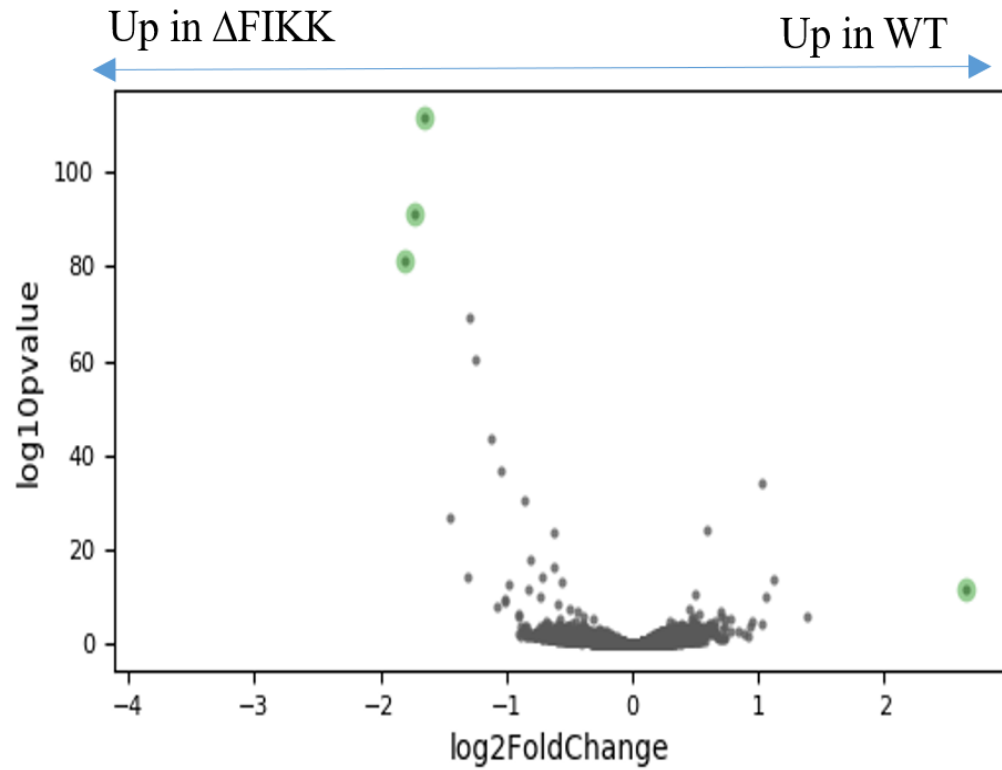
Differential expression of genes between Pru Δ HPT and Pru Δ HPT Δ FIKK3. Twelve genes were differentially expressed based on an adjusted p value of <0.05 and a Log₂ fold change of at least 1.5. Alignment and analysis was performed using Deqseq with statistical significance calculated using the Benjamini-hochberg method.



Product Description	log2FoldChange	padj	log10_pvalue
DnAK-TPR	-1.61996	1.48E-33	32.83103
hypothetical protein	-1.91115	4.07E-89	88.39032
RuvB family 2 protein	-1.65839	1.85E-113	112.7322
FIKK kinase, putative	2.852037	1.73E-14	13.76228

Figure 22: Differentially Expressed Genes Between Pru Δ HPT and Δ FIKK Clones at 24 Hours Under SNP Stress

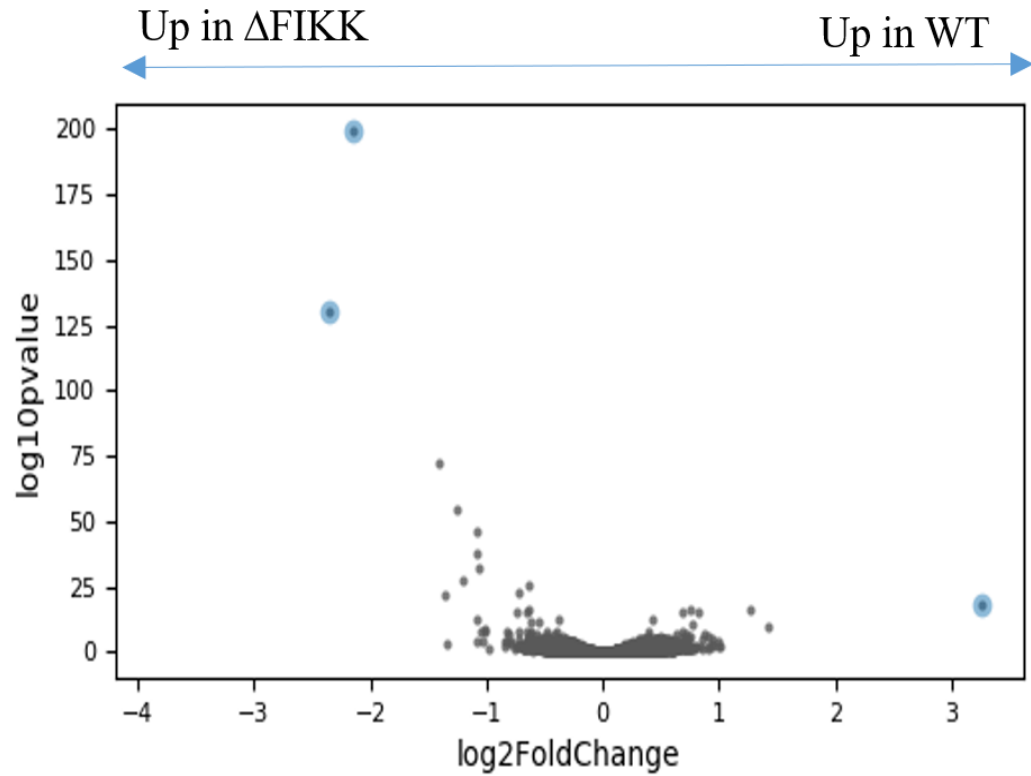
Four genes were statistically significant based on an adjusted p value <0.05 Log₂ fold change of at least 1.5 Alignment and analysis was performed using Deqseq with statistical significance calculated using the Benjamini-hochberg method.



Product Description	log2FoldChange	pvalue
HXGPRT	1.72388	3.25E-95
hypothetical protein	-1.80511	3.20E-85
RuvB family 2 protein	-1.6487	4.66E-116
FIKK kinase, putative	2.652368	6.27E-15

Figure 23: Differentially Expressed Genes Between Pru Δ HPT and Δ FIKK Clones at 48 Hours Under SNP Stress

Four genes were statistically significant based on an adjusted p value <0.05 Log₂ fold change of at least 1.5 Alignment and analysis was performed using Deqseq with statistical significance calculated using the Benjamini-hochberg method.



Product Description	log2FoldChange	padj
hypothetical protein	-2.35129	3.25E-131
RuvB family 2 protein	-2.15118	1.73E-200
FIKK kinase, putative	3.267567	4.21E-19

Figure 24: Differentially Expressed Genes Between Pru Δ HPT and Δ FIKK Clones at 72 Hours Under SNP Stress

Three genes were statistically significant based on an adjusted p value <0.05 Log₂ fold change of at least 1.5 Alignment and analysis was performed using Deqseq with statistical significance calculated using the Benjamini-hochberg method.

Aim 2: Functional Characterization of the FIKK Kinase for Acute Infection

In Aim 1 we attempted to characterize the FIKK deletion by examining the effects of the FIKK deletion on the global transcriptome and proteome of the parasite. In Aim 2 we evaluated whether the *T. gondii* FIKK kinase contributes to the lytic cycle of the Type II strain of the parasite and its ability to cause acute infection.

The FIKK Kinase is Not Required for the Parasites' Lytic Cycle *in vitro*.

Localization to the basal end of the parasite in association with the basal complex suggested a potential role for the FIKK kinase in parasite replication. Our previous study showed no role for the FIKK kinase in the lytic cycle in Type I RH parasites (72). However, RH is a lab strain that is extensively adapted for growth as a “professional tachyzoite”. Thus we evaluated the importance of the FIKK kinase in the lytic cycle of the Type II Prugnaud (Pru) strain, as unlike RH, Pru remains capable of differentiating between tachyzoites and bradyzoites in acute versus chronic infection respectively. Thus the effect of FIKK gene deletion in the Prugnaud strain of *T. gondii* on parasite replication and the parasites' lytic cycle were evaluated. In Aim 2, the parasite's lytic cycle in HFF cells as well as individual steps in the parasite's lytic cycle was compared between WT, FIKK deleted parasites, and FIKK kinase complemented parasites. of the parasite lytic cycle (Figure 25).

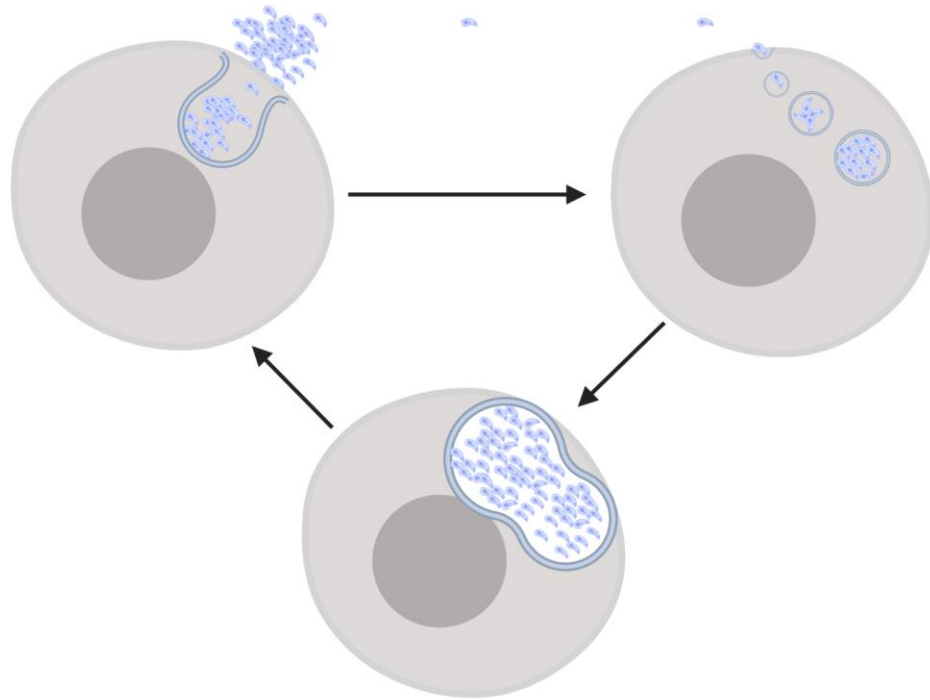


Figure 25: Parasite Lytic Cycle

The parasite's lytic cycle consists of parasite invasion of host cells, formation of a PV, replication within the host cell PV, and lysis of the host cell releasing the parasites to reinvade other host cells.

There is No Gross Impact of the FIKK Gene Deletion on Parasite *in vitro* Growth in HFF Cells

The parasite lytic cycle is dependent on parasite gliding motility to reach host cells, invasion of host cells, replication in the PV, and parasite egress to re-initiate the lytic cycle in new host cells. Gross defects in *T. gondii*'s lytic cycle are assessed by evaluating the ability of the parasite to form plaques in an HFF cell monolayer. The presence of plaques shows that the parasite can complete multiple sequential rounds of its lytic cycle. The size of the plaques in the HFF cell monolayer created by each parasite provides an additional measure of how effectively the parasite completes multiple lytic cycles in order to create a spreading zone of lysis over time in the HFF cell monolayer. To compare the lytic cycle of wild type parasites, FIKK gene deleted parasites and FIKK complemented clones their ability to form comparable plaques in HFF cells was evaluated. Plaques were compared in both stressed HFF cells as well as non-stressed HFF cells to evaluate the effect of biological stress on the parasite's lytic cycle. As shown in Figure 26 wild type, Δ FIKK and FIKK complemented parasites were all able to form plaques in HFF cell monolayers. Furthermore, the average size of each plaque, which reflects the zone of HFF cell lysis over time, was similar for wild type, Δ FIKK and FIKK complemented parasites. However, in the presence of exogenous stress, also referred to as bradyzoite-inducing conditions, there was a slight increase in the size of plaques created by the Δ FIKK clones that was restored in complemented clones. Thus the deletion of the FIKK gene did not grossly affect the parasites' lytic cycle *in vitro* in HFF cells in the absence of exogenous stress but moderately enhanced the parasite lytic cycle in bradyzoite-inducing conditions (stressed conditions).

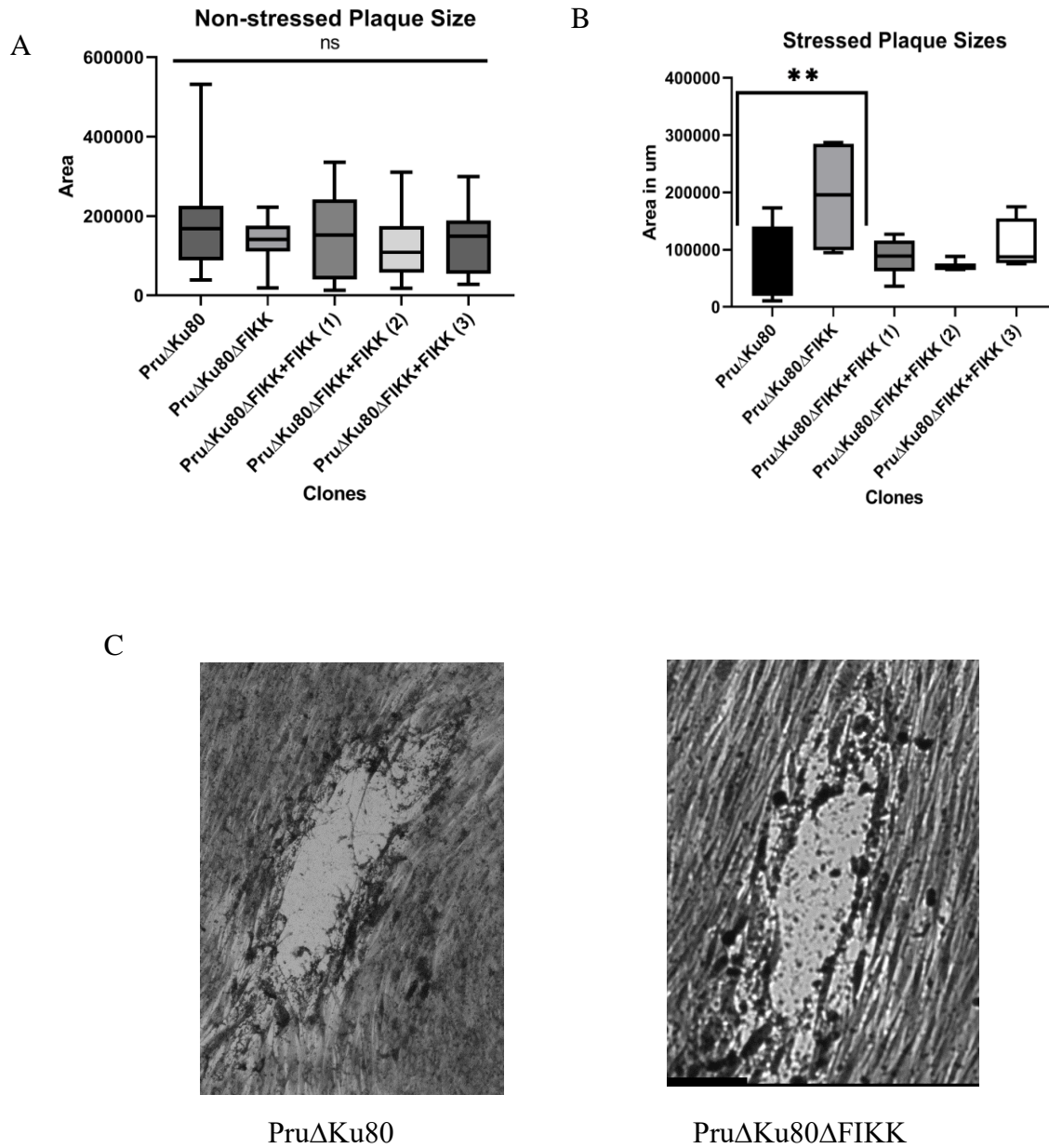


Figure 26: Plaque Sizes of PruΔKu80, ΔFIKK, and FIKK Kinase Complemented Clones

A. Plaque areas of clones under standard growth conditions (D10 medium at 37°C) for 5-7 days. The area of the zone of HFF cell lysis was measured and the mean and SD is shown. B. Plaque area after growth in bradyzoite inducing conditions (MPA stress for extracellular parasites for four hours). The area of the zone of HFF cell lysis was measured and the mean and SD is shown. C. Example of a plaque from PruΔKu80 and ΔFIKK clones. Average plaque size was the same in PruΔKu80 and ΔFIKK clones in the absence of exogenous stress; however a slight increase in plaque size was seen in ΔFIKK parasites grown under stress conditions. Analysis was performed in Graphpad Prism using a one way ANOVA with Tukey post-hoc test. All clones were compared to each other. ** p<0.001.

Deletion of the FIKK Kinase Does Not Impact the Efficiency of Parasite Invasion of HFF Cells.

It was clear from the plaque assay that both WT and Δ FIKK parasites formed similar plaques over 5-7 days. However, a plaque assay is unable to identify changes in the efficiency of parasite invasion; how quickly are parasites able to invade cells. The efficiency of parasite invasion is determined using an invasion assay, also known as an in vs out assay. The assay uses a short pulse of parasite challenge of HFF cells and evaluates how many parasites are able to invade during this short exposure versus how many remain extracellular. Differential permeabilization is combined with antibody staining of parasites to differentiate extracellular parasites from intracellular parasites. As shown in Figure 27, there was no marked deficiency in the invasion efficiency between the wild-type and Δ FIKK clones.

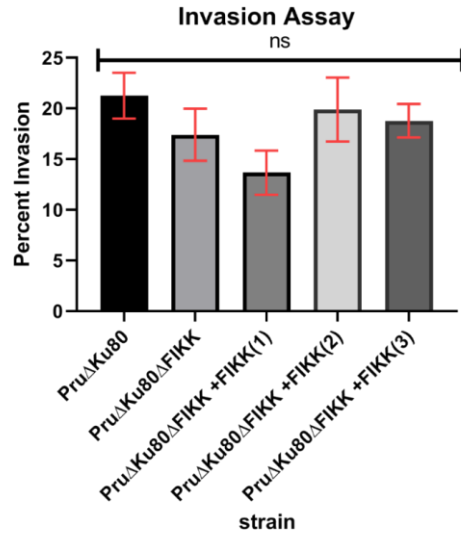
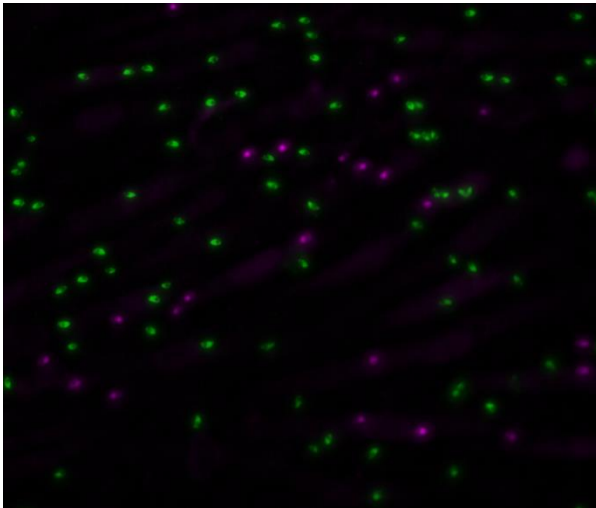


Figure 27: Parasite Invasion Assay

Parasite invasion efficiency was determined by measuring the total number of parasites (green and purple) versus the number of intracellular parasites (purple) after a short HFF challenge pulse of parasites. The picture shows a florescent microscope field that shows intracellular parasites (purple) versus total parasites (green and purple). The percent of in intracellular parasites compared to total parasites is shown in the graph. The statistical analysis was done using a one way ANOVA with a Tukey post hoc test comparing the clones to each other. Bars are mean with red error bars showing the 95% Confidence Interval.

The FIKK Kinase Does Not Alter Parasite Replication Within a PV

To determine whether the deletion of the FIKK kinase impacted replication of the Pru strain of *T. gondii* the number of parasites within parasitophorous vacuoles in HFF cells were measured over time. Parasite replication was directly measured by comparing the number of intracellular parasites per PV 24 and 48 hours post-invasion. As shown in Figure 28, there was no significant difference between WT and FIKK deficient parasites in terms of parasite replication in the presence or absence of bradyzoite inducing conditions.

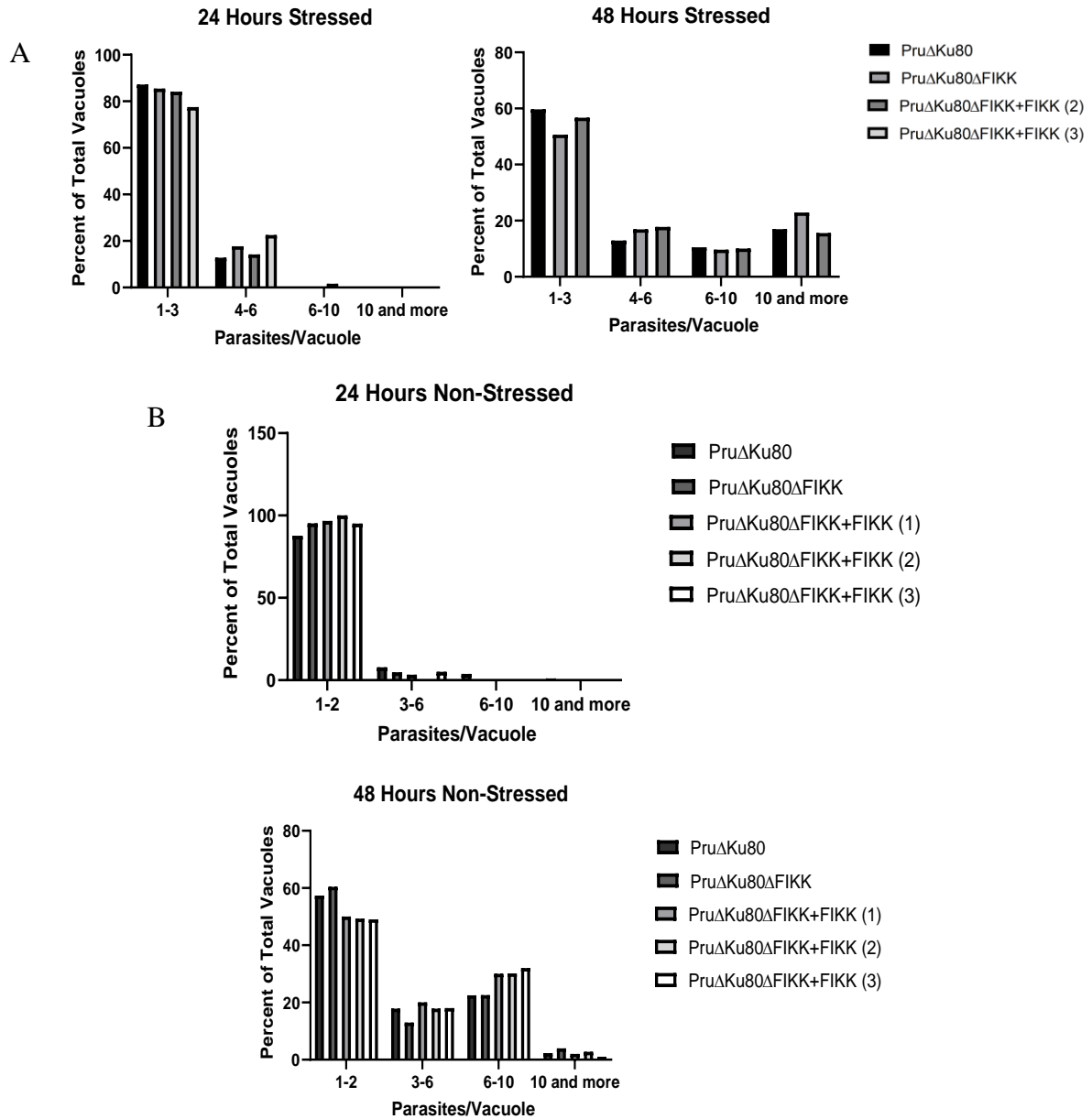


Figure 28: Parasite Replication of WT and FIKK Deficient Parasites in the Presence and Absence of Exogenous Stress

A total of 100 vacuoles were counted per clone per time point. Part A clones under Stressed conditions (MPA treatment), Part B non-stressed. Analysis was done using a one way ANOVA with a Tukey post hoc test comparing the mean parasite per vacuole number between the clones. No significant differences were found between the clones.

The FIKK Kinase is Important for Parasite Virulence During Acute Infection *in vivo*

Although the FIKK kinase was not critical for the parasite's lytic cycle, it is clear that infection *in vivo* is more complicated than the lytic cycle *in vitro* in HFF cells. Therefore, we evaluated whether the deletion of the FIKK kinase impacted parasite virulence during acute infection in mice. Three groups of 5 C57BL/6 mice per group were inoculated intraperitoneally with 200 parasites. The number of viable parasites per each inoculate was confirmed by plaque assay of parasites in HFF cells after injection of the mice was complete. Acute infection symptoms manifested within 2 weeks of infection indicating sickness in all mice. Mice were kept and monitored for 30 days, and euthanized if they showed moribund behaviors (slow movement, shaking, and cold body temperature). Mice infected with wild-type parasites were all euthanized on day 8 post-infection as infected mice were all moribund. Mice infected with Pru Δ FIKK complement 2 were euthanized on day 9 post-infection as they were all moribund. One mouse infected with Pru Δ FIKK complement 3 was moribund behavior on day 13 post infection and was sacrificed. The 3 remaining mice were sacrificed on day 14 post-infection when they became moribund. All of the the mice infected with Pru Δ ku80 Δ FIKK showed symptoms of infection but subsequently recovered. They survived up to day 30 post infection at which point they were euthanized at the end of the experiment (Figure 29).

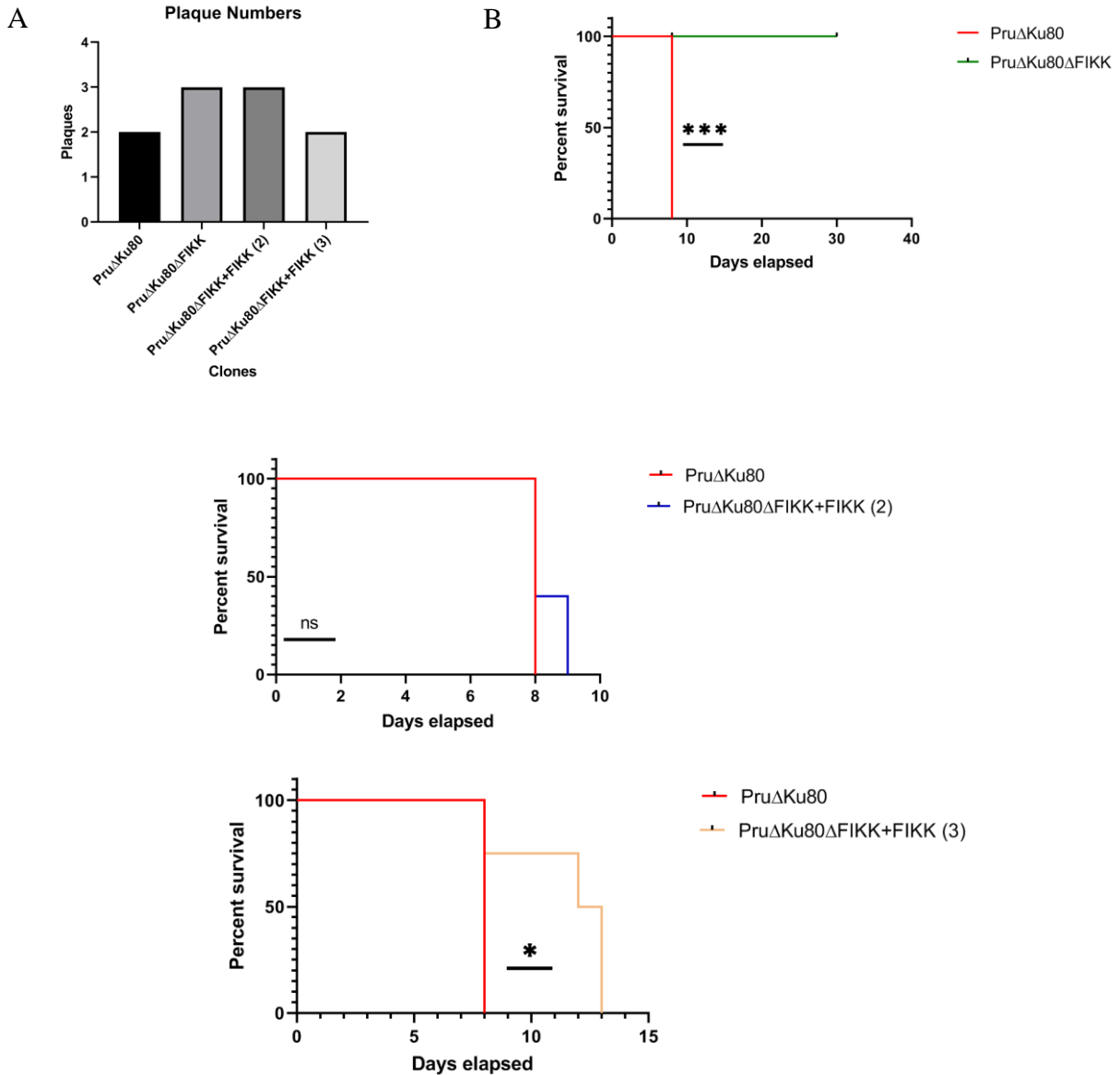


Figure 29: Survival Curves of Acute Infection

A: Mice were infected IP with 200 parasites. Parasite dose for each clone was confirmed by counting the number of HFF plaques in a plaque assay. B: Survival curves of mice infected with WT, Δ FIKK and FIKK complemented clones. Mice infected with Δ FIKK parasites survived acute infection, recovered and appeared healthy through the 30 days post-infection. Mice infected with Pru Δ Ku80 had a similar mortality to mice infected with FIKK complement 2. However, complement 3 showed a minor difference in survival. Statistical analysis was performed using the Log-rank test * $p < 0.05$ *** $p < 0.001$.

Aim 3: Functional Characterization of the FIKK Kinase in Chronic Infection

The FIKK Kinase is Important for Cyst Formation *in vitro*

In Aim 3 we evaluated whether the *T. gondii* FIKK kinase contributed to cyst formation and ultimately chronic infection. Tachyzoite to bradyzoite differentiation as well as cyst formation can be induced *in vitro* in HFF cells in response to exogenous stress. These stresses are typically referred to as bradyzoite-inducing conditions. Wild type parasites, Δ FIKK parasites and complemented clones were compared to determine if the FIKK kinase was important for tachyzoite to bradyzoite differentiation and cyst formation *in vitro* in HFF cells and *in vivo* in mice. FIKK gene deletions in the Pru Δ HPT lines as well as the Pur Δ Ku80 lines were also compared.

Bradyzoite inducing conditions *in vitro* include nitric oxide exposure, nutrient deprivation, alkaline pH stress, and exposure to anti-*Toxoplasma* drugs. We first determined whether the FIKK kinase contributed to parasite cyst formation in response to NO (SNP). Three independent gene deletions for the FIKK gene were assessed, two in the Pru Δ HPT parental parasites and one in the Pru Δ HPT Δ Ku80. Cyst numbers relative to tachyzoites in PVs was evaluated by fluorescence microscopy. DBA staining was used to identify cysts compared to PVs. Cysts were defined as any vacuole positive for CST1 staining with a defined cyst wall around the edge. As shown in Figure 30 and Figure 31, Δ FIKK parasites did not form cysts in the presence of SNP for three days. In contrast, both WT and FIKK complement parasites readily formed cysts in response to SNP.

To determine whether the deletion of the FIKK kinase was important for a general conserved pathway important for tachyzoite to bradyzoite differentiation and cyst formation or just a pathway specific to NO, Δ FIKK parasites were examined to determine

whether they were impaired for cyst formation induced by a panel of established parasite bradyzoite/cyst-inducing conditions. As shown in Figures 27 and 28, Δ FIKK parasites failed to form cysts in response to all of the bradyzoite/cyst-inducing conditions. Additionally, the impact of FIKK gene deletion on spontaneous cyst formation in the absence of exogenous stress was all evaluated. Δ FIKK parasites were also unable to spontaneously convert to cysts in the absence of exogenous inducers of bradyzoites/cysts (Figure 31).

Initial characterization of the importance of the FIKK kinase in cyst formation was performed using the Pru Δ HPT Δ FIKK clones and Pru Δ Ku80 Δ FIKK clones. Our results show that cyst production was impaired for all FIKK gene deleted clones regardless of the parental clones or bradyzoite/cyst-inducing conditions. We also compared the the Pru Δ Ku80, Δ FIKK, and complemented clones to confirm that deletion of the FIKK gene prevented cyst formation by parasites and complementation of the mutants with the FIKK gene restored cyst formation. Complementation of Δ FIKK parasites restored cyst production in the parasites. (Figure 30, Figure 31, Figure 32).

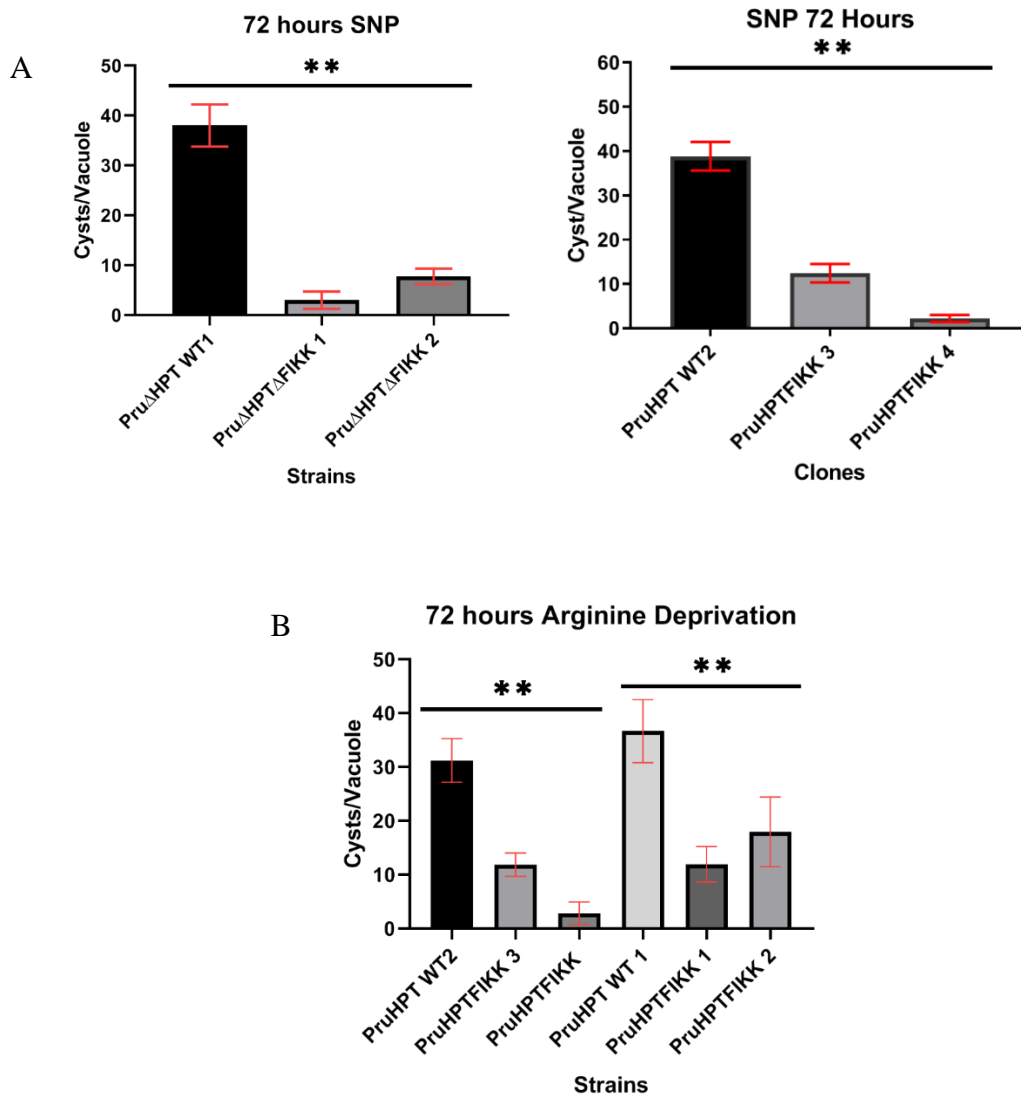


Figure 30: Cyst Formation *in vitro* by Pru Δ HPT and Pru Δ HPT Δ FIKK Clones
 Pru Δ HPT and Δ FIKK clones were inoculated into HFF cells and stressed using different conditions for 72 hours. A. Cyst production in response to exogenous SNP; B Cyst production in response to arginine starvation. Statistical analysis was performed using ANOVA with a Tukey post hoc test. Comparisons were made between the wild-types and their respective groups of Δ FIKK clones with the wild-type significantly different from their Δ FIKK clones, the Δ FIKK clones were not significantly different from each other. Bars are mean with 95% confidence interval. ** $p < 0.01$

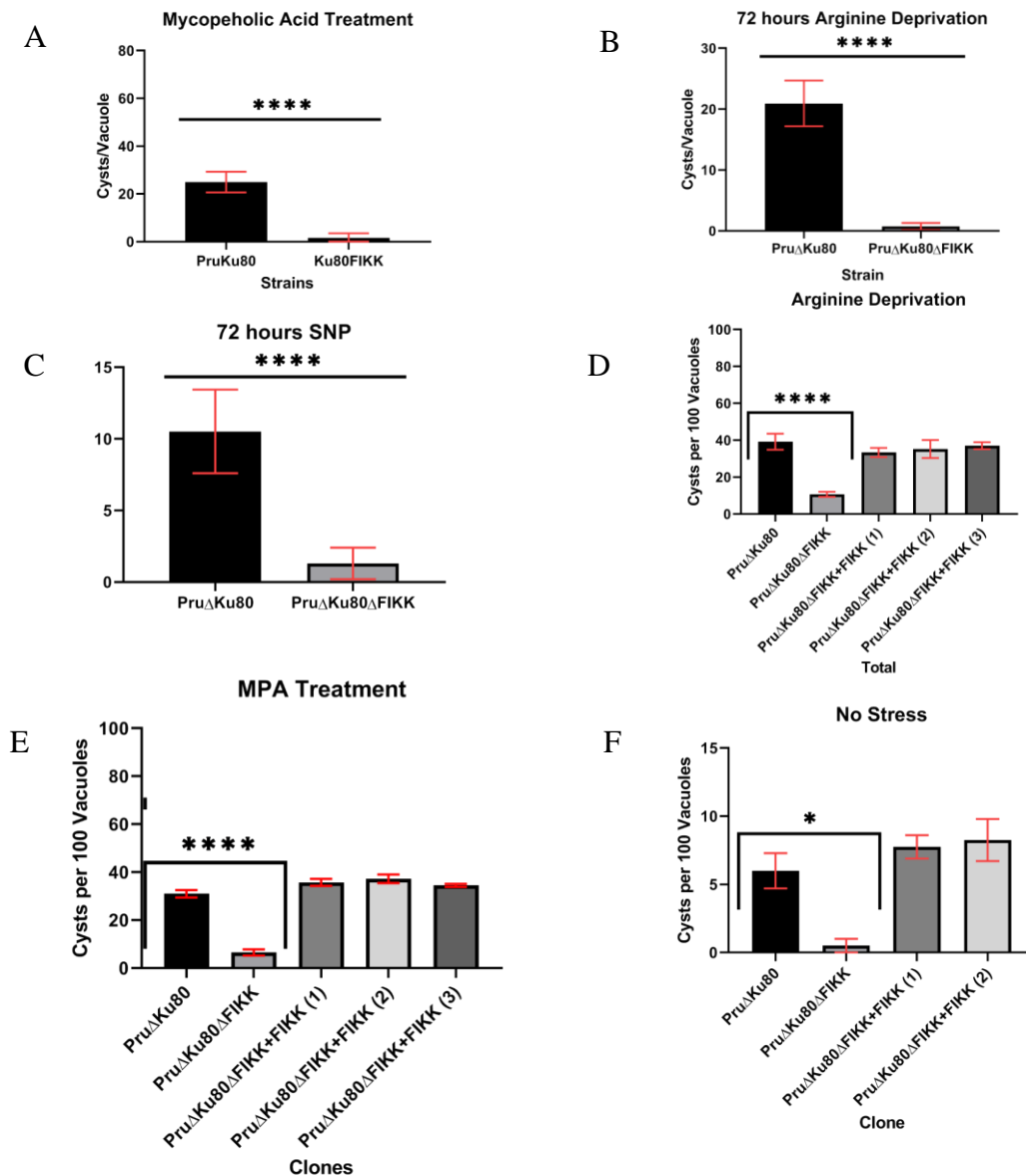


Figure 31: Cyst Formation *in vitro* Pru Δ Ku80.

Cyst formation was statistically significantly different between Pru Δ Ku80 wild-type and Δ FIKK Clones but not between wild-type and complemented clones. Unpaired student's T-test was used to compare two clones, a one way ANOVA was used to compare more than two with a Tukey post hoc test also used to compare groups. Comparisons were made between wild-type and Δ FIKK clones and when present between wild-type, Δ FIKK, and complemented clones. The wild-type clone was significantly different from the Δ FIKK clone, FIKK complements were not different from the wild-type clone. Any statistically significant differences between clones is annotated with asterisks. Bars are mean with 95% confidence interval. * $p < 0.05$ **** $P < 0.0001$

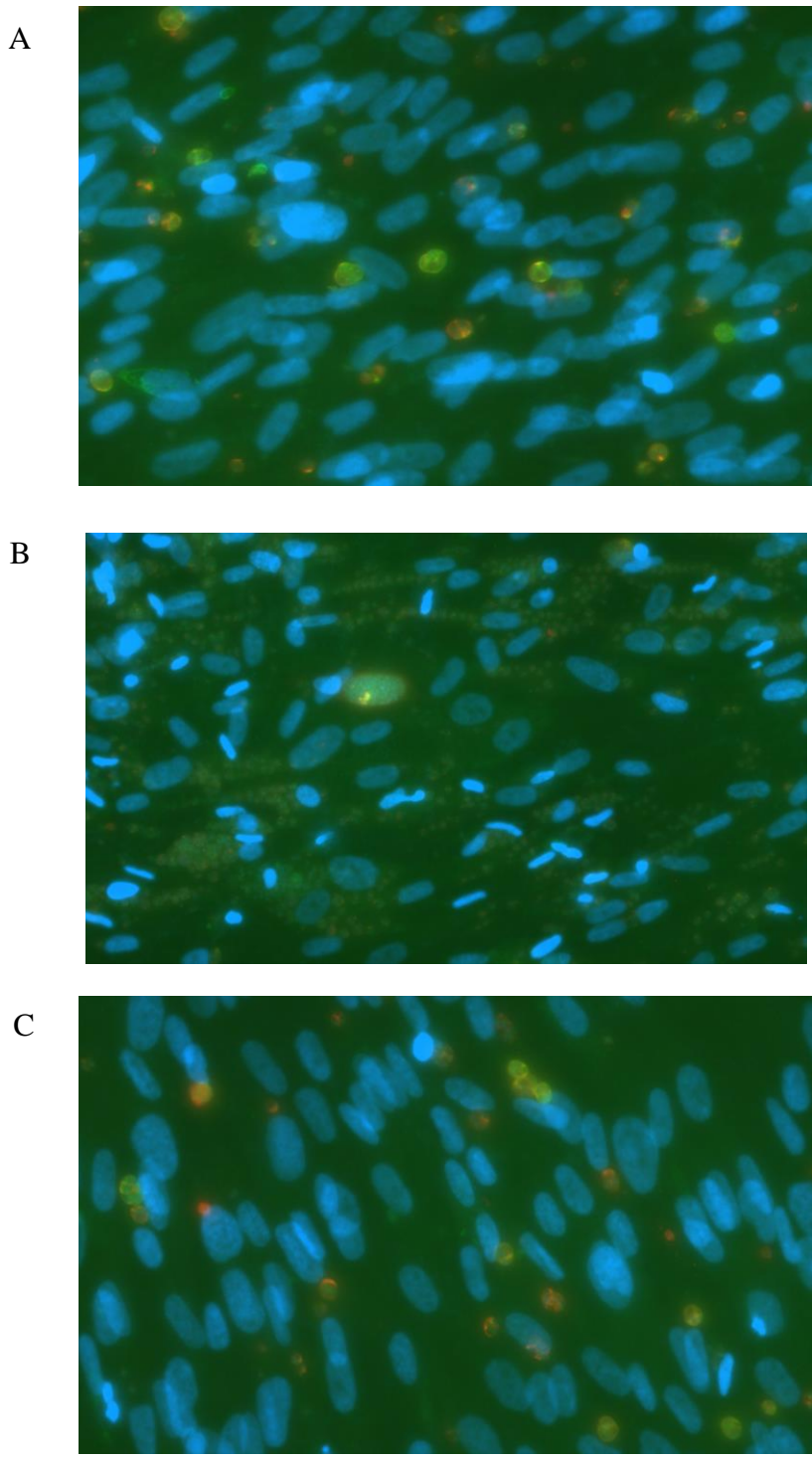


Figure 32: Cysts *in vitro*
In vitro cyst in HFF cells. A. Pru Δ Ku80, B. Pru Δ Ku80 Δ FIKK, C. Pru Δ Ku80 Δ FIKK + FIKK 1. Cysts are stained green with FITC-DBA, Parasites are stained red, and counterstained with DAPI.

The FIKK Kinase is Important for Establishment of Chronic Infection in Mice

Our results indicate that the FIKK kinase is important for cyst formation *in vitro* in HFF cells in response to a variety of known cyst inducing conditions. Thus we evaluated the importance of the FIKK kinase to the establishment of chronic infection. To evaluate chronic infection in mice a parasite dose that allows the parasite to survive the initial acute stage of infection but yet results in significant cyst formation 30 days post-infection must be used. We first compared the two sets of independent FIKK gene deletion in the Pru Δ HPT line wild in CD1 outbred mice. These mice are relatively more resistant to the acute and chronic stages of infection. Thus, CD1 outbred mice are more likely to survive acute infection with *T. gondii* to establish chronic infection. In independent experiments CD1 outbred mice were challenged ip with either 500 parasites (Pru Δ HPT compared to wild-type 2) or 2000 parasites (Pru Δ HPT compared to wild-type 1).

As shown in Figure 33, in one experiment the Δ FIKK clones had significantly fewer cysts in the brain at 30 days post-infection compared to WT in CDI outbred mice. In a second experiment Δ FIKK clones also had fewer cysts than WT mice but the result was not significant. The high standard deviation associated with cyst numbers in mice is due to the genetic heterogeneity in the CD-1 outbred mice. Therefore, in a subsequent experiment we used inbred BALB/C mice. In this experiment we compared the Pu Δ Ku80 parasites with its respective Δ FIKK and FIKK complemented clones. Mice were inoculated IP with 200 parasites. 30 days post-infection mice were euthanized and brains were stained for cysts using florescent-conjugated DBA and examined by florescence microscopy.

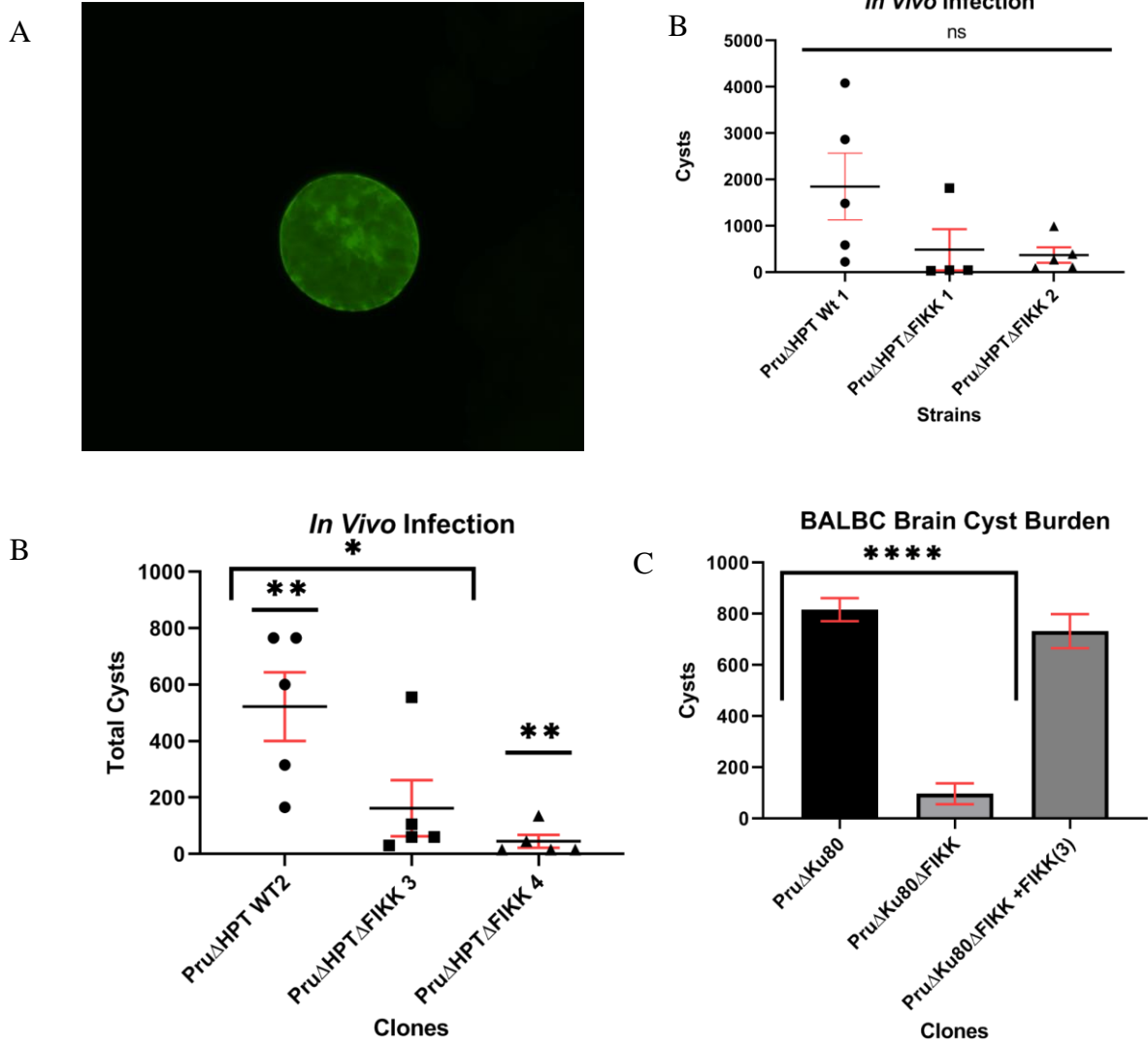


Figure 33: Infection with Δ FIKK Parasites Results in Decreased Numbers of Brain Cysts
 A. Picture of a DBA-stained brain cyst from mice infected with WT parasites. B. Number of brain cysts following infection of CD1 outbred mice with WT parasites or Δ FIKK clones. C. Number of brain cysts following infection of CD1 outbred mice with WT parasites and Δ FIKK clones from an independent electroporation then in B. C. Number of cysts in the brains of BALB/c mice 30 days post-infection with Pru Δ ku80, Δ FIKK clones and FIKK complemented clones. Analysis was performed using ANOVA with a Tukey test * $p < 0.05$ ** $p < 0.01$ **** $p < 0.0001$

The FIKK Kinase is Important for Tachyzoite Differentiation to Bradyzoites.

Previous experiments showed that removal of the FIKK gene from the genome negatively affected the parasite's ability to form cysts both *in vitro* and *in vivo*.

Tachyzoite to bradyzoite transition and the resulting production of cysts is a complicated and multistep process. Transition between stages involves changes in the expression of more than a thousand genes, production of cyst wall components and their trafficking to the PVM, remodeling of the PVM to form a nascent cyst wall and inner membrane. In our previous studies we showed that the FIKK kinase is required for efficient formation of cysts in response to cyst-inducing conditions. The question remained where in this process of cyst formation the FIKK kinase is required. First, we evaluated whether the FIKK kinase was required for one of the earliest steps in cyst production; the initiation of tachyzoite differentiation to bradyzoites. Thus we evaluated whether parasites deficient for the FIKK kinase increased their expression of canonical markers specific for bradyzoites as compared to tachyzoites in response to cyst inducing conditions.

Extracellular WT and Δ FIKK clones were exposed for 4 hours to bradyzoite/cyst inducing conditions prior to allowing the parasites to invade an HFF cell monolayer.

Bradyzoite/cyst-inducing conditions were maintained in the parasite-infected culture for 24, 48, and 72 hours. Parasites were lysed at each time point, RNA isolated and qRT-PCR was performed to evaluate the expression of a panel of canonical bradyzoite genes Bag1 which is a surface marker of bradyzoites, LDH2, and ENO1 metabolic genes expressed in bradyzoites, and cyst wall proteins CST1, BPK1, and MCP4. We found a marked reduction in the expression of bradyzoite associated genes in the

Pru Δ HPT Δ FIKK and similar, though not as sharp, reduction in bradyzoite markers in Pru Δ Ku80 Δ FIKK that returned to the wild-type baseline in the complements (Figure 34). These results indicated a role for the *Tg*FIKK in regulating these genes. Since it was clear that the Δ FIKK parasites were impaired for tachyzoite to bradyzoite differentiation, we evaluated early events associated with entry of tachyzoites into the bradyzoite differentiation pathway at the G1 cell cycle checkpoint. The current determinants that are important for entry into the bradyzoite differentiation pathway are unknown, but we examined expression of members of the Ap2 transcription factors that have been shown to be important in the process of tachyzoite to bradyzoite differentiation. We examined the expression of the Ap2 transcription factors over time in Pru Δ Ku80 line and the clones made from it. We examined the expression at a baseline (4 hours extracellularly) to 24, 48, and 72 hours under stress (MPA stress) to examine if there was a difference in expression under bradyzoite inducing conditions. The factors examined were a series known to be involved in tachyzoite to bradyzoite transition (Figure 35, Figure 36). We found only a minor difference of expression in two factors in the Δ FIKK line Ap2IX-4 at 48 hours, and Ap2IV-3 at 4 hours.

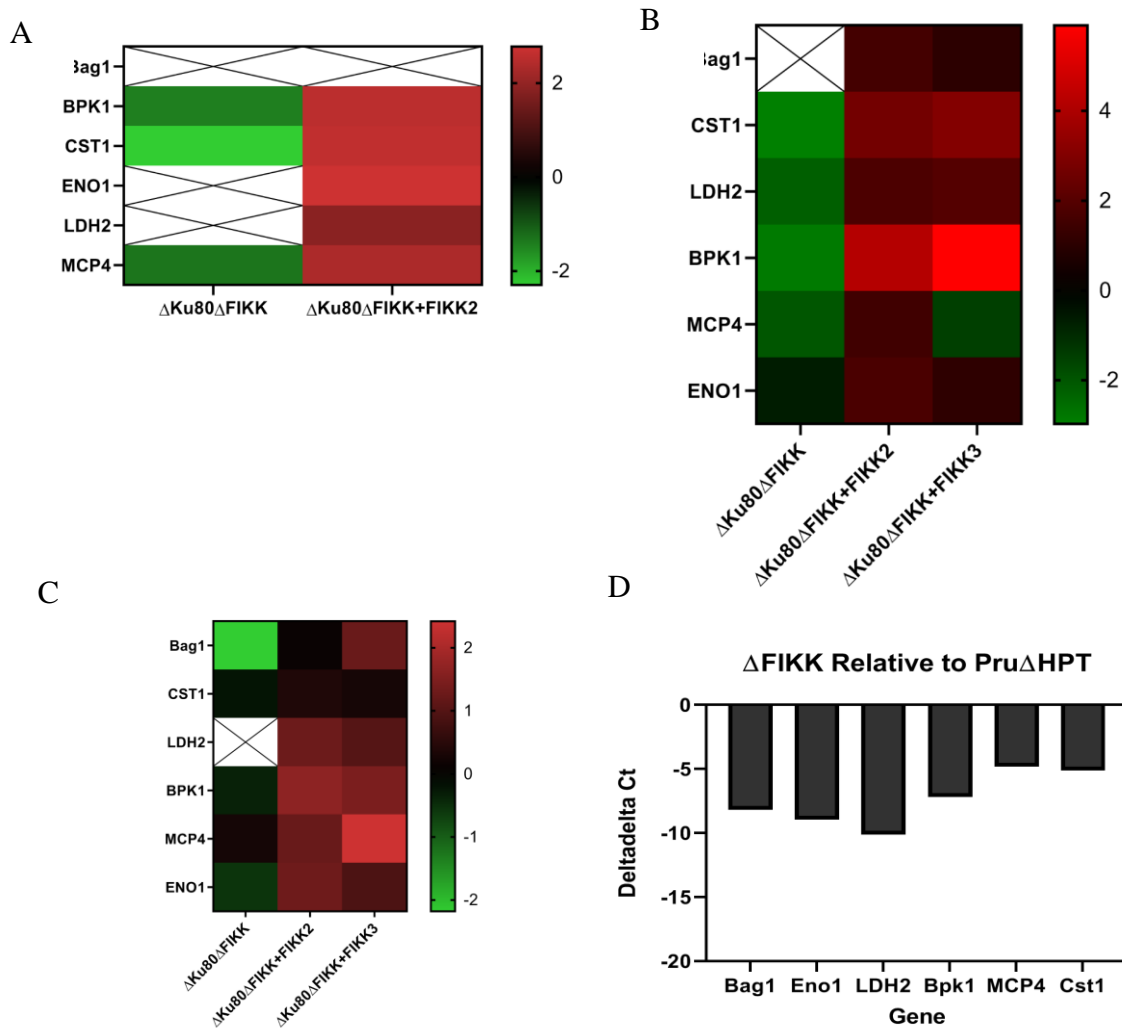


Figure 34: Expression of Canonical Bradyzoite Marker in WT versus $\Delta FIKK$ Parasites Cultured in Bradyzoite/cyst-inducing Conditions.

Expression of canonical bradyzoite associated markers in WT versus $\Delta FIKK$ parasites. qRT-PCR was performed with primers listed in Table 5 for each gene. Expression was normalized using the housekeeping gene tubulin (Tub1) and quantified using the $\Delta\Delta Ct$ method. Parts A-C Pru $\Delta Ku80\Delta FIKK$ and FIKK complement compared to Pru $\Delta Ku80$ wild-type at 24, 48, and 72 hours post-infection. Part D. Pru ΔHpt and Pru $\Delta HPT\Delta FIKK$ compared at 72 hours post-infection.

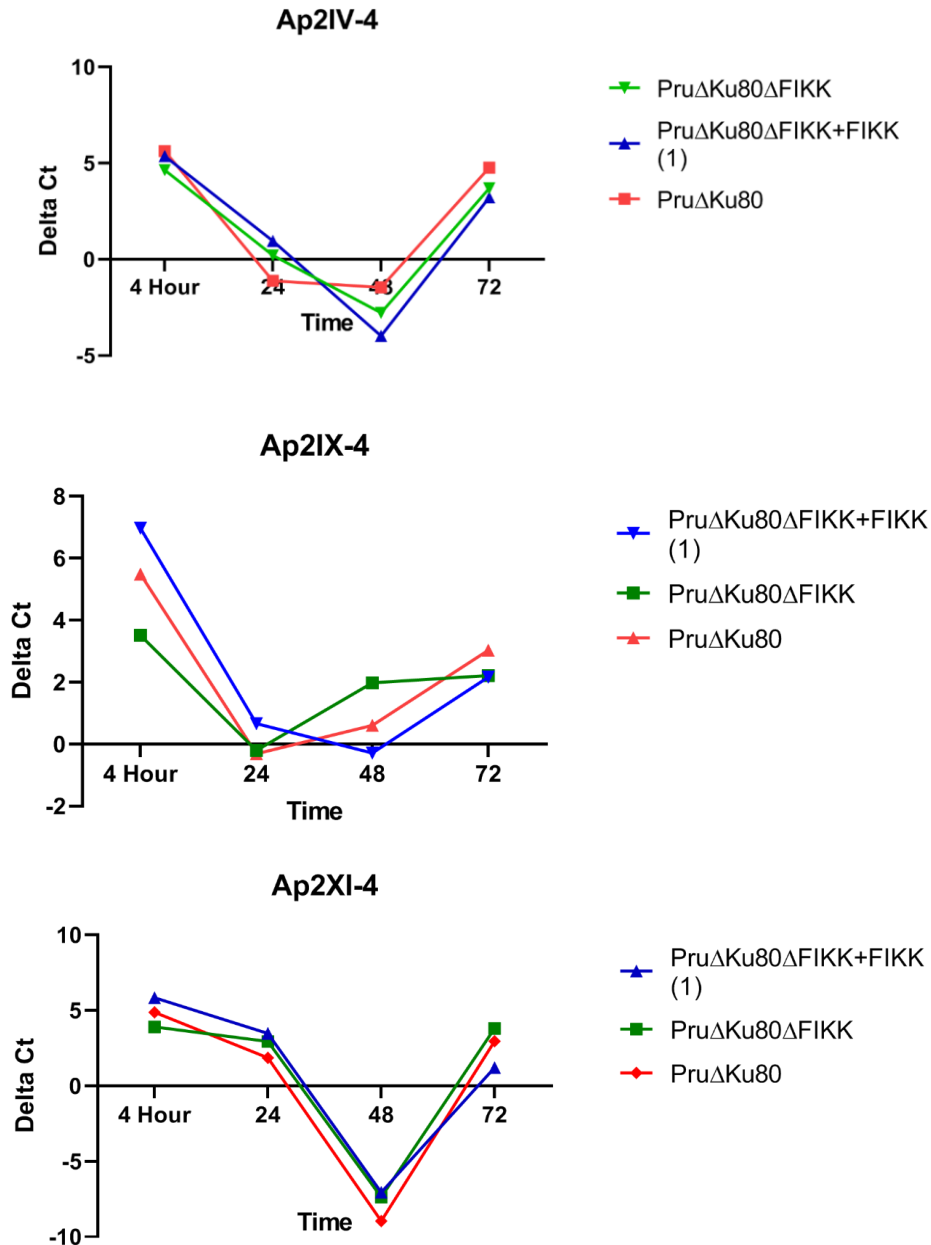


Figure 35: Expression of Ap2 Transcription Factors in WT Parasites, Δ FIKK Clones and FIKK Complemented Parasites
 Differential expression of these Ap2 transcription factors in tachyzoites and bradyzoites are associated with stage differentiation. Plots are the Δ Ct for the various genes, expression normalized to Tub1, at different time points under stress conditions (MPA treatment).

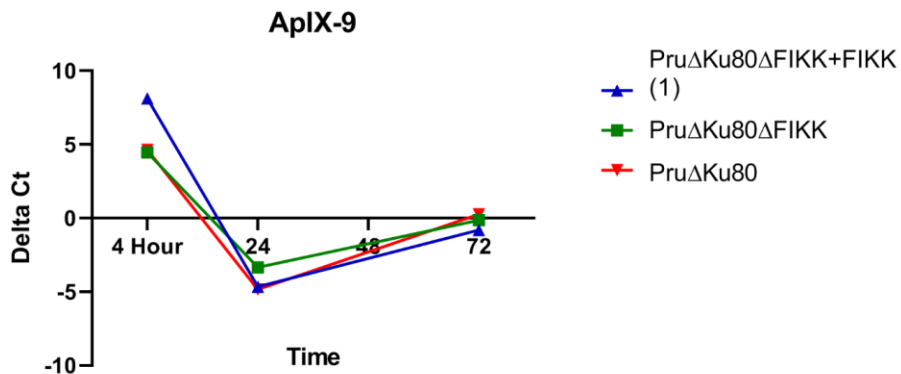
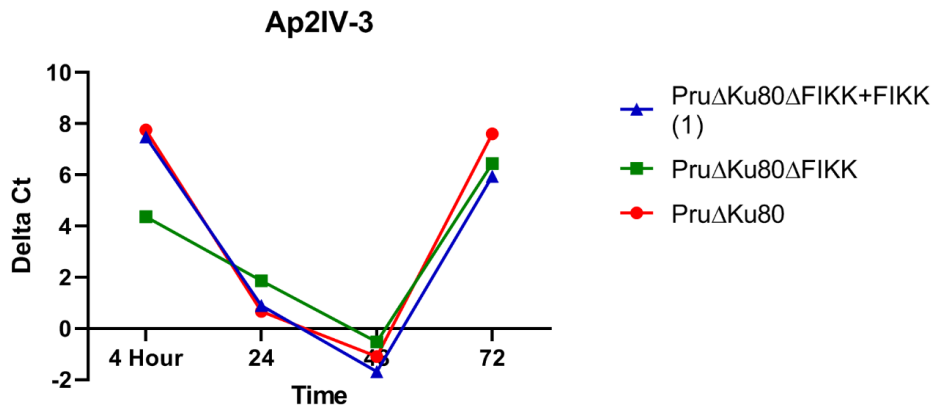
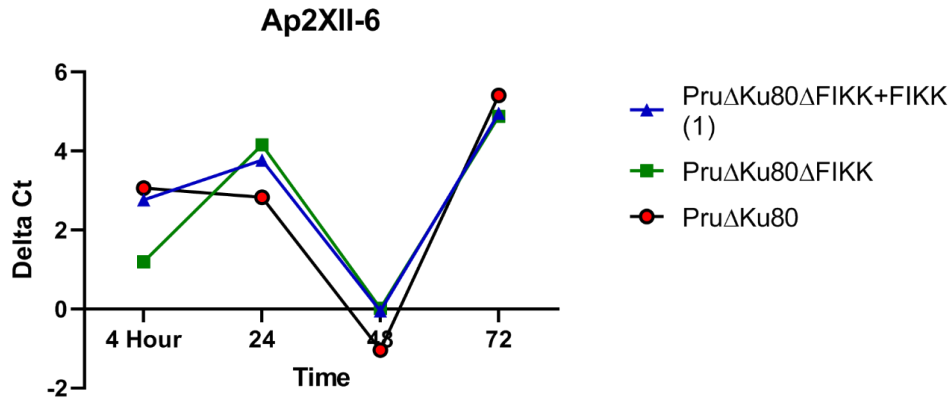


Figure 36: Expression of Ap2 Transcription Factors in WT Parasites, Δ FIKK Clones and FIKK Complemented Parasites
 Differential expression of these Ap2 transcription factors in tachyzoites and bradyzoites are associated with stage differentiation. Plots are the Δ Ct for the various genes, expression normalized to Tub1, at different time points under stress conditions (MPA treatment)

FIKK Target Search

The sequence targeted for phosphorylation by *Tg*FIKK are currently unknown. The two closest homologous to *Tg*FIKK are *P. falciparum* FIKK 8 and the FIKK kinase in *Cryptosporidium parvum* (Figure 37). While the *Tg*FIKK is significantly larger than either of the homologs in *Plasmodium falciparum* and *Cryptosporidium parvum*, the three proteins have a high degree of homology at the C terminal ends where the kinase domain is located. Previous studies have determined a motif targeted by both *Cp*FIKK and *Pf*FIKK8 (58). We performed a search in ToxoDB.org for proteins containing this motif. 59 genes were found to contain this protein motif in the *T. gondii* genome. While most are hypothetical proteins a few known transcription factors were discovered including four known Ap2 transcription factors (Ap2VIII-2, Ap2XII-4, Ap2III-2, and Ap2IX-9) Ap2IX-9 is known to be important for bradyzoite differentiation. While annotated as a repressor or bradyzoite associated genes Ap2IX-9 expression increases during stage differentiation and is theorized to keep the parasite in a “holding pattern” during the transition (56). (Table 7).

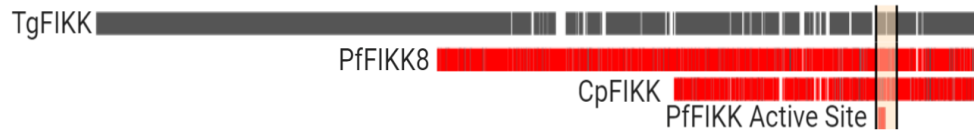


Figure 37: Alignment of *TgFIKK*, *PfFIKK8*, *PfFIKK8* Active site, and *CpFIKK*
 Alignment of the *TgFIKK*, *PfFIKK8*, *CpFIKK*, proteins, and the *PfFIKK8* active site. The *TgFIKK* is significantly longer than the other two FIKK proteins while all three proteins have a high degree of homology at the C-terminus. The three proteins have a 33% pairwise identity. The catalytic kinase domain is intact in all three of the proteins.

Table 7: Genes in the *T. gondii* Genome that Contain the Putative FIKK Target Sequence

Gene.ID	Product. Description
TGME49_202070	hypothetical protein
TGME49_204380	hypothetical protein
TGME49_208400	hypothetical protein
TGME49_208710	DNA/RNA non-specific endonuclease
TGME49_209510	hypothetical protein
TGME49_209850	RNA recognition motif-containing protein
TGME49_212130	phospholipase, patatin family protein
TGME49_214900	hypothetical protein
TGME49_215370	hypothetical protein
TGME49_217490	hypothetical protein
TGME49_217855	hypothetical protein
TGME49_218550	PIK3R4 kinase-related protein
TGME49_223550	hypothetical protein
TGME49_225090	hypothetical protein
TGME49_226280	ribosomal protein L28, putative
TGME49_227000	hypothetical protein
TGME49_228380	hypothetical protein
TGME49_232240	hypothetical protein
TGME49_233120	Ap2 domain transcription factor Ap2VIII-2
TGME49_234200	hypothetical protein
TGME49_238970	hypothetical protein
TGME49_239420	protein kinase
TGME49_240370	Toxoplasma gondii family E protein
TGME49_243970	hypothetical protein
TGME49_247700	Ap2 domain transcription factor Ap2XII-4
TGME49_252870	hypothetical protein
TGME49_253440	cell-cycle-associated protein kinase SRPK, putative
TGME49_260640	autophagy protein apg9 protein
TGME49_261490	hypothetical protein
TGME49_261610	hypothetical protein
TGME49_262950	hypothetical protein
TGME49_263610	hypothetical protein
TGME49_264670	DNA polymerase family B protein
TGME49_266930	general transcription factor IIH polypeptide 3 GTF2H3
TGME49_268020	transporter, major facilitator family protein
TGME49_268035	hypothetical protein
TGME49_268370	non-specific serine/threonine protein kinase
TGME49_270060	hypothetical protein

TGME49_270720	hypothetical protein
TGME49_270930	hypothetical protein
TGME49_270940	hypothetical protein
TGME49_285230	PRP38 family protein
TGME49_288420	hypothetical protein
TGME49_289280	hypothetical protein
TGME49_292300	DNA-directed RNA polymerase III RPC8
TGME49_299150	Ap2 domain transcription factor Ap2III-3
TGME49_305640	metallo-beta-lactamase domain-containing protein
TGME49_306400	hypothetical protein
TGME49_306620	Ap2 domain transcription factor Ap2IX-9
TGME49_307570	glycerol-3-phosphate dehydrogenase (gpdh), putative
TGME49_312420	hypothetical protein
TGME49_313030	hypothetical protein
TGME49_313140	isocitrate dehydrogenase
TGME49_313270	hypothetical protein
TGME49_313590	hypothetical protein
TGME49_314055	splicing factor, putative
TGME49_315810	tRNA nucleotidyltransferase/poly(A) polymerase family protein
TGME49_315950	zinc finger, C3HC4 type (RING finger) domain-containing protein
TGME49_326500	hypothetical protein

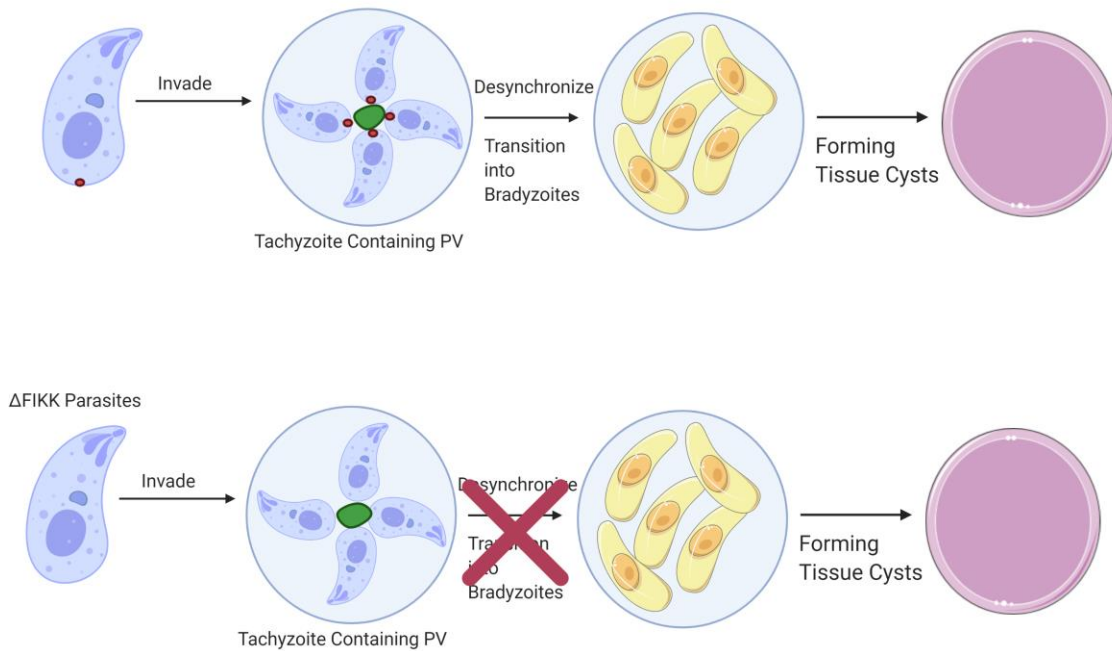


Figure 38: Schematic Model of the Current Model of Where and How the FIKK Kinase Functions in Parasite Cyst Formation.

Normal parasites (top row) with the FIKK localized to the basal end of the parasite (red dot) invade and form PVs with residual bodies linking the parasites together at the basal end. This residual body forms a bridge to synchronize the parasite through cell-cell communication. During stage differentiation this bridge is lost as parasites transition to bradyzoites. The FIKK deleted parasites (bottom row) and invade and form PVS with residual body linkages, however something is lost during the transition process. Perhaps the ability to desynchronize, or the loss of an ability to signal between the parasites necessary to start the transition.

Discussion

FIKK kinases are a unique family of kinases specific for the Apicomplexa. Most Apicomplexa parasites have a single FIKK kinase but the family is enlarged in *Plasmodium falciparum* and absent in the piroplasms. The function of the FIKK kinases in the Apicomplexa is poorly understood. However, in *Plasmodium* they have been implicated in cytoskeletal alterations in infected red blood cells, particularly in erythrocyte membranes. FIKK kinases in *Plasmodium falciparum*, and *Cryptosporidium parvum* have been shown to have serine threonine phosphorylation activity. Preliminary data from another laboratory has shown the *T. gondii* FIKK kinase also has kinase activity. However, to date our labs and others have been unable to purify the *T. gondii* FIKK kinase catalytic domain as it appears to be unstable and prone to degradation (data not shown).

In a previous study, our laboratory performed an initial characterization of the *T. gondii* FIKK kinase in the virulent RH strain of the parasite. This is a lab-adapted strain originally purified from an infected person that is adapted to growth as a tachyzoite in cell culture. The RH strain is extremely virulent in mice; a single parasite is lethal in 6-10 days. Endogenous tagging of the 3' end of the RH-FIKK kinase with YFP revealed it localized to the basal complex of the parasite in association with the basal complex protein MORN1. A YFP-tagged FIKK protein and a Ty-tagged FIKK protein both localized to the parasite basal complex apical to inner membrane complex protein-5 and Centrin-2. The basal complex is an organelle that is critical for parasite replication (4, 26). MORN-1 in the parasite complex is critical for the formation of a basal contractile ring that is important to segregate daughter cells during endodyogeny. However MORN1 and the basal complex is also present in mature parasites suggesting a possible role in

addition to daughter cell formation and segregation (26). Deletion of the FIKK kinase in the RH strain did not impact parasite replication (72). This may not be surprising because unlike the basal complex protein MORN1 and other known basal complex proteins, the FIKK kinase only localizes to the basal complex of mature parasites and it is not found in daughter cells during parasite division by endodyogeny (72).

The goal of the current study was to evaluate the importance of the *T. gondii* FIKK kinase in a parasite strain that remained capable of completing the parasite mammalian cycle that includes replication as a tachyzoite during acute infection and stage differentiation to bradyzoites contained in tissue cysts to establish chronic infection. The Type II genotype *T. gondii* strains are the most common cause of toxoplasmosis in humans (13). They are virulent in mice but are often called avirulent because they are less virulent than the Type I genotypes of the parasite that includes the RH strain. Thus we deleted the FIKK gene in the Type II genotype Prugnaud strain of *T. gondii* and examined the effect on the parasite's lytic cycle, differentiation from tachyzoites to bradyzoites to form encysted parasites and during acute and chronic infection in mouse models of toxoplasmosis. We also complemented the Δ FIKK clones with the FIKK kinase expressed under the control of its endogenous promoter as a transgene integrated into the parasite UPT locus. Our studies show the *T. gondii* FIKK kinase is important for the ability of the parasite to initiate stage differentiation from tachyzoites to bradyzoites. Parasites deficient for the FIKK kinase are impaired for cyst production both *in vitro* in cell culture in response to exogenous bradyzoite/cyst-inducing conditions and *in vivo* in mice.

***Tg*FIKK is Not Important for the Parasite's Lytic Cycle**

Our study indicates no significant role for *Tg*FIKK in parasite replication in either the virulent RH strain that replicates primarily as a tachyzoite or the less virulent Prugnaud strain that retains its ability to interconvert between tachyzoites and bradyzoites. Deletion of the FIKK gene did not have a significant effect on the parasite's lytic cycle in HFF cells as determined by plaque assays *in vitro*. Furthermore, studies focused on specific steps in the parasite's lytic cycle including efficient parasite invasion, and replication revealed no significant defect in Δ FIKK parasites.

Δ FIKK Parasites Retain Growth Characteristics of Tachyzoites When Exposed to Bradyzoite-differentiation Conditions.

A difference in plaque size was found with the Δ FIKK clone producing larger plaques under exogenous bradyzoite-inducing conditions stress. In contrast, no difference was seen in plaque size in no stress conditions. Our interpretation of these data in light of our other findings, is that the Δ FIKK parasites remain as tachyzoites in bradyzoite-inducing conditions. Thus the ability to persist as replication-competent tachyzoites instead of differentiation into slow-growing bradyzoites, results in increased plaque size in HFF cells in bradyzoite-inducing conditions (Figure 26)

The *Tg*FIKK Kinase Has a Moderate Impact on Acute Infection in Mice

The acute infection in mice is mediated by the tachyzoite stage of the parasite. Our studies show that the deletion of the FIKK kinase does impact acute infection with *T. gondii* in the mouse model. C57BL/6 mice infected with wild type or FIKK complemented parasites died during acute infection. In contrast, none of the mice infected with the Δ FIKK parasites died during acute infection, although they did

transiently exhibit sick behavior including ruffled fur. It is unclear whether the reason that the Δ FIKK parasite is less lethal during acute infection is a consequence of their impaired cyst production or some other undiscovered defect in parasite fitness *in vivo*. Other studies have shown that cyst formation can occur as early as 1-day post-infection (12); thus it is possible that tachyzoite differentiation to bradyzoites and even cyst formation may alter the host immune response or the parasite during acute infection. This would certainly align with our other data that showed a marked deficiency in cyst formation. However, the mice were carefully monitored for signs of sickness over the course of the experiment, with all the mice showing symptoms around day 7 post-infection. This would indicate that all of the mice, including those infected with the Δ FIKK clones, developed a systemic and symptomatic infection. However, only the mice infected with the Δ FIKK clone were able to resolve the symptoms of acute infection and recover.

It is also possible that the Δ FIKK parasites were less virulent during acute infection because they retain surface proteins and other immunogenic proteins associated with tachyzoites since they are impaired for differentiation from tachyzoites to bradyzoites. Tachyzoites, unlike bradyzoites, generate a robust cell-mediated immune response that may be important for the parasite to avoid killing its host during acute infection. *T. gondii* parasites need to replicate during acute infection and disseminate systemically in order to establish a chronic infection that can transmit the parasite through carnivorousism. Thus the parasite has evolved mechanisms that enable robust replication and dissemination but also stimulates a cell-mediated immune response that most often prevents lethal acute infection. In contrast, to tachyzoites, bradyzoites appear

to be less immune-stimulatory, and bradyzoites contained in tissue cysts are largely non-immunogenic. Since the Δ FIKK parasites cannot transition to bradyzoites properly, the prolonged tachyzoite stage may result in a more potent clearance of parasites by the increased stimulatory effect on host immunity. Studies have shown that constitutive expression of certain *T. gondii* proteins during infection can have a strong immunogenic effect. One of these immune stimulatory genes is the tachyzoite marker Sag1(59). It is also possible the Δ FIKK parasites may have dysregulation in tachyzoite and bradyzoite genes that alter either parasite fitness or immunity. Studies of the Ap2 transcription factors, particularly Ap2IV-3, and Ap2IX-4 have speculated on the paradoxical nature of how a “bradyzoite repressor” can be upregulated during tachyzoite to bradyzoite stage differentiation. The current working hypothesis is that the transition is a carefully regulated process in which the parasite can produce many highly immunogenic proteins that cannot be safely expressed until the bradyzoite transition is complete and proper mature cysts have been formed (64). That dysregulation of this process may result in the expression of “late bradyzoite genes” far earlier than the parasite needs and that this could actually increase the immune response of the host. The list of known bradyzoite genes is long, with ~1000 genes known to be changed between tachyzoites and bradyzoites. So our results are by no means exhaustive, and it is still possible that some genes are being expressed in a dysregulated manner in our Δ FIKK clones that could cause the mutant parasites to be cleared more easily by the host. While such a dysregulation is possible, we have not seen any unusual expression of bradyzoite-associated genes when their expression was studied over time (Figure 34). It would seem based on our results that the Δ FIKK parasites are not initiating an early step important for

tachyzoite to bradyzoite differentiation, and in some way, this is moderately impacting fitness during acute infection.

TgFIKK is Important for Early Events that Regulate Tachyzoite to Bradyzoite Differentiation.

Our results indicate that the FIKK kinase is important for a conserved pathway that results in cyst formation in response to all known exogenous mediators that induce cyst formation. The Δ FIKK clones showed a marked reduction in cyst formation *in vitro* for all exogenous stress conditions that were tested. Furthermore, the Δ FIKK parasites were also impaired for spontaneous cyst formation (Figure 30, Figure 31). We concluded from these experiments that the FIKK kinase is important in the cyst formation process irrespective of the presence or source of exogenous stress.

The process of cyst formation from tachyzoites is a stepwise process in which the parasite has to change its epigenetic profile and gene expression, followed by the expression of necessary genes for bradyzoites and cysts, and then the trafficking of components for the cyst wall out of the parasite and to the PVM where they can be assembled into the cyst wall. We first considered a role for the FIKK kinase in assembling the cyst wall based on previous studies that suggest the presence of a pore in the posterior end of the parasite. The parasite intramembrane complex (IMC) is located just beneath the plasma membrane from the anterior to the posterior poles of the parasite. It is interrupted only by a micropore (MP) located in the posterior end of the parasite near or part of the parasite basal complex. This pore is believed to be the primary portal through which secretion of vesicles necessary to form the intracyst network, and possibly the cyst wall, takes place (71). Electron micrographs have shown the presence of membrane bound vesicles being trafficked out of the posterior end of the parasite These

membrane bound vesicles appear to contain proteins similar to those in the cyst matrix and ultimately the cyst wall (71). Also a tubular vesicular network called the IVN that links the parasite and PV membrane has been shown to be associated with the posterior end of the parasite (38, 55). Thus far we have no definitive data that rigorously proves or disproves a potential role for the parasite basal complex or FIKK kinase in the structure or function of this posterior pore. No qualitative difference could be seen between the few cysts formed by the Δ FIKK clones and the wild-type and FIKK complement clones. We also evaluated whether Δ FIKK parasites appeared blocked in a step directly related to cyst wall formation. However, there was no evidence that Δ FIKK parasites created partial cyst walls or accumulated cyst wall products in the PV that failed to be exported to a nascent cyst wall (data not shown). Thus we currently have no evidence that the FIKK kinase is important for the export of cyst wall components to form a nascent cyst wall. During our initial study of the Pru Δ HPT Δ FIKK we examined the expression of Ap2 transcription factors and bradyzoite associated genes at 72 hours under stress conditions and found that the Δ FIKK clones had an expression profile more like that of tachyzoites than like bradyzoites (Figure 35, Figure 36). These differences supported the hypothesis that the Δ FIKK clones were not capable of transitioning into the bradyzoite stage. Thus we compared wild type, Pru Δ Ku80, the Δ FIKK clone and the FIKK complements in bradyzoite/cyst-inducing conditions to determine how early Δ FIKK parasites showed a difference in the expression of tachyzoite and bradyzoite genes known to be involved in tachyzoite bradyzoite interconversion. The three-best studied Ap2 genes known to be involved in cyst formation are Ap2IV-3, Ap2IX-4, and Ap2IX-9. We compared the change in expression of these genes by qRT-PCR at key time points after exposure of

wild type, Δ FIKK and FIKK complemented parasites to bradyzoite/cyst-inducing conditions (Figure 35, Figure 36), and evaluated our results against the known functions of these AP2 transcription factors in regulation of tachyzoite to bradyzoite differentiation. We examined expression from an extracellular time point without stress, compared to 24, 48, and 72 hours post-infection after 4 hours of external MPA/CO₂ starvation stress in order to induce differentiation to bradyzoites. We had hoped that by comparing the normalized expression values (Δ Ct) of the genes between the clones over time some pattern could be seen in which the Δ FIKK clone would be different from the wild-type and complement clones. A modest difference unique to the Δ FIKK parasites was found at the 4 hour extracellular time point for Ap2IV-3. Interestingly Ap2IV-3 is considered an activator of bradyzoite transition and so its higher level earlier in wild type and FIKK complement parasite clones suggest that in the absence of the FIKK kinase parasites may respond to exogenous signals that trigger tachyzoite to bradyzoite differentiation or that parasites are impaired for entry into the bradyzoite differentiation pathway. The Δ FIKK clone also differs in its expression of Ap2IX-4 at 48 hours. Its expression is decreased in the Δ FIKK clone, like wild type and FIKK complement parasites in intracellular parasites exposed to bradyzoite-inducing conditions. However, its expression is elevated at 48 hours only in Δ FIKK parasites. Ap2IX-4 is considered a bradyzoite repressor and a falloff in expression of this factor is important for the parasite to enter into the process. This may suggest that the Δ FIKK parasites may be impaired for entry into the bradyzoite differentiation process but may also upregulate its expression of Ap2IX-4 in prolonged bradyzoite-inducing conditions. Although preliminary, these studies suggest that the FIKK kinase may play a multifactorial role in maintaining the parasite as a tachyzoite and

preventing its entry into a bradyzoite differentiation pathway. It is worth noting that we examined expression at the AP2s at the transcript level and many published studies used tagged forms of the AP2 transcription factors to evaluate protein expression. Recently a master regulator of bradyzoite transition called BFD1 has been identified (87). We attempted to detect this gene by qRT-PCR but could not find a difference between the Pru Δ Ku80 wild-type and Δ FIKK clones.

RNA sequencing was performed to determine if there were significant differences between the wild-type Pru Δ HPT and Δ FIKK clones. Based on a cutoff of 1.5 fold differential expression and an adjusted p value of less than 0.05, it was very clear that deletion of the FIKK kinase did not strongly impact global gene expression during normal *in vitro* growth conditions in cell culture in HFF cells. Fewer than 10 genes had differential expression in the Δ FIKK clones compared to WT. Most genes that were differentially expressed between WT and Δ FIKK clones are annotated as hypothetical proteins. Thus we are unable to currently prioritize the changes based on gene annotation or function domains that might inform function. The only consistently different gene at all time points was RuvB2 which is a component of the holiday junction important for homologous directed repair, a pathway in *T. gondii* upregulated in the tachyzoite stage (27). No genes were found to be different in the proteomic and phosphoproteomic data for the wild type and Δ FIKK parasites in the absence of exogenous stress. However, we were unable to purify the parasite and PV from the HFF cells and thus the depth of detection of proteins and phosphorylated proteins was limited. Consistent with a lack of sufficient depth for the proteomics study, the FIKK kinase was not present in the proteome or phosphoproteome data.

The exact mechanism of how the FIKK kinase contributes to tachyzoite to bradyzoite differentiation is unknown. The FIKK kinase substrates or associated proteins are also unknown. Another group (58) has identified potential protein targets of the closest homologous to TgFIKK in *Plasmodium* and *Cryptosporidium*. These FIKK8 homologs identified a motif consisting of a serine with arginine residues at the +3 and -3 positions with two hydrophobic amino acids in between as being a potential target. A search of the *T. gondii* genome database (ToxoDB) using a motif search based on this residue sequence identified 59 hits that were found to be positive for this motif. Three Ap2 transcription factors were in this list, Ap2XII-4, Ap2III-3, and Ap2IX-9. Ap2IX-9 is a repressor of bradyzoite genes (64). However we could not find information about the other Ap2 transcription factors. Most of the genes on the list are hypothetical proteins. However some have been annotated with at least one being a zinc finger containing protein which are known to bind DNA however no information on this protein could be found.

The FIKK Kinase is Important for Chronic Infection.

Our comparison of chronic infection with wild type, Δ FIKK and FIKK complement parasite clones revealed that the FIKK kinase was important for the presence of cysts in the brain of infected mice 30 days post-infection. However, the studies show that cysts can still form in the absence of the FIKK kinase, but the number is dramatically reduced both *in vitro* and *in vivo* during chronic infection. The low number of cysts in the brains of infected mice is likely a reflection of the inefficiency of tachyzoite to bradyzoite differentiation and cyst formation in the absence of the FIKK gene. However it is also possible that fitness defects associated with the deletion of the FIKK kinase during acute

infection may also impact the number of brain cysts. A comparison of parasite numbers in tissues over the time course of acute and chronic infection is needed to ultimately dissect differences during acute or chronic infection.

In summary our studies have shown that the FIKK kinase in *T. gondii* is critical for tachyzoite to bradyzoite differentiation as well as cyst formation *in vitro* and *in vivo* during chronic infection. However, a role for the FIKK kinase in other aspects of cyst formation cannot be ruled out. Our studies also suggest that the deletion of the FIKK kinase also impacts parasite fitness during acute infection, that may be dependent or independent of the host immune response. The FIKK complement clones that were created have both an HA and BirA tag in the 3' end of the protein. Both of these tags will be useful in future studies to identify other proteins that either directly interact with the FIKK kinase or are near neighbors. The fact that we were able to identify a process for successful complementation of the Δ FIKK clones with the FIKK kinase also will allow us to mutate important putative catalytic residues in the FIKK kinase to definitively show whether FIKK kinase activity is critical for its role in tachyzoite to bradyzoite differentiation. If the kinase residues are critical, future studies will identify proteins phosphorylated by the FIKK kinase both in the presence and absence of exogenous stress. Our current working hypothesis is that the FIKK kinase phosphorylates/associates with a subset of distinct proteins in the basal complex of mature parasites, this association/regulation of these proteins is important for the transition to bradyzoites, which involves de-linking and desynchronization of the parasite before the transition to bradyzoites (Figure 38). On a larger scale, our data suggest the the parasite basal complex

in mature parasites may have direct functions that regulation stage differentiation in addition to its known role in parasite endodyogeny.

References

1. **Ajzenberg D, Cogné N, Paris L, et al.** Genotype of 86 *Toxoplasma gondii* Isolates Associated with Human Congenital Toxoplasmosis, and Correlation with Clinical Findings. *The Journal of Infectious Diseases*. 2002;186(5):684-689.
2. **Altschul SF, Wootton JC, Zaslavsky E, Yu Y-K.** The Construction and Use of Log-Odds Substitution Scores for Multiple Sequence Alignment. *PLOS Computational Biology*. 2010;6(7).
3. **Behnke MS, Wootton JC, Lehmann MM, et al.** Coordinated Progression through Two Subtranscriptomes Underlies the Tachyzoite Cycle of *Toxoplasma gondii*. *PLOS ONE*. 2010;5(8):e12354.
4. **Blader IJ, Coleman BI, Chen C-T, Gubbels M-J.** Lytic Cycle of *Toxoplasma gondii* : 15 Years Later. *Annual Review of Microbiology*. 2015;69(1):463-485.
5. **Bohne W, Gross U, Ferguson DJP, Heesemann J.** Cloning and characterization of a bradyzoite-specifically expressed gene (hsp30/bag1) of *Toxoplasma gondii*, related to genes encoding small heat-shock proteins of plants. *Molecular Microbiology*. 1995;16(6):1221-1230.
6. **Bougdour A, Maubon D, Baldacci P, et al.** Drug inhibition of HDAC3 and epigenetic control of differentiation in Apicomplexa parasites. *Journal of Experimental Medicine*. 2009;206(4):953-966.
7. **Buchholz KR, Bowyer PW, Boothroyd JC.** Bradyzoite Pseudokinase 1 Is Crucial for Efficient Oral Infectivity of the *Toxoplasma gondii* Tissue Cyst. *Eukaryotic Cell*. 2013;12(3):399-410.
8. **Castro-Elizalde KN, Hernández-Contreras P, Ramírez-Flores CJ, et al.** Mycophenolic acid induces differentiation of *Toxoplasma gondii* RH strain tachyzoites into bradyzoites and formation of cyst-like structure in vitro. *Parasitol Res*. 2018;117(2):547-563.
9. **Chao CC, Anderson WR, Hu S, Gekker G, Martella A, Peterson PK.** Activated Microgila Inhibit Multiplication of *Toxoplasma gondii* via a Nitric Oxide Mechanism. *Clinical Immunology and Immunopathology*. 1993;67(2):178-183.
10. **Chatton E, Blanc G.** Notes and Reflections on the *Toxoplasma* and Toxoplasmosis of the Gundi. *Arch Inst Pasteur*. 1917.
11. **Clough B, Frickel E-M.** The *Toxoplasma* Parasitophorous Vacuole: An Evolving Host-Parasite Frontier. *Trends in Parasitology*. 2017;33(6):473-488.
12. **Cristina MD, Marocco D, Galizi R, Proietti C, Spaccapelo R, Crisanti A.** Temporal and Spatial Distribution of *Toxoplasma gondii* Differentiation into

Bradyzoites and Tissue Cyst Formation In Vivo. *Infection and Immunity*. 2008;76(8):3491-3501.

13. **Croken MM, Ma Y, Markillie LM, et al.** Distinct Strains of *Toxoplasma gondii* Feature Divergent Transcriptomes Regardless of Developmental Stage. *PLOS ONE*. 2014;9(11):e111297.
14. **Croken MM, Qiu W, White MW, Kim K.** Gene Set Enrichment Analysis (GSEA) of *Toxoplasma gondii* expression datasets links cell cycle progression and the bradyzoite developmental program. *BMC Genomics*. 2014;15(1):1-13.
15. **Dalmaso MC, Onyango DO, Naguleswaran A, Sullivan WJ, Angel SO.** *Toxoplasma* H2A Variants Reveal Novel Insights into Nucleosome Composition and Functions for this Histone Family. *Journal of Molecular Biology*. 2009;392(1):33-47.
16. **Denkers EY, Gazzinelli RT.** Regulation and Function of T-Cell-Mediated Immunity during *Toxoplasma gondii* Infection. *Clin Microbiol Rev*. 1998;11(4):569-588.
17. **Desmots G, Couvreur J, Alison F, Baudelot J, Gerbeaux J, Lelong M.** Etude épidémiologique sur la toxoplasmose: de l'influence de la cuisson des viandes de boucherie sur la fréquence de l'infection humaine. *Revue française d'études cliniques et biologiques*. 1965.
18. **Doerig C, Billker O, Haystead T, Sharma P, Tobin AB, Waters NC.** Protein kinases of malaria parasites: an update. *Trends in Parasitology*. 2008;24(12):570-577.
19. **Doerig C, Billker O, Pratt D, Endicott J.** Protein kinases as targets for antimalarial intervention: Kinomics, structure-based design, transmission-blockade, and targeting host cell enzymes. In: *Biochimica et Biophysica Acta - Proteins and Proteomics*. Vol 1754. Elsevier; 2005:132-150.
20. **Dubey JP.** Advances in the life cycle of *Toxoplasma gondii*. *Int J Parasitol*. 1998;28(7):1019-1024.
21. **Dubey JP, Lindsay DS, Speer CA.** Structures of *Toxoplasma gondii* tachyzoites, bradyzoites, and sporozoites and biology and development of tissue cyst. *Clin Microbiol Rev*. 1998;11(2):267-299.
22. **Dubey JP, Miller NL, Frenkel JK.** The *Toxoplasma gondii* Oocyst From Cat Feces. *J Exp Med*. 1970;132(4):636-662.
23. **Dunn D, Wallon M, Peyron F, Petersen E, Peckham C, Gilbert R.** Mother-to-child transmission of toxoplasmosis: Risk estimates for clinical counselling. *Lancet*. 1999;353(9167):1829-1833.

24. **Dupont CD, Christian DA, Hunter CA.** Immune response and immunopathology during toxoplasmosis. *Semin Immunopathol.* 2012;34(6):793-813.
25. **Dzierszynski F, Nishi M, Ouko L, Roos DS.** Dynamics of *Toxoplasma gondii* Differentiation. *Eukaryotic Cell.* 2004;3(4):992-1003.
26. **Engelberg K, Ivey FD, Lin A, et al.** A MORN1-associated HAD phosphatase in the basal complex is essential for *Toxoplasma gondii* daughter budding. *Cellular Microbiology.* 2016;18(8):1153-1171.
27. **Fenoy IM, Bogado SS, Contreras SM, Gottifredi V, Angel SO.** The knowns unknowns: Exploring the homologous recombination repair pathway in *Toxoplasma gondii*. *Frontiers in Microbiology.* 2016;7:1-15.
28. **Fox BA, Gigley JP, Bzik DJ.** *Toxoplasma gondii* lacks the enzymes required for de novo arginine biosynthesis and arginine starvation triggers cyst formation. *Int J Parasitol.* 2004;34(3):323-331.
29. **Francia ME, Striepen B.** Cell division in apicomplexan parasites. *Nature Reviews Microbiology.* 2014;12(2):125-136.
30. **Frenkel JK.** *Toxoplasma* In and Around Us. *BioScience.* 1973;23(6):343-352.
31. **Frenkel JK, Dubey JP, Miller NL.** *Toxoplasma gondii* in Cats: Fecal Stages Identified as Coccidian Oocysts. *Science.* 1970;167(3919):893-896.
32. **Gajria B, Bahl A, Brestelli J, et al.** ToxoDB: an integrated *Toxoplasma gondii* database resource. *Nucleic Acids Res.* 2008;36(Database issue):D553-D556.
33. **Gay-Andrieu F, Marty P, Pialat J, Sournies G, Laforte TD de, Peyron F.** Fetal toxoplasmosis and negative amniocentesis: necessity of an ultrasound follow-up. *Prenatal Diagnosis.* 2003;23(7):558-560.
34. **Gazzinelli RT, Hakim FT, Hieny S, Shearer GM, Sher A.** Synergistic role of CD4+ and CD8+ T lymphocytes in IFN-gamma production and protective immunity induced by an attenuated *Toxoplasma gondii* vaccine. *The Journal of Immunology.* 1991;146(1):286-292.
35. **Gissot M, Kelly KA, Ajioka JW, Greally JM, Kim K.** Epigenomic Modifications Predict Active Promoters and Gene Structure in *Toxoplasma gondii*. *PLOS Pathogens.* 2007;3(6):e77.
36. **Gross U, Bohne W, Soète M, Dubremetz JF.** Developmental differentiation between tachyzoites and bradyzoites of *Toxoplasma gondii*. *Parasitology Today.* 1996.

37. **Gubbels M-J, Vaishnav S, Boot N, Dubremetz J-F, Striepen B.** A MORN-repeat protein is a dynamic component of the *Toxoplasma gondii* cell division apparatus. *J Cell Sci.* 2006;119(Pt 11):2236-2245.
38. **Guevara RB, Fox BA, Falla A, Bzik DJ.** *Toxoplasma gondii* Intravacuolar-Network-Associated Dense Granule Proteins Regulate Maturation of the Cyst Matrix and Cyst Wall . *mSphere.* 2019;4(5).
39. **Harris MT, Jeffers V, Martynowicz J, True JD, Mosley AL, Sullivan WJ.** A novel GCN5b lysine acetyltransferase complex associates with distinct transcription factors in the protozoan parasite *Toxoplasma gondii*. *Mol Biochem Parasitol.* 2019;232:111203.
40. **Hartley WJ, Marshall SC.** Toxoplasmosis as a cause of ovine perinatal mortality. *New Zealand Veterinary Journal.* 1957;5(4):119-124.
41. **He X, Grigg ME, Boothroyd JC, Garcia KC.** Structure of the immunodominant surface antigen from the *Toxoplasma gondii* SRS superfamily. *Nature Structural Biology.* 2002;9(8):606-611.
42. **Hong D-P, Radke JB, White MW.** Opposing Transcriptional Mechanisms Regulate *Toxoplasma* Development. *mSphere.* 2017;2(1):1-30.
43. **Howe DK, Sibley LD.** *Toxoplasma gondii* Comprises Three Clonal Lineages: Correlation of Parasite Genotype with Human Disease. *Journal of Infectious Diseases.* 1995;172(6):1561-1566.
44. **Hutchison WM.** Experimental transmission of *Toxoplasma gondii*. *Nature.* 1965;206(987):961-962.
45. **Jeffers V, Tampaki Z, Kim K, Sullivan WJ.** A Latent Ability to Persist: Differentiation in *Toxoplasma gondii*. *Cell Mol Life Sci.* 2018;75(13):2355-2373.
46. **Jeninga MD, Quinn JE, Petter M.** ApiAP2 Transcription Factors in Apicomplexan Parasites. *Pathogens.* 2019;8(2).
47. **Jones JL, Kruszon-Moran D, Wilson M, McQuillan G, Navin T, McAuley JB.** *Toxoplasma gondii* infection in the United States: Seroprevalence and risk factors. *American Journal of Epidemiology.* 2001;154(4):357-365.
48. **Kang H, Remington JS, Suzuki Y.** Decreased Resistance of B Cell-Deficient Mice to Infection with *Toxoplasma gondii* Despite Unimpaired Expression of IFN- γ , TNF- α , and Inducible Nitric Oxide Synthase. *The Journal of Immunology.* 2000;164(5):2629-2634.
49. **Kim K.** The Epigenome, Cell Cycle, and Development in *Toxoplasma*. *Annual Review of Microbiology.* 2018;72(1):479-499.

50. **Konrad C, Queener SF, Wek RC, Sullivan WJ.** Inhibitors of eIF2 α Dephosphorylation Slow Replication and Stabilize Latency in *Toxoplasma gondii*. *Antimicrobial Agents and Chemotherapy*. 2013;57(4):1815-1822.
51. **Lerliche MA, Dubremetz JF.** Exocytosis of *Toxoplasma gondii* dense granules into the parasitophorous vacuole after host cell invasion. *Parasitology research*. 1990;76(7):559-562.
52. **Liu T, White MW, Sullivan WJ.** *Toxoplasma gondii* AP2IX-4 Regulates Development. 2017;2(2):1-16.
53. **Mercier C, Dubremetz JF, Rauscher B, Lecordier L, Sibley LD, Cesbron-Delauw MF.** Biogenesis of nanotubular network in *Toxoplasma* parasitophorous vacuole induced by parasite proteins. *Molecular Biology of the Cell*. 2002;13(7):2397-2409.
54. **Montoya JG, Liesenfeld O.** Toxoplasmosis. *The Lancet*. 2004;363(9425):1965-1976.
55. **Muñiz-Hernández S, González del Carmen M, Mondragón M, et al.** Contribution of the Residual Body in the Spatial Organization of *Toxoplasma gondii* Tachyzoites within the Parasitophorous Vacuole. *Journal of Biomedicine and Biotechnology*. 2011;2011:e473983.
56. **Narasimhan J, Joyce BR, Naguleswaran A, et al.** Translation Regulation by Eukaryotic Initiation Factor-2 Kinases in the Development of Latent Cysts in *Toxoplasma gondii*. *J Biol Chem*. 2008;283(24):16591-16601.
57. **Nardelli SC, Che F-Y, Monerri NCS de, et al.** The Histone Code of *Toxoplasma gondii* Comprises Conserved and Unique Posttranslational Modifications. *mBio*. 2013;4(6).
58. **Osman KT, Lou HJ, Qiu W, et al.** Biochemical characterization of FIKK8 - A unique protein kinase from the malaria parasite *Plasmodium falciparum* and other apicomplexans. *Molecular and Biochemical Parasitology*. 2015;201(2):85-89.
59. **Pagheh AS, Sarvi S, Sharif M, et al.** *Toxoplasma gondii* surface antigen 1 (SAG1) as a potential candidate to develop vaccine against toxoplasmosis: A systematic review. *Comparative Immunology, Microbiology and Infectious Diseases*. 2020;69:101414.
60. **Painter HJ, Campbell TL, Llinás M.** The Apicomplexan AP2 family: integral factors regulating *Plasmodium* development. *Mol Biochem Parasitol*. 2011;176(1):1-7.
61. **Periz J, Whitelaw J, Harding C, et al.** *Toxoplasma gondii* F-actin forms an extensive filamentous network required for material exchange and parasite maturation. Akhmanova A, ed. *eLife*. 2017;6:e24119.

62. **Porter SB, Sande MA.** Toxoplasmosis of the Central Nervous System in the Acquired Immunodeficiency Syndrome. *New England Journal of Medicine.* 1992;327(23):1643-1648.
63. **Radke JB, Lucas O, De Silva EK, et al.** ApiAP2 transcription factor restricts development of the Toxoplasma tissue cyst. *Proceedings of the National Academy of Sciences of the United States of America.* 2013;110(17):6871-6876.
64. **Radke JB, Worth D, Hong D, et al.** Transcriptional repression by ApiAP2 factors is central to chronic toxoplasmosis. *PLoS Pathogens.* 2018;14(5):1-26.
65. **Radke JR, Guerini MN, Jerome M, White MW.** A change in the premitotic period of the cell cycle is associated with bradyzoite differentiation in Toxoplasma gondii. *Molecular and Biochemical Parasitology.* 2003;131(2):119-127.
66. **Radke JR, Striepen B, Guerini MN, Jerome ME, Roos DS, White MW.** Defining the cell cycle for the tachyzoite stage of Toxoplasma gondii. *Molecular and Biochemical Parasitology.* 2001;115(2):165-175.
67. **Rawal BD.** Toxoplasmosis. A dye-test survey on Sera from vegetarians and meat eaters in Bombay. *Trans R Soc Trop Med Hyg.* 1959;53(1):61-63.
68. **Ruthenburg AJ, Li H, Patel DJ, Allis CD.** Multivalent engagement of chromatin modifications by linked binding modules. *Nat Rev Mol Cell Biol.* 2007;8(12):983-994.
69. **Saksouk N, Bhatti MM, Kieffer S, et al.** Histone-Modifying Complexes Regulate Gene Expression Pertinent to the Differentiation of the Protozoan Parasite Toxoplasma gondii. *Molecular and Cellular Biology.* 2005;25(23):10301-10314.
70. **Saksouk N, Bhatti MM, Kieffer S, et al.** Histone-Modifying Complexes Regulate Gene Expression Pertinent to the Differentiation of the Protozoan Parasite Toxoplasma gondii. *Molecular and Cellular Biology.* 2005;25(23):10301-10314.
71. **Sibley LD, Niesman IR, Parmley SF, Cesbron-Delauw MF.** Regulated secretion of multi-lamellar vesicles leads to formation of a tubulovesicular network in host-cell vacuoles occupied by Toxoplasma gondii. *Journal of Cell Science.* 1995;108(4):1669-1677.
72. **Skariah S, Walwyn O, Engelberg K, et al.** The FIKK kinase of Toxoplasma gondii is not essential for the parasite's lytic cycle. *International Journal for Parasitology.* 2016;46(5-6):323-332.
73. **Striepen B, Jordan CN, Reiff S, Dooren GG van.** Building the Perfect Parasite: Cell Division in Apicomplexa. *PLOS Pathogens.* 2007;3(6):e78.

74. **Sullivan WJ, Narasimhan J, Bhatti MM, Wek RC.** Parasite-specific eIF2 (eukaryotic initiation factor-2) kinase required for stress-induced translation control. *Biochemical Journal*. 2004;380(2):523-531.
75. **Suss-Toby E, Zimmerberg J, Wardt GE.** Toxoplasma invasion: The parasitophorous vacuole is formed from host cell plasma membrane and pinches off via a fission pore (cell capacitance/intracellular parasite/endocytosis). *National Institutes of Health*. 1996;93:8413-8418.
76. **Suzuki Y, Claflin J, Wang X, Lengi A, Kikuchi T.** Microglia and macrophages as innate producers of interferon-gamma in the brain following infection with *Toxoplasma gondii*. *International Journal for Parasitology*. 2005;35(1):83-90.
77. **Suzuki Y, Orellana MA, Schreiber RD, Remington JS.** Interferon-gamma: the major mediator of resistance against *Toxoplasma gondii*. *Science*. 1988;240(4851):516-518.
78. **Swierzy IJ, Lüder CGK.** Withdrawal of skeletal muscle cells from cell cycle progression triggers differentiation of *Toxoplasma gondii* towards the bradyzoite stage. *Cellular Microbiology*. 2015;17(1):2-17.
79. **Tait ED, Jordan KA, Dupont CD, et al.** Virulence of *Toxoplasma gondii* Is Associated with Distinct Dendritic Cell Responses and Reduced Numbers of Activated CD8+ T Cells. *The Journal of Immunology*. 2010;185(3):1502-1512.
80. **Taverna SD, Li H, Ruthenburg AJ, Allis CD, Patel DJ.** How chromatin-binding modules interpret histone modifications: lessons from professional pocket pickers. *Nature Structural & Molecular Biology*. 2007;14(11):1025-1040.
81. **Torgerson PR, Mastroiacovo P.** The global burden of congenital toxoplasmosis: a systematic review. *Bulletin of the World Health Organization*. 2013;91(7):501-508.
82. **Tosetti N, Dos Santos Pacheco N, Soldati-Favre D, Jacot D.** Three F-actin assembly centers regulate organelle inheritance, cell-cell communication and motility in *Toxoplasma gondii*. Lappalainen P, Akhmanova A, eds. *eLife*. 2019;8:e42669.
83. **Travier L, Mondragon R, Dubremetz JF, et al.** Functional domains of the *Toxoplasma* GRA2 protein in the formation of the membranous nanotubular network of the parasitophorous vacuole. *International Journal for Parasitology*. 2008;38(7):757-773.
84. **Tu V, Mayoral J, Sugi T, et al.** Enrichment and Proteomic Characterization of the Cyst Wall from In Vitro *Toxoplasma gondii* Cysts. *mBio*. 2019;10(2).
85. **Tu V, Mayoral J, Yakubu RR, et al.** MAG2, a *Toxoplasma gondii* Bradyzoite Stage-Specific Cyst Matrix Protein. *mSphere*. 2020;5(1).

86. **Tu V, Tomita T, Sugi T, et al.** The Toxoplasma gondii Cyst Wall Interactome. *mBio*. 2020;11(1).
87. **Waldman BS, Schwarz D, Wadsworth II MH, Saeij J, Shalek AK, Lourido S.** Identification of a Master Regulator of Differentiation in Toxoplasma. *SSRN Electronic Journal*. 2019:1-23.
88. **Wang J, Dixon SE, Ting L-M, et al.** Lysine Acetyltransferase GCN5b Interacts with AP2 Factors and Is Required for Toxoplasma gondii Proliferation. *PLoS Pathogens*. 2014;10(1):e1003830.
89. **Ward P, Equinet L, Packer J, Doerig C.** Protein kinases of the human malaria parasite Plasmodium falciparum: the kinome of a divergent eukaryote. *BMC Genomics*. 2004;5(1):79.
90. **Wek RC, Jiang H-Y, Anthony TG.** Coping with stress: eIF2 kinases and translational control. *Biochem Soc Trans*. 2006;34(1):7-11.
91. **Wolf A, Cowen D, Paige B.** Human Toxoplasmosis: Occurrence in Infants as an Encephalomyelitis Verification by Transmission to Animals. *Science*. 1939;89(2306):226-227.
92. **Yahiaoui B, Dzierszynski F, Bernigaud A, Slomianny C, Camus D, Tomavo S.** Isolation and characterization of a subtractive library enriched for developmentally regulated transcripts expressed during encystation of Toxoplasma gondii. *Mol Biochem Parasitol*. 1999;99(2):223-235.
93. **Yamamoto M, Ma JS, Mueller C, et al.** ATF6 β is a host cellular target of the Toxoplasma gondii virulence factor ROP18. *Journal of Experimental Medicine*. 2011.
94. **Yang S, Parmley SF.** A bradyzoite stage-specifically expressed gene of Toxoplasma gondii encodes a polypeptide homologous to lactate dehydrogenase. *Molecular and Biochemical Parasitology*. 1995;73(1):291-294.
95. **Yang S, Parmley SF.** Toxoplasma gondii expresses two distinct lactate dehydrogenase homologous genes during its life cycle in intermediate hosts. *Gene*. 1997;184(1):1-12.
96. **Yap GS, Sher A.** Effector Cells of Both Nonhemopoietic and Hemopoietic Origin Are Required for Interferon (IFN)- γ - and Tumor Necrosis Factor (TNF)- α -dependent Host Resistance to the Intracellular Pathogen, Toxoplasma gondii. *J Exp Med*. 1999;189(7):1083-1092.
97. **Zhang YW, Halonen SK, Ma YF, Wittner M, Weiss LM.** Initial Characterization of CST1, a Toxoplasma gondii Cyst Wall Glycoprotein. *Infect Immun*. 2001;69(1):501-507.